A Partial Prehistory of the Southwest Silk Road: Archaeometallurgical Networks along the Sub-Himalayan Corridor

T.O. Pryce, Simon Carrignon, Mélissa Cadet, Kay Thwe Oo, Saw Naing Oo, Thu Thu Win, Arkar Aye, Baptiste Pradier, Bérénice Bellina, Peter Petchey, et al.

A partial prehistory of the Southwest Silk Road: Archaeometallurgical networks along the sub-Himalayan corridor

Journal:	*Cambridge Archaeological Journal*
Manuscript ID	CAJ-2023-0011.R1
Manuscript Type:	Research Article
Date Submitted by the Author:	n/a
Complete List of Authors:	Pryce, Thomas; Centre National de la Recherche Scientifique, UMR 7065 Institut de Recherche sur les archéomatériaux Carrignon, Simon; Cambridge University, Department of Archaeology Cadet, Mélissa; Academia Sinica, Institute of History and Philology Naing Oo, Kay; Independent scholar Naing Oo, Saw; Independent scholar Thu Win, Thu; Independent scholar Aye, Arkar; Independent scholar Pradier, Baptiste; Université de Paris Nanterre, UMR 8068 TEMPS Bellina, Bérénice; Centre National de la Recherche Scientifique, UMR 8068 TEMPS Le Meur, Clémence; Ecole Pratique des Hautes Etudes Petchey, Peter; University of Otago Radivojevic, Miljana; University College London, Institute of Archaeology
Manuscript Keywords:	Southwest Silk Roads, Archaeometallurgy, Lead isotope analysis, Myanmar, Yunnan, Southeast Asia, Prehistory, Complex Networks Analysis, Leiden Algorithm Community Analysis
Abstract:	Historical phenomena often have prehistoric precedents, with this paper we investigate the potential for archaeometallurgical analyses and networked data processing to elucidate the progenitors of the Southwest Silk Road in Mainland Southeast Asia and southern China. We present original microstructural, elemental and lead isotope data for 40 archaeological copper-base metal samples, mostly from the UNESCO-listed site of Halin, and lead isotope data for 25 geological copper-mineral samples, also from Myanmar. We combined these data with existing datasets (N=98 total) and compared them to the 1000+ sample late prehistoric archaeometallurgical database available from Cambodia, Laos, Thailand, Vietnam and Yunnan. Lead isotope data, contextualised for alloy, find location and date, were interpreted manually for intra-site, inter-site and inter-regional consistency, which hint at significant multi-scalar connectivity from the late 2nd millennium BC. To test this interpretation statistically, the archaeological lead isotope data were then processed using regionally-adapted production-derived consistency parameters. Complex networks analysis using the Leiden community detection algorithm established groups of artefacts sharing lead isotopic consistency. Introducing the geographic component allowed for the identification of communities of sites with consistent assemblages. The four major communities were consistent with the manually interpreted exchange networks and suggest southern sections of the Southwest Silk Road were active in the late 2nd millennium BC.

A partial prehistory of the Southwest Silk Road: Archaeometallurgical networks along the sub-Himalayan corridor

T. O. Pryce, Simon Carrignon, Mélissa Cadet, Kay Thwe Oo, Saw Naing Oo, Thu Thu Win, Arkar Aye, Baptiste Pradier, Bérénice Bellina, Clémence Le Meur, Peter Petchey, Miljana Radivojević

T. O. Pryce*

Email: oliver.pryce@cnrs.fr

Author Contributions: Paste the author contributions here.

Designed research: TOP

Performed research: TOP, KTO, SNO, TTW, AA, MC, BP, BB, CLM, PP, MR

Analyzed data: TOP, SC, MC

Wrote the paper: TOP, SC, MC, MR

Submitting author biography

T. O. Pryce is a Senior Researcher for the French Centre for Scientific Research since 2013. He is a member of the *Institut de Recherche sur les ArchéoMATériaux* (UMR 7065) since 2022 and was previously member of *Préhistoire et Technologie* (UMR 7055). Pryce has been Director of the French Archaeological Mission in Myanmar since 2012, until its suspension in 2021. He is Director of the BROGLASEA/SEALIP since 2008 and has conducted archaeometallurgical research in Southeast Asia since 2004. Pryce was previously postdoctoral researcher at the French Institute of Research for Development in 2013, and the University of Oxford from 2009 to 2012.

Competing Interest Statement:

We declare no competing interests.

Keywords: Southwest Silk Roads, Archaeometallurgy, Lead isotope analysis, complex networks, community detection, Myanmar, Yunnan, Southeast Asia, Prehistory.

Abstract

Historical phenomena often have prehistoric precedents, with this paper we investigate the potential for archaeometallurgical analyses and networked data processing to elucidate the progenitors of the Southwest Silk Road in Mainland Southeast Asia and southern China. We present original microstructural, elemental and lead isotope data for 40 archaeological copper-base metal samples, mostly from the UNESCO-listed site of Halin, and lead isotope data for 25 geological copper-mineral samples, also from Myanmar. We combined these data with existing datasets (N=98 total) and compared them to the 1000+ sample late prehistoric archaeometallurgical database available from Cambodia, Laos, Thailand, Vietnam and Yunnan. Lead isotope data, contextualised for alloy, find location and date, were interpreted manually for intra-site, inter-site and inter-regional consistency, which hint at significant multi-scalar connectivity from the late 2nd millennium BC. To test this interpretation statistically, the archaeological lead isotope data were then processed using regionally-adapted production-derived consistency parameters. Complex networks analysis using the Leiden community detection algorithm established groups of artefacts sharing lead isotopic consistency. Introducing the geographic component allowed for the identification of communities of sites with consistent assemblages. The four major communities were consistent with the manually interpreted exchange networks and suggest southern sections of the Southwest Silk Road were active in the late 2nd millennium BC.

Introduction

The 'Silk Road' (SR) has been a source of perennial academic and public interest since the term was introduced in the late 19th century (von Richthofen 1877), but the historiography of the concept can be traced to the medieval (Polo 1918) and antique (Claudius 1406) periods. The diachronic, predominantly, east-west interactions represented by the SR are widely acknowledged to have massively stimulated the civilizations of participating populations, with long-distance movements of goods, far more varied than those implied eponymously, modes of thought, technologies and people. It is a truism to state the SR's pertinence to the modern world, encapsulated since 2013 by China's 'Belt and Road Initiative', but the SR's origin has been a longstanding topic of discussion, and one complicated by the fact there are numerous 'roads'. Of course, the SR of popular imagination involves camels and caravanserai spanning the desertic steppe, and these routes (there are many) are indeed of massive importance historically; and of particular relevance to the history of metallurgy in eastern Asia (e.g. Linduff & Mei 2009). However, this paper concerns the origins of the Southwest Silk Road (SSR), which remains less well known than their supra-Himalayan counterparts, or even their nautical variants, the Maritime Silk Roads (MSR) (e.g. Bellina 2014; Bellina *et al.* 2019).

In Mandarin, the SSR is known as the 茶馬道, or 'Tea Horse Road', these being the chief goods known to have moved to the Chinese imperial capital of Chang'an in Shaanxi province. The SSR routes varied over time, with four main variations attested historically for the mid-1st to early 2nd millennia AD (Figure 1), connecting Chang'an to Chengdu in Sichuan province, Dian/Dali in Yunnan province, before continuing west to northern Myanmar (Mian), Bangladesh, India (Yandu); while alternate branches went south to northern Vietnam (Jiaozhi), Laos, Thailand and Cambodia (Yang 2004; 2008). Knowledge of earlier, pre-3rd c. AD, SSR routes is limited to Yunnan, Sichuan and Shaanxi provinces (plus *Jiaozhi*, northern Vietnam, Figure 2) as the other Mainland Southeast Asian (MSEA) territories were, at that juncture, 'prehistoric'. With this paper, we wish to question whether these trans-regional montane and riverine social interaction networks linking MSEA and southern China may be older, possibly considerably older, than the textual sources allow for.

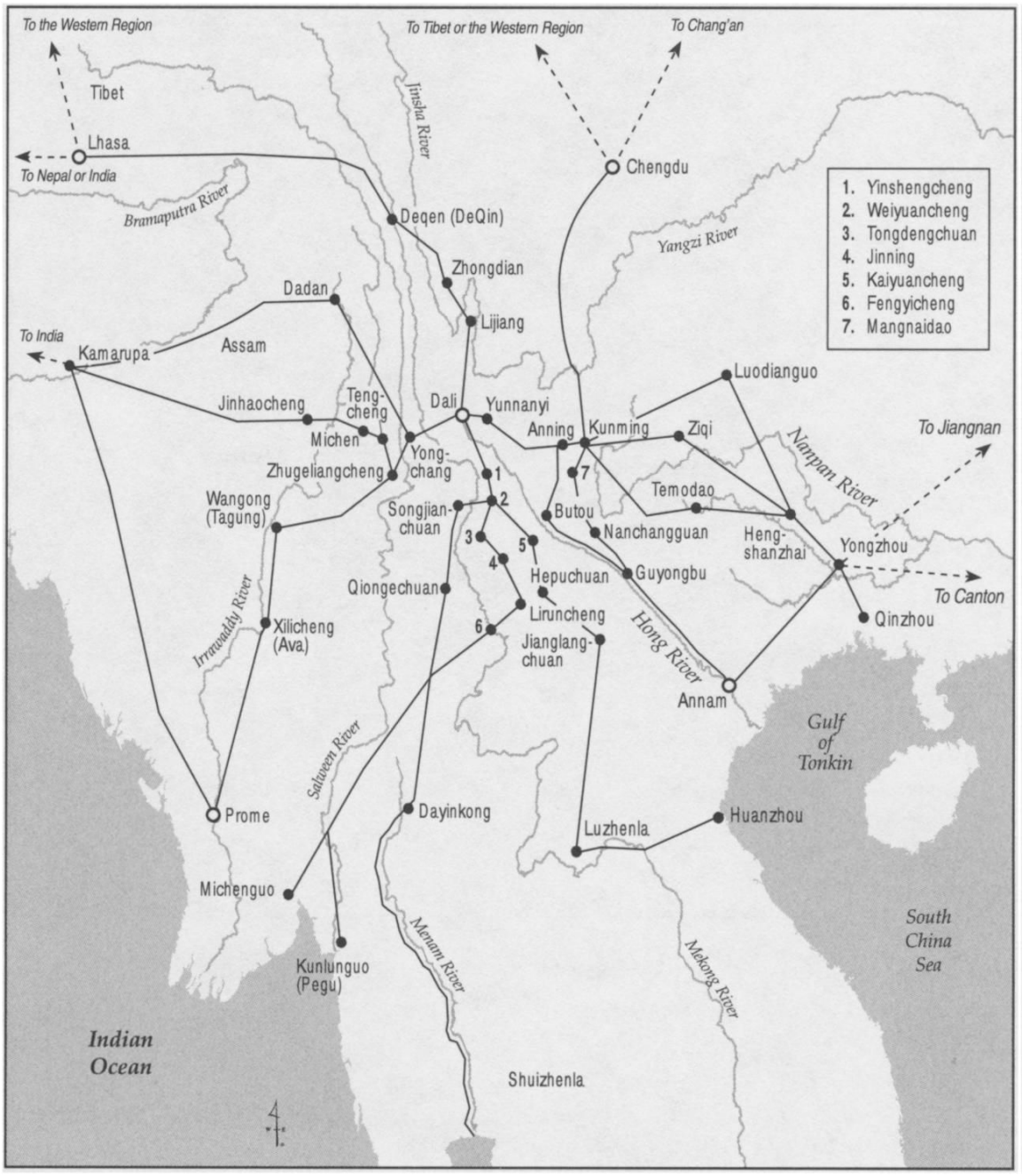

Figure 1: The SSR during the Nanzhao-Dali period, 7th-13th c. AD, reproduced with permission from (Yang 2004: Map 2).

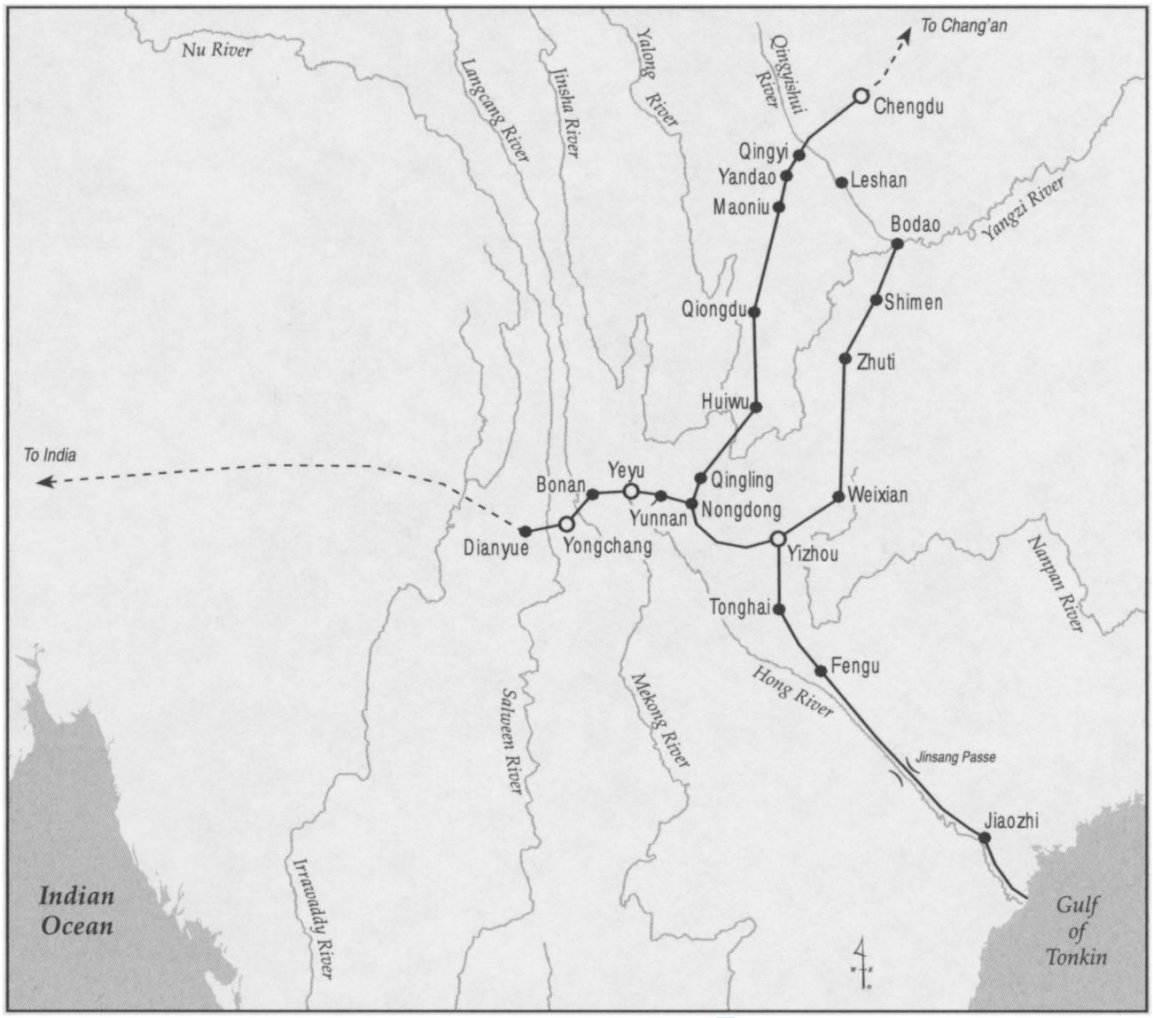

Figure 2: The SSR before the 3rd c. BC, reproduced with permission from (Yang 2004: Map 1), with the exclusion of Mainland Southeast Asia due to lack of textual sources.

Archaeological evidence for horses and tea in early China is quite abundant (e.g. Jiang *et al.* 2021; Li *et al.* 2020; Lu *et al.* 2016; Wan 2013) but practically absent from prehistoric Southeast Asia. Therefore, alternative means of identifying proto-SSR interaction networks must comprise materials that a) might have been exchanged, and b) might be detected archaeologically. Within the Maritime Silk Road system, Southeast Asian forest products, including exotic woods, resins and spices, were famously in demand by more westerly consumers, located as far as the Mediterranean basin (Bellina *et al.* 2019; Bellina & Glover 2004). It is certainly conceivable that some of these materials were not available in southern China, despite some overlap in ecological conditions, and that detailed and fortuitous future MSEA sampling programmes could recover evidence for their being supplied north; as per the recent association of sappanwood and lead and copper ingot exchange in a 17th c. AD wreck in the Gulf of Siam (Venunan *et al.* 2022). More readily identifiable would be the exchange of semi-precious stones, for which there are precedents in the form of Taiwanese nephrite (Hung *et al.* 2007), agate and carnelian beads produced by highly skilled artisans (Bellina 2003; Bellina *et al.* 2019), as well as recent evidence

for lower-skilled production of carnelian beads in Neolithic north-central Myanmar (Georjon *et al.* 2021).

Of course, pottery should provide the bulk of our evidence, and the Yunnan Neolithic 'incised and impressed' ("i&I") wares are indeed detected from Thai and Vietnamese Neolithic sites spanning the mid-3rd to late-2nd millennia BC (Higham 2017; Rispoli 2007; Sarjeant 2014), as well as potentially early-mid 3rd millennium BC deposits from north-central Myanmar (Hudson & Lwin 2012; Pautreau *et al.* 2010; Pryce *et al.* in press). However, we do not wish to emphasise the possibility of a proto-SSR commencing up to 5000 BP at this time. Few of these Neolithic pottery assemblages have been evaluated within a strict *chaîne opératoire* framework (as per Favereau *et al.* 2018), meaning the claimed homologies have not been reliably demonstrated. Furthermore, there are as yet no equivalent shared typewares for the Yunnan and MSEA Bronze Age and Iron Age periods (which have notably close chronologies, Higham *et al.* 2015; Pryce *et al.* 2018b; in press; Yao *et al.* 2020), and thus pottery studies currently fail the test of chronological contiguity.

As glass is either inexistent-to-vanishingly-rare in MSEA or Chinese contexts prior to the mid-first millennium BC (excluding Chinese faience and frits of the late 2nd/early 1st mill. BC, Fuxi 2009; Huang 2020) and trace element datasets compatible with those of MSEA (e.g. Dussubieux & Bellina 2018) are as yet unavailable in Yunnan, we therefore turn to metals to reach back to the late 2nd millennium BC. Prehistoric precious and ferrous metals having only received fleeting attention, here we investigate the potential to push back the early dating of the more southerly SSR routes using copper-base archaeometallurgical evidence. Recent copper/bronze provenance papers have established tentative but nuanced protohistoric linkages between northern Vietnam (*Jiaozhi*) and the rest of MSEA (Pryce *et al.* 2022a), and from these areas into Yunnan (Pryce *et al.* 2022b). In this paper we add new data from Myanmar, which potentially completes an arc of interaction between northern MSEA and southern China. We also offer original data treatments in an attempt to firm up our trans-regional interpretations. The latest metal samples come from recently excavated Bronze (late 2nd/early-mid 1st millennia BC), Iron Age (mid-late 1st millennium BC, Pyu (1st millennium AD) and Bagan (early 2nd millennium AD) period sites and selected copper mineralisations in north-central Myanmar, as analysed by the ANR 'Bronze and Glass as Cultural Catalysts and Tracers in Early Southeast Asia' project (SEALIP-BROGLASEA). Additionally, we have a few samples from a newly-discovered Iron Age site in southern Myanmar, likely related to the Maritime Silk Road itself (Bellina *et al.* 2018).

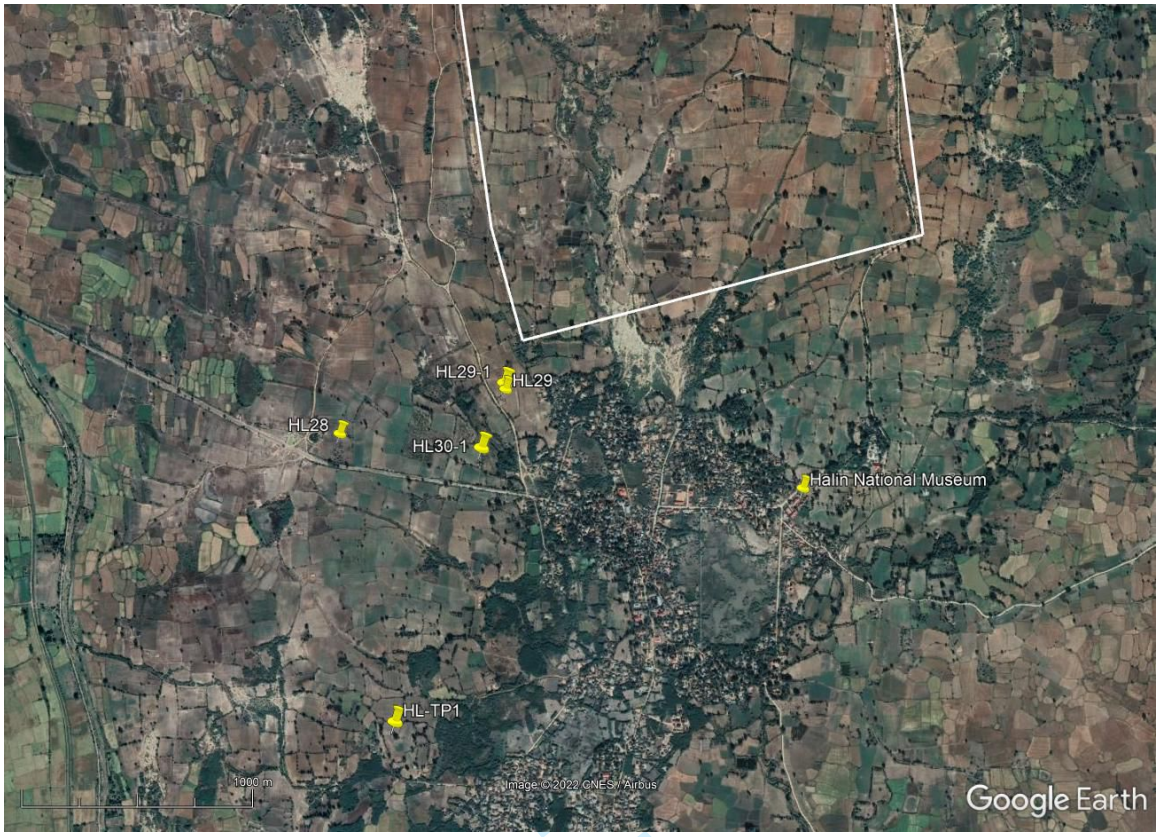

Figure 3: Excavations yielding copper-base artefacts for the present study, with respect to Halin village, the National Museum, and the southern part of the Pyu city wall (white line approximation).

The bulk of archaeological sites concerned for our new data: HL30-1, HL29, HL29-1, HL28 and HL-TP1, are located in the southwestern environs of the UNESCO-listed Pyu citystate of Halin, (museum, 95.818957°E, 22.453651°N), ca. 15 km west of the Irrawaddy River in Sagaing Division (Figure 3). The monumental ruins of the Pyu city account for Halin's fame but the presence of prehistoric deposits spanning back to a mid-3rd millennium Neolithic, as well subsequent Bagan remains, allows the possibility of investigating over 4000 years of Myanmar's history; from first farmers to the formation, and decline, of the first states (Pryce *et al.* in press). Understanding the impact of external cultural influence is essential to this endeavour, and the SSR in its developed and nascent forms could conceivably have played a significant role. Reconstructing social interaction networks is a task well-suited, for post-Neolithic societies, to archaeometallurgy and, in particular, lead isotope-based provenance research (Pryce *et al.* 2022a; 2022b).

HL29-1, HL30-1 and HL-TP1 were excavated by the *Mission Archéologique Française au Myanmar* between 2017 and 2020, while HL28 and HL29 were excavated by Myanma archaeologists in 2009-2010. HL29-1 was a multiphase deposit with a Bronze Age cemetery, Pyu cremation burials and Bagan occupation deposit. HL30-1 contained a Neolithic cemetery, a Bronze Age occupation deposit and an Iron Age cemetery. HL-TP1 was a mid-Bronze Age, Iron Age, Pyu and Bagan period occupation and salt production locale. HL28 and HL29 were Iron and Bronze Age cemeteries, respectively, whose assemblages were sampled by the lead author in 2019. For a summary of Halin archaeology see Pryce *et al.* (in press).

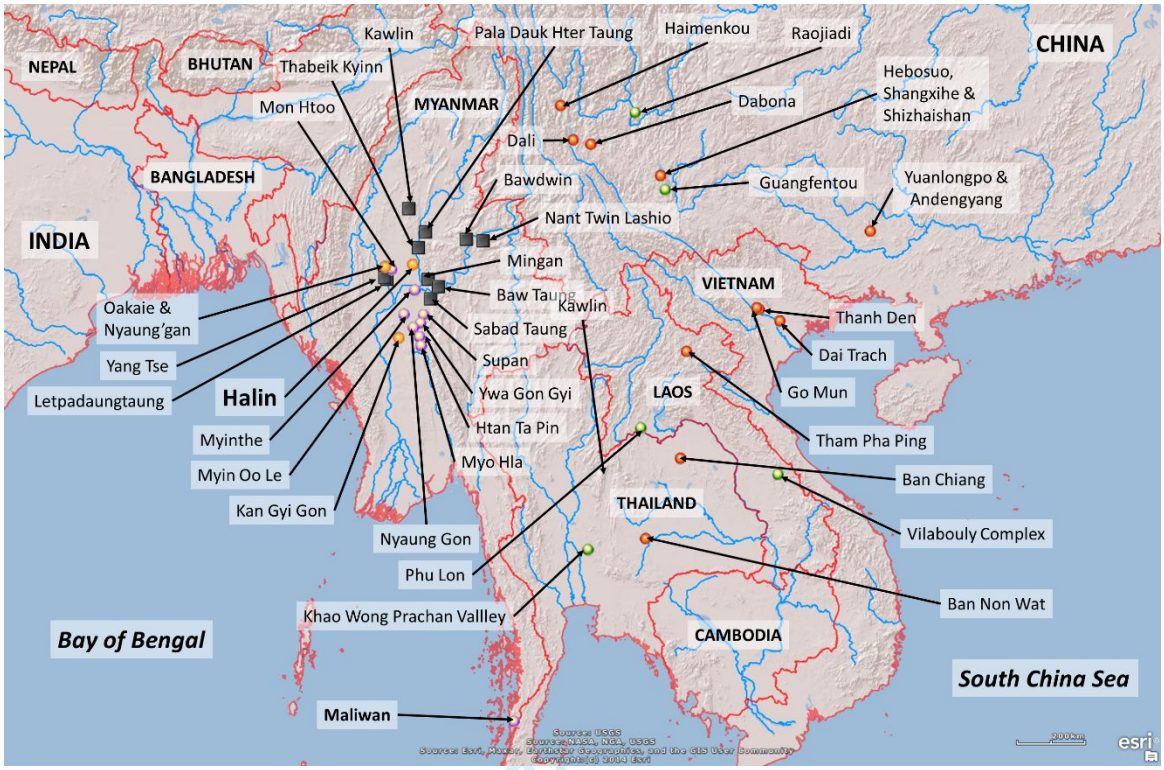

Figure 4: Map showing the present study sites/locations, terrain, major rivers and national boundaries. Black squares represent sampled mineralisations, pink circles represent Myanmar Iron Age consumption sites (excavated by the MAFM under the direction of J.-P. Pautreau), orange circles represent Myanmar Bronze Age – Bagan period consumption sites excavated by the MAFM (under the direction of the lead author), and red circles other consumption sites cited in the paper. Green circles represent the documented prehistoric copper producing centres with lead isotope characterisations.

A total of 38 Halin copper-base artefacts spanning over 2000 years of metal consumption were analysed, including: four axes, four bangles, six rings, seven bells, five spearheads, ten wires, one casting spillage and one plate-like fragment (Figure 5, Table 1). Their typological, technological, elemental and lead isotopic data add to the 32 published Myanmar samples (Dussubieux & Pryce 2016; Pryce *et al.* 2018a; 2014). In the absence of early copper mining and smelting evidence in Myanmar, as well as geological data generally, we also collected 25 geological samples from nine copper mineralisations in Sagaing Division, Mandalay Division, Kachin State and Shan State, to gain some handle on regional geological variation (Figure 3, Table 1). The three southern Myanmar samples come from the littoral settlement of Maliwan (98.623468°E, 10.324234°N), recently excavated by the French Archaeological Project in Peninsular Myanmar and Thailand (Bellina *et al.* 2018).

Table 1: Current study samples, names and context information.

	SEALIP ID	Site	Sample type	Artefact	Context	Catalogue	Reference	Period *	Mass	Corrosion
1	SEALIP/MY/BAW/1	Baw Mountain, Kyaukse	Mineral	Cu mineral	surface collection			geological	-	-
2	SEALIP/MY/BAW/2	Baw Mountain, Kyaukse	Mineral	Cu mineral	surface collection			geological	-	-
3	SEALIP/MY/BAW/3	Baw Mountain, Kyaukse	Mineral	Cu mineral	surface collection			geological	-	-
4	SEALIP/MY/BWD/1	Bawdwin	Mineral	Cu mineral	surface collection			geological	-	-
5	SEALIP/MY/BWD/2	Bawdwin	Mineral	Cu mineral	surface collection			geological	-	-
6	SEALIP/MY/KAW/1	Kawlin	Mineral	Cu mineral	surface collection			geological	-	-
7	SEALIP/MY/KAW/2	Kawlin	Mineral	Cu mineral	surface collection			geological	-	-
8	SEALIP/MY/KAW/3	Kawlin	Mineral	Cu mineral	surface collection			geological	-	-
9	SEALIP/MY/MIN/1	Mingan	Mineral	Cu mineral	surface collection			geological	-	-
10	SEALIP/MY/MIN/2	Mingan	Mineral	Cu mineral	surface collection			geological	-	-
11	SEALIP/MY/MIN/3	Mingan	Mineral	Cu mineral	surface collection			geological	-	-
12	SEALIP/MY/NTL/1	Nant Twin village	Mineral	Cu mineral	surface collection			geological	-	-
13	SEALIP/MY/NTL/2	Nant Twin village	Mineral	Cu mineral	surface collection			geological	-	-
14	SEALIP/MY/NTL/3	Nant Twin village	Mineral	Cu mineral	surface collection			geological	-	-
15	SEALIP/MY/PDHT/1	Pala Dauk Hter Taung	Mineral	Cu mineral	surface collection			geological	-	-
16	SEALIP/MY/PDHT/2	Pala Dauk Hter Taung	Mineral	Cu mineral	surface collection			geological	-	-
17	SEALIP/MY/PDHT/3	Pala Dauk Hter Taung	Mineral	Cu mineral	surface collection			geological	-	-
18	SEALIP/MY/ST/1	Sabad Taung	Mineral	Cu mineral	surface collection			geological	-	-
19	SEALIP/MY/ST/2	Sabad Taung	Mineral	Cu mineral	surface collection			geological	-	-
20	SEALIP/MY/ST/3	Sabad Taung	Mineral	Cu mineral	surface collection			geological	-	-
21	SEALIP/MY/TKN/1	Thabeik Kyinn	Mineral	Cu mineral	surface collection			geological	-	-
22	SEALIP/MY/TKN/2	Thabeik Kyinn	Mineral	Cu mineral	surface collection			geological	-	-
23	SEALIP/MY/TKN/3	Thabeik Kyinn	Mineral	Cu mineral	surface collection			geological	-	-
24	SEALIP/MY/YTCM/1	Yang Tse Copper	Mineral equivalent	Cu ingot	personal collection			modern	-	low
25	SEALIP/MY/HL28/1	Halin HL28	Consumption artefact	wire bundle	MoC excavation	2013/2/3-A		IA	8,05	low
26	SEALIP/MY/HL28/2	Halin HL28	Consumption artefact	wire bundle	MoC excavation	2013/2/3-B		IA	9,75	low
27	SEALIP/MY/HL28/3	Halin HL28	Consumption artefact	wire bundle	MoC excavation	2013/2/3-C		IA	7,85	low
28	SEALIP/MY/HL28/4	Halin HL28	Consumption artefact	wire bundle multi	MoC excavation	2013/2/3-D		IA	7,95	low
29	SEALIP/MY/HL28/5	Halin HL28	Consumption artefact	wire bundle multi	MoC excavation	2013/2/3-D		IA	-	low
30	SEALIP/MY/HL28/6	Halin HL28	Consumption artefact	wire bundle multi	MoC excavation	2013/2/3-D		IA	-	low
31	SEALIP/MY/HL28/7	Halin HL28	Consumption artefact	wire bundle	MoC excavation	2013/2/3-E		IA	10,1	low
32	SEALIP/MY/HL28/8	Halin HL28	Consumption artefact	wire bundle	MoC excavation	2013/2/3-F		IA	3,9	low
33	SEALIP/MY/HL28/9	Halin HL28	Consumption artefact	wire bundle	MoC excavation	2013/2/3-G		IA	6,55	low
34	SEALIP/MY/HL28/10	Halin HL28	Production artefact	possible casting spillage	MoC excavation	2013/2/3-H		IA	9,5	medium
35	SEALIP/MY/HL28/11	Halin HL28	Consumption artefact	wire bundle	MoC excavation	2013/2/3-I		IA	7,9	low
36	SEALIP/MY/HL28/12	Halin HL28	Consumption artefact	large bell/rattle	MoC excavation	04/02/2014		IA	189,65	low
37	SEALIP/MY/HL28/13	Halin HL28	Consumption artefact	small bell/rattle	MoC excavation	2013/2/5-A		IA	39,6	low
38	SEALIP/MY/HL28/14	Halin HL28	Consumption artefact	small bell/rattle	MoC excavation	2013/2/5-B		IA	25,15	medium
39	SEALIP/MY/HL28/15	Halin HL28	Consumption artefact	small bell/rattle	MoC excavation	2013/2/5-C		IA	15	medium
40	SEALIP/MY/HL28/16	Halin HL28	Consumption artefact	small bell/rattle	MoC excavation	2013/2/5-D		IA	19,4	low
41	SEALIP/MY/HL28/17	Halin HL28	Consumption artefact	small bell/rattle	MoC excavation	2013/2/5-E		IA	18,15	low
42	SEALIP/MY/HL28/18	Halin HL28	Consumption artefact	small bell/rattle	MoC excavation	2013/2/5-F		IA	16,95	medium
43	SEALIP/MY/HL29/1	Halin HL29	Consumption artefact	pseudo spear head	MoC excavation	2013/2/1		?	18,6	low
44	SEALIP/MY/HL29/2	Halin HL29	Consumption artefact	pseudo spear head	MoC excavation	2013/2/2		?	20,25	low
45	SEALIP/MY/HL29/3	Halin HL29	Consumption artefact	pseudo spear head	MoC excavation	2013/2/8		?	13,45	low
46	SEALIP/MY/HL29/4	Halin HL29	Consumption artefact	axe	MoC excavation	2013/2/6		?	243,8	medium
47	SEALIP/MY/HL29/5	Halin HL29	Consumption artefact	axe	MoC excavation	2013/2/7		?	243,15	high
48	SEALIP/MY/HL29/6	Halin HL29	Consumption artefact	asymmetric curved axe	HL29 Burial 14	2006	2016/2/38	?	243	
49	SEALIP/MY/HL29/7	Halin HL29	Consumption artefact	spearhead	HL29 Burial 8 Skeleton 11	2001	2016/2/34	?	216	
50	SEALIP/MY/HL29/8	Halin HL29	Consumption artefact	spearhead	HL29 Burial 6 Skeleton 14	2005	2016/2/39	?	230	
51	SEALIP/MY/HL29-1/1	Halin HL29-1	Consumption artefact	bangle	B12, Context 1043	1540		BA	2,45	high
52	SEALIP/MY/HL29-1/2	Halin HL29-1	Consumption artefact	bangle	B12, Context 1043, A	1541a		BA	4,9	high
53	SEALIP/MY/HL29-1/3	Halin HL29-1	Consumption artefact	bangle	B12, Context 1043, B	1541b		BA	4,5	high
54	SEALIP/MY/HL29-1/4	Halin HL29-1	Consumption artefact	bangle (double line)	B12, Context 1043, C	1541c		BA	4,05	high
55	SEALIP/MY/HL29-1/5	Halin HL29-1	Consumption artefact	axe	B30, Context 1076	1659		BA	214,85	low
56	SEALIP/MY/HL29-1/6	Halin HL29-1	Consumption artefact	flat ring	B28, Context 1080	1648		BA	29,5	low
57	SEALIP/MY/HL29-1/7	Halin HL29-1	Consumption artefact	ring	B1, Context 1021	1506		Bagan	47	low
58	SEALIP/MY/HL29-1/8	Halin HL29-1	Consumption artefact	spiral square section ring	Jar burial, Context 1018	-		Bagan	1,262	
60	SEALIP/MY/HL30-1/1	Halin HL30-1	Consumption artefact	ring	HL30-1/7027	7539		IA	2,6	
61	SEALIP/MY/HLTP1/1	Halin HLTP1	Consumption artefact	platy fragment	HL-TP1/4001			Bagan		high
62	SEALIP/MY/HLTP1/2	Halin HLTP1	Consumption artefact	ring fragment	HL-TP1/6519			Bagan		high
63	SEALIP/MY/MLW/1	Maliwan	Consumption artefact	fragment	TP6/6003			IA		low
64	SEALIP/MY/MLW/2	Maliwan	Consumption artefact	fragment	TP6/6003			IA		low
65	SEALIP/MY/MLW/3	Maliwan	Consumption artefact	fragment	TP6/6003			IA		low
	* only MAFM-excavated samples have radiometric dating									

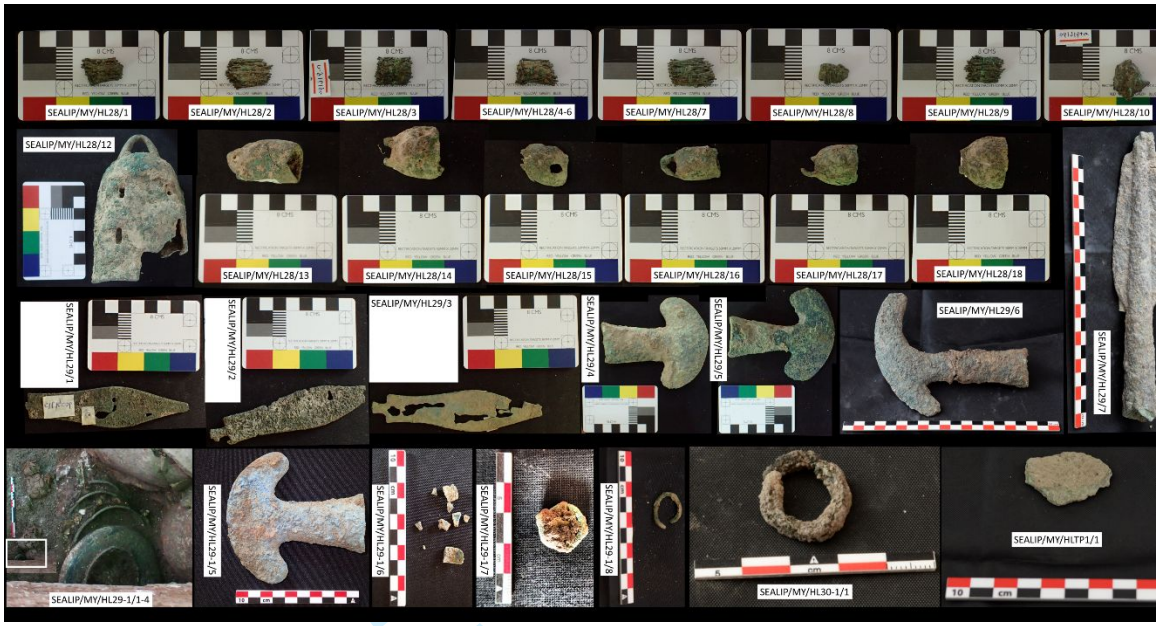

Figure 5: The study's archaeological artefacts. Please note missing image for SEALIP/MY/HLTP1/2.

Methodology

Optical Microscopy (OM)

The metal samples were mounted in epoxy resin, ground with silicon carbide paper (from 800 to 4000 grits) and then polished using diamond suspensions (1 and 0.25 µm). After etching with alcoholic ferric chloride, microstructural evidence for thermo-mechanical treatments was investigated using an optical microscope (Leica DLLM). Mineral samples were not studied by OM.

X-ray Fluorescence (XRF)

XRF was used for the OM samples' bulk elemental composition of major, minor and (some) trace elements, conducted at the *Laboratoire Archéomatériaux et Prévision de l'Altération* (LAPA-IRAMAT/CEA) in Saclay, France. XRF data were acquired using a NITON XL 3t GOLDD+ portable XRF analyser in 'laboratory mode' (fixed stand), with a max 40 kV accelerating voltage in the 'alloys' mode. Accuracy and precision were assessed with eleven Certified Reference Materials (Table 2). Good results for majors and minor components were confirmed but note that light elements at low concentrations like phosphorous, silicon, aluminium, magnesium and sulphur were not reliably detected due to non-vacuum conditions. The analyses were performed on the OM mounted and polished sections using a 3 mm beam diameter, which allowed for reliable results as long as the sample was larger than this. Three such spot analyses were made for each sample to account for corrosion and inclusions.

Scanning Electron Microscopy with Energy Dispersive Spectrometry (SEM-EDS)

Small and/or corroded OM/XRF samples were carbon coated for analysis in a JEOL 7001F instrument, in order to establish the bulk composition of samples less 3 mm in diameter, those with intergranular corrosion, and to study any inclusions. Both secondary electron (SE) and backscattered electron (BSE) modes were used, using a 20 kV accelerating voltage, a 10 mm working distance with an Oxford Silicon Drift Detector, and processed using Oxford Instruments Aztec software.

The detection limit was fixed at 0.5 wt.% with a count rate of 4000/s (detection time of 40 s), which gave good spectral resolution with respect to background noise. We consider the relative quantification error (2 σ) is circa 10% of the measured value. SEM-EDS accuracy was evaluated using the same CRMs as used for the pXRF analysis, and we obtained good results for the major elements (Table 2). Bulk compositions for each sample were obtained by a mean of 3-4 areas scan (0.4 mm^2) per sample. The analyses were performed in areas without corrosion products, when possible.

Table 2: CRMs for the present study, as analysed with pXRF, SEM-EDS and with certified values given. Data given to 1d.p.

SAMPLE	Sb	Sn	Bi	Pb	Zn	Cu	Ni	Co	Fe	Mn	Al	S
B10 pXRF	1,2	7,2	*bdl*	4,1	2,9	83,2	1,1	*bdl*	0,2	*bdl*	*bdl*	*bdl*
B10 SEM-EDS	1,7	6,6	*bdl*	3,6	3,0	82,7	1,0	*bdl*	*bdl*	*bdl*	*bdl*	*bdl*
B10 certified value	1,1	7,0	0,0	4,1	2,8	83,7	1,0	0,0	0,2	0,0	0,2	0,0
B12 pXRF	0,1	10,1	*bdl*	0,2	0,7	85,2	2,8	*bdl*	0,2	0,2	*bdl*	*bdl*
B12 SEM-EDS	*bdl*	9,5	*bdl*	*bdl*	0,9	84,9	3,1	*bdl*	*bdl*	*bdl*	*bdl*	*bdl*
B12 certified value	0,1	9,6	0,0	0,2	0,6	85,7	2,6	0,0	0,2	0,2	0,1	0,0
51.13-4 pXRF	*bdl*	0,3	*bdl*	0,1	0,4	91,0	*bdl*	*bdl*	1,9	0,9	4,9	*bdl*
51.13-4 SEM-EDS	*bdl*	*bdl*	*bdl*	*bdl*	0,7	87,7	*bdl*	*bdl*	1,9	1,1	7,8	*bdl*
51.13-4 certified value	0,0	0,3	0,0	0,0	0,3	88,8	0,1	0,0	1,8	0,9	7,3	0,0
71.32-4 pXRF	0,3	6,4	*bdl*	4,3	7,1	80,5	0,8	*bdl*	0,4	*bdl*	*bdl*	*bdl*
71.32-4 SEM-EDS	*bdl*	6,4	*bdl*	3,1	7,3	81,8	0,8	*bdl*	0,4	*bdl*	*bdl*	*bdl*
71.32-4 certified value	0,3	6,5	0,1	4,4	6,5	80,5	0,7	0,0	0,4	0,1	0,1	0,0
SRM-500 pXRF	*bdl*	*bdl*	*bdl*	*bdl*	0,1	99,7	0,1	*bdl*	*bdl*	*bdl*	*bdl*	*bdl*
SRM-500 SEM-EDS	*bdl*	*bdl*	*bdl*	*bdl*	0,4	99,4	*bdl*	*bdl*	*bdl*	*bdl*	*bdl*	*bdl*
SRM-500 certified value	0,0	0,0	0,0	0,0	0,0	99,7	0,1	0,0	0,0	0,0	0,0	0,0
C1123 pXRF	*bdl*	*bdl*	*bdl*	*bdl*	*bdl*	97,4	*bdl*	2,5	*bdl*	*bdl*	*bdl*	*bdl*
C1123 SEM-EDS	*bdl*	*bdl*	*bdl*	*bdl*	*bdl*	96,5	*bdl*	3,4	*bdl*	*bdl*	*bdl*	*bdl*
C1123 certified value	0,0	0,0	0,0	0,0	0,0	97,4	0,0	2,3	0,0	0,0	0,0	0,0
SRM1275 pXRF	*bdl*	*bdl*	*bdl*	*bdl*	*bdl*	86,9	10,7	*bdl*	1,6	0,4	*bdl*	*bdl*
SRM1275 SEM-EDS	*bdl*	*bdl*	*bdl*	*bdl*	*bdl*	87,9	10,1	*bdl*	1,5	0,5	*bdl*	*bdl*
SRM1275 certified value	0,0	0,0	0,0	0,0	0,1	88,2	9,8	0,0	1,5	0,4	0,0	0,0
L-20-1 pXRF	*bdl*	0,5	*bdl*	0,3	14,4	84,2	0,2	*bdl*	*bdl*	0,1	*bdl*	*bdl*
L-20-1 SEM-EDS	*bdl*	0,5	*bdl*	*bdl*	14,6	84,0	*bdl*	*bdl*	*bdl*	*bdl*	*bdl*	*bdl*
L-20-1 certified value	0,0	0,5	0,0	0,3	13,3	85,2	0,2	0,0	0,0	0,1	0,1	0,0
B21 pXRF	0,2	5,3	*bdl*	3,7	6,5	82,2	1,3	*bdl*	0,3	*bdl*	*bdl*	*bdl*
B21 SEM-EDS	*bdl*	5,2	*bdl*	3,9	7,0	82,2	1,3	*bdl*	*bdl*	*bdl*	*bdl*	*bdl*
B21 certified value	0,2	5,1	0,0	3,8	6,2	83,0	1,2	0,0	0,3	0,0	0,1	0,0
B31 pXRF	0,5	8,0	*bdl*	10,6	0,8	79,4	0,6	*bdl*	*bdl*	*bdl*	*bdl*	*bdl*
B31 SEM-EDS	1,8	8,0	*bdl*	9,9	1,1	78,6	0,5	*bdl*	*bdl*	*bdl*	*bdl*	*bdl*
B31 certified value	0,5	7,7	0,0	11,8	0,8	78,6	0,5	0,0	0,0	0,0	0,0	0,0
UZ-52-3 pXRF	0,1	1,0	*bdl*	0,1	18,0	80,3	0,1	*bdl*	0,3	*bdl*	*bdl*	*bdl*
UZ-52-3 SEM-EDS	*bdl*	1,0	*bdl*	*bdl*	18,2	80,2	*bdl*	*bdl*	*bdl*	*bdl*	*bdl*	*bdl*
UZ-52-3 certified value	0,1	1,1	0,0	0,1	17,0	81,1	0,1	0,0	0,3	0,0	0,0	0,0

Multi Collector – Inductively Coupled Plasma – Mass Spectrometer (MC-ICP-MS)

Lead isotope analysis (LIA) was conducted at the *Service d'Analyse des Roches et des Minéraux* of the Centre for Petrographic and Geochemical Research (SARM-CRPG) in Nancy, France, using MC-ICP-MS after lead extraction (Manhes *et al.* 1980). Thallium NIST SRM 997 was used to correct for instrumental mass bias and all parameters were adjusted to obtain the closest values relative to NIST SRM 981, as determined by DSTIMS (Thirlwall 2002). More details about SARM-CRPG lead isotope analysis are available in (Aebischer *et al.* 2015; Cloquet *et al.* 2006).

As per the SEALIP/BROGLASEA programmes, LIA was used to look for 'consistency' with known and characterised production systems, in recognition that there could be other, as yet uncharacterised, primary and/or secondary production systems, as well as mixing, alloying and recycling impacting interpretation (e.g. Budd et al., 1993; Pryce et al., 2014, 2011b; Wilson and Pollard, 2001). These consistencies were judged by proximity of data points on $^{208}Pb/^{204}Pb$ vs $^{206}Pb/^{204}Pb$ and $^{207}Pb/^{204}Pb$ vs $^{206}Pb/^{204}Pb$ biplots for traditional manual interpretation.

Complex networks analysis

As this paper will evoke with examples from the internally-manageable Myanma LI datasets, manual LI interpretation is unsuited to detecting pertinent anthropological patterning in very large datasets. Therefore, the available LI data for all Bronze Age metal objects, ores and slags from MSEA and southern China were processed using a complex networks analysis approach termed 'community detection' (or modularity analysis). Previous applications in southeastern Europe used the 'Louvain' algorithm (Radivojević & Grujić 2018) as applied to elemental data but here we opted for an improved 'Leiden' algorithm (Traag *et al.* 2019) for our LI data, although both Louvain and Leiden algorithms present similar robustness on archaeological data (Grujić & Radivojević forthcoming). Our application of complex networks analysis in this paper is novel and required substantial method development, which will be detailed in the discussion (and available at https://github.com/simoncarrignon/bronze-age-ssr). We do not consider our method definitive but do contest that it is offering reliable and archaeologically/geochemically-justified preliminary rationalisations of large datasets that merits dissemination at this juncture.

Our current protocol requires a definition of 'consistency' for lead isotope ratios that takes into account Southeast Asia's and southern China's high geological diversity as well as the variability of known prehistoric copper production LI signatures. For each of the three ^{204}Pb-denominated ratios (those most geologically sensitive), the difference between any pair of artefacts' LI ratios must be as small or smaller than our production-defined thresholds in ordered to be considered *potentially* consistent – i.e. subject to human evaluation of the algorithmic proposition. Applying this measure to the whole dataset allows us firstly to identify groups/modules of artefacts that exhibit the strongest connections within the group and weaker connections outside of it, as outlined by Radivojević & Grujić (2018). Secondly we calculate the same strength/weakness of connectivity but now between sites/assemblages, using the principle that if a high density of artefacts from sites belong to the same module, those sites *potentially* share a meaningful link.

Results

To save space, only new Myanma data are presented in text but will be considered with reference to previous national datasets (calculations available online at https://github.com/simoncarrignon/bronze-age-ssr, see also Dussubieux & Pryce 2016; Pryce *et al.* 2018a; 2014).

Table 3: Elemental compositions for metal and mineral samples, and working techniques for metal samples. SEM-EDS and pXRF data are given to 1d.p..

#	Sample	Site	Object	O	Ba	Sb	Sn	Cd	Pd	Ag	Ru	Mo	Nb	Zr	Bi	Pb	Se	As	Au	W	Zn	Cu	Ni	Co	Fe	Mn	Cr	V	Ti	Al	S	Cl	P	Si	Mg	Analytical total	Analytical technique	Corrosion products	Probable alloy	Working techniques
1	SEALIP/MY/HL28/1	Halin HL28	wire bundle	4,7	bdl	bdl	bdl	bdl	bdl	bdl	bdl	bdl	bdl	bdl	bdl	bdl	bdl	bdl	bdl	bdl	bdl	93,4	bdl	bdl	0,2	bdl	bdl	bdl	bdl	1,4	0,3	bdl	0,1	bdl	100,0	SEM-EDS	Medium	copper	As cast
2	SEALIP/MY/HL28/2	Halin HL28	wire bundle	bdl	bdl	bdl	bdl	bdl	bdl	bdl	0,0	0,0	bdl	bdl	bdl	bdl	bdl	0,0	bdl	bdl	bdl	99,1	bdl	bdl	0,8	bdl	bdl	bdl	bdl	bdl	bdl	bdl	bdl	bdl	bdl	100,0	pXRF	Low	copper	As cast
3	SEALIP/MY/HL28/3	Halin HL28	wire bundle	1,2	bdl	bdl	bdl	bdl	bdl	bdl	bdl	bdl	bdl	bdl	bdl	bdl	bdl	bdl	bdl	bdl	bdl	97,5	bdl	bdl	0,4	bdl	bdl	bdl	bdl	bdl	0,9	bdl	bdl	0,0	bdl	100,0	SEM-EDS	Low	copper	As cast
4	SEALIP/MY/HL28/4	Halin HL28	wire bundle multi	bdl	bdl	bdl	bdl	bdl	bdl	bdl	0,0	bdl	bdl	bdl	bdl	bdl	bdl	0,0	bdl	bdl	bdl	99,5	bdl	bdl	0,4	bdl	bdl	bdl	bdl	bdl	bdl	bdl	bdl	bdl	bdl	100,0	pXRF	Low	copper	As cast
5	SEALIP/MY/HL28/5	Halin HL28	wire bundle multi	bdl	bdl	bdl	bdl	bdl	bdl	bdl	0,0	bdl	bdl	bdl	bdl	bdl	bdl	0,0	bdl	bdl	bdl	98,8	bdl	bdl	0,4	bdl	bdl	bdl	bdl	bdl	0,8	bdl	bdl	bdl	bdl	99,9	pXRF	Low	copper	As cast
6	SEALIP/MY/HL28/6	Halin HL28	wire bundle multi	bdl	bdl	bdl	bdl	bdl	bdl	bdl	bdl	bdl	bdl	bdl	bdl	bdl	bdl	0,0	bdl	bdl	bdl	97,5	bdl	bdl	0,5	bdl	bdl	bdl	bdl	bdl	1,2	bdl	bdl	0,8	bdl	100,0	pXRF	Low	copper	As cast
7	SEALIP/MY/HL28/7	Halin HL28	wire bundle	bdl	bdl	bdl	bdl	bdl	bdl	bdl	0,0	0,0	bdl	bdl	bdl	bdl	bdl	0,0	bdl	bdl	bdl	99,5	bdl	bdl	0,4	bdl	bdl	bdl	bdl	bdl	bdl	bdl	bdl	bdl	bdl	100,0	pXRF	Low	copper	As cast
8	SEALIP/MY/HL28/8	Halin HL28	wire bundle	1,2	bdl	bdl	bdl	bdl	bdl	bdl	bdl	bdl	bdl	bdl	bdl	bdl	bdl	bdl	bdl	bdl	bdl	97,2	bdl	bdl	0,5	bdl	bdl	bdl	bdl	bdl	1,1	bdl	bdl	0,1	bdl	100,0	SEM-EDS	Low	copper	As cast
9	SEALIP/MY/HL28/9	Halin HL28	wire bundle	1,8	bdl	bdl	bdl	bdl	bdl	bdl	bdl	bdl	bdl	bdl	bdl	bdl	bdl	bdl	bdl	bdl	bdl	96,1	bdl	bdl	0,3	bdl	bdl	bdl	bdl	bdl	1,1	0,4	bdl	0,3	bdl	100,0	SEM-EDS	Low	copper	As cast
10	SEALIP/MY/HL28/10	Halin HL28	possible casting spillage	17,5	bdl	bdl	15,7	bdl	bdl	bdl	bdl	bdl	bdl	bdl	bdl	bdl	bdl	bdl	bdl	bdl	bdl	66,3	bdl	bdl	bdl	bdl	bdl	bdl	bdl	bdl	bdl	bdl	bdl	0,4	0,1	0,2	100,2	SEM-EDS	High	bronze	As cast
11	SEALIP/MY/HL28/11	Halin HL28	wire bundle	bdl	bdl	bdl	bdl	bdl	bdl	bdl	0,0	0,0	bdl	bdl	bdl	bdl	bdl	0,0	bdl	bdl	bdl	99,2	bdl	bdl	0,8	bdl	bdl	bdl	bdl	bdl	bdl	bdl	bdl	bdl	bdl	100,0	pXRF	Low	copper	As cast
12	SEALIP/MY/HL28/12	Halin HL28	large bell/rattle	bdl	bdl	bdl	4,5	bdl	bdl	bdl	bdl	0,0	0,0	bdl	bdl	bdl	bdl	0,0	bdl	bdl	bdl	92,7	bdl	bdl	0,1	bdl	bdl	bdl	bdl	bdl	bdl	bdl	bdl	2,6	bdl	100,0	pXRF	Medium	bronze	As cast
13	SEALIP/MY/HL28/13	Halin HL28	small bell/rattle	bdl	bdl	bdl	bdl	bdl	bdl	bdl	bdl	0,1	0,1	bdl	bdl	bdl	bdl	bdl	bdl	bdl	bdl	99,4	bdl	bdl	bdl	bdl	bdl	bdl	bdl	bdl	bdl	bdl	bdl	bdl	bdl	99,6	pXRF	Low	copper	Hammered/annealed
14	SEALIP/MY/HL28/14	Halin HL28	small bell/rattle	bdl	bdl	bdl	4,2	bdl	bdl	bdl	bdl	bdl	bdl	bdl	bdl	bdl	bdl	bdl	bdl	bdl	bdl	80,3	bdl	bdl	bdl	bdl	bdl	bdl	bdl	bdl	bdl	bdl	bdl	bdl	bdl	84,5	SEM-EDS	High	bronze	As cast
15	SEALIP/MY/HL28/15	Halin HL28	small bell/rattle	bdl	bdl	bdl	4,2	bdl	bdl	bdl	bdl	bdl	bdl	bdl	bdl	bdl	bdl	bdl	bdl	bdl	bdl	83,4	bdl	bdl	bdl	bdl	bdl	bdl	bdl	bdl	bdl	bdl	bdl	bdl	bdl	87,6	SEM-EDS	High	bronze	As cast
16	SEALIP/MY/HL28/16	Halin HL28	small bell/rattle	bdl	bdl	bdl	1,2	bdl	bdl	bdl	bdl	0,0	0,0	bdl	bdl	bdl	bdl	0,0	bdl	bdl	bdl	98,0	bdl	bdl	bdl	bdl	bdl	bdl	bdl	bdl	bdl	bdl	bdl	bdl	0,7	100,0	pXRF	Medium	bronze	As cast
17	SEALIP/MY/HL28/17	Halin HL28	small bell/rattle	bdl	bdl	bdl	11,0	bdl	bdl	bdl	bdl	0,0	0,0	0,0	bdl	bdl	bdl	0,0	bdl	bdl	bdl	88,2	bdl	bdl	bdl	bdl	bdl	bdl	bdl	bdl	bdl	bdl	bdl	bdl	0,6	100,0	pXRF	Medium	bronze	As cast
18	SEALIP/MY/HL28/18	Halin HL28	small bell/rattle	bdl	bdl	bdl	6,2	bdl	bdl	bdl	bdl	bdl	bdl	bdl	bdl	bdl	bdl	bdl	bdl	bdl	bdl	80,1	bdl	bdl	bdl	bdl	bdl	bdl	bdl	bdl	bdl	bdl	bdl	bdl	0,6	86,9	SEM-EDS	High	bronze	As cast
19	SEALIP/MY/HL29/1	Halin HL29	pseudo spear head	bdl	bdl	bdl	1,5	bdl	bdl	bdl	bdl	bdl	bdl	bdl	bdl	bdl	bdl	bdl	bdl	bdl	bdl	97,8	bdl	bdl	bdl	bdl	bdl	bdl	bdl	bdl	bdl	bdl	bdl	bdl	bdl	99,3	SEM-EDS	High	bronze	As cast
20	SEALIP/MY/HL29/2	Halin HL29	pseudo spear head	bdl	bdl	bdl	bdl	bdl	bdl	bdl	bdl	bdl	bdl	bdl	bdl	bdl	bdl	0,0	bdl	bdl	bdl	96,7	bdl	bdl	1,7	bdl	bdl	bdl	bdl	bdl	0,2	bdl	bdl	1,3	bdl	100,0	pXRF	Low	copper	As cast
21	SEALIP/MY/HL29/3	Halin HL29	pseudo spear head	bdl	bdl	bdl	bdl	bdl	bdl	bdl	bdl	bdl	bdl	bdl	bdl	0,1	bdl	0,0	bdl	bdl	bdl	99,5	bdl	bdl	0,5	bdl	bdl	bdl	bdl	bdl	bdl	bdl	bdl	bdl	bdl	100,1	pXRF	Low	copper	As cast
22	SEALIP/MY/HL29/4	Halin HL29	axe	20,2	bdl	bdl	5,4	bdl	bdl	bdl	bdl	bdl	bdl	bdl	bdl	bdl	bdl	bdl	bdl	bdl	bdl	63,6	bdl	bdl	bdl	bdl	bdl	bdl	bdl	bdl	bdl	bdl	bdl	10,6	0,1	bdl	100,0	SEM-EDS	High	bronze	As cast
23	SEALIP/MY/HL29/5	Halin HL29	axe	50,2	bdl	bdl	bdl	bdl	bdl	bdl	bdl	bdl	bdl	bdl	bdl	bdl	bdl	bdl	bdl	bdl	bdl	7,3	bdl	bdl	5,3	bdl	bdl	bdl	bdl	8,1	bdl	0,5	bdl	22,6	2,2	96,2	SEM-EDS	High	copper	Corroded
24	SEALIP/MY/HL29/6	Halin HL29	asymmetric curved axe	bdl	bdl	bdl	11,4	bdl	bdl	bdl	bdl	bdl	bdl	bdl	bdl	bdl	bdl	bdl	bdl	bdl	bdl	88,1	0,0	bdl	0,0	bdl	bdl	bdl	bdl	bdl	bdl	bdl	bdl	bdl	bdl	99,6	pXRF	High	bronze	As cast
25	SEALIP/MY/HL29/7	Halin HL29	spearhead	bdl	bdl	bdl	15,9	bdl	bdl	bdl	bdl	bdl	bdl	bdl	bdl	0,6	bdl	bdl	bdl	bdl	bdl	82,9	bdl	bdl	bdl	bdl	0,1	0,0	0,1	bdl	bdl	bdl	bdl	bdl	bdl	99,6	pXRF	High	bronze	As cast
26	SEALIP/MY/HL29/8	Halin HL29	spearhead	bdl	bdl	bdl	5,2	bdl	bdl	bdl	bdl	bdl	0,1	bdl	bdl	0,4	bdl	bdl	bdl	bdl	bdl	91,5	bdl	bdl	1,6	bdl	0,1	0,1	0,3	bdl	bdl	bdl	bdl	bdl	bdl	99,3	pXRF	High	bronze	Corroded
27	SEALIP/MY/HL29-1/1	Halin HL29-1	bangle	bdl	bdl	bdl	10,8	0,1	bdl	bdl	bdl	bdl	bdl	bdl	bdl	0,4	bdl	0,1	bdl	bdl	0,3	87,1	bdl	bdl	1,0	bdl	bdl	bdl	bdl	bdl	bdl	bdl	bdl	0,3	bdl	100,0	pXRF	Medium	bronze	As cast
28	SEALIP/MY/HL29-1/2	Halin HL29-1	bangle	bdl	bdl	bdl	9,8	bdl	bdl	bdl	bdl	bdl	bdl	bdl	bdl	0,2	bdl	0,1	bdl	bdl	0,1	87,1	bdl	bdl	2,3	bdl	bdl	bdl	bdl	bdl	0,1	bdl	bdl	0,2	bdl	100,0	pXRF	Medium	bronze	Annealed
29	SEALIP/MY/HL29-1/3	Halin HL29-1	bangle	bdl	bdl	bdl	8,6	bdl	bdl	bdl	bdl	bdl	bdl	bdl	0,0	0,1	bdl	0,1	bdl	bdl	0,1	90,9	bdl	bdl	0,1	bdl	bdl	bdl	bdl	bdl	bdl	bdl	bdl	0,1	bdl	100,0	pXRF	Medium	bronze	Hammered
30	SEALIP/MY/HL29-1/4	Halin HL29-1	bangle (double line)	bdl	bdl	bdl	6,9	bdl	bdl	bdl	bdl	0,0	bdl	bdl	bdl	0,3	bdl	0,1	bdl	bdl	0,4	86,4	bdl	0,0	4,3	bdl	bdl	bdl	bdl	bdl	bdl	bdl	bdl	1,7	bdl	100,0	pXRF	Medium	bronze	Hammered/annealed
31	SEALIP/MY/HL29-1/5	Halin HL29-1	axe	16,4	bdl	bdl	6,5	bdl	bdl	bdl	bdl	bdl	bdl	bdl	bdl	bdl	bdl	bdl	bdl	bdl	bdl	73,3	bdl	bdl	bdl	bdl	bdl	bdl	0,1	1,2	0,9	1,1	1,0	bdl	100,4	SEM-EDS	High	bronze	Corroded
32	SEALIP/MY/HL29-1/6	Halin HL29-1	flat ring	bdl	bdl	bdl	2,0	bdl	bdl	bdl	bdl	0,0	bdl	bdl	bdl	0,1	bdl	bdl	bdl	bdl	0,1	97,9	bdl	bdl	bdl	bdl	bdl	bdl	bdl	bdl	bdl	bdl	bdl	bdl	bdl	100,0	pXRF	Low	bronze	Hammered/annealed
33	SEALIP/MY/HL29-1/7	Halin HL29-1	spiral square section ring	bdl	bdl	bdl	5,8	bdl	bdl	bdl	bdl	bdl	bdl	bdl	0,0	0,1	bdl	0,1	bdl	bdl	0,1	93,9	bdl	bdl	0,1	bdl	bdl	bdl	bdl	bdl	bdl	bdl	bdl	bdl	bdl	100,0	pXRF	Medium	bronze	As cast
34	SEALIP/MY/HL29-1/8	Halin HL29-1	ring	bdl	bdl	0,1	bdl	bdl	bdl	bdl	bdl	bdl	bdl	bdl	bdl	1,5	bdl	bdl	bdl	bdl	bdl	96,4	bdl	bdl	0,1	bdl	0,1	0,0	0,0	bdl	bdl	bdl	bdl	bdl	bdl	98,4	pXRF	Low	leaded copper	Hammered/annealed
35	SEALIP/MY/HL30-1/1	Halin HL30-1	ring	bdl	bdl	bdl	9,5	bdl	bdl	bdl	bdl	bdl	bdl	bdl	bdl	0,2	bdl	bdl	bdl	bdl	bdl	89,3	bdl	bdl	0,6	bdl	bdl	bdl	bdl	bdl	bdl	bdl	bdl	bdl	bdl	99,7	pXRF	High	bronze	As cast
36	SEALIP/MY/HLTP1/1	Halin HLTP1	platy fragment	bdl	bdl	1,5	29,3	bdl	bdl	bdl	bdl	bdl	bdl	bdl	bdl	0,1	bdl	bdl	bdl	bdl	bdl	67,6	bdl	bdl	0,8	bdl	bdl	bdl	0,2	bdl	bdl	bdl	bdl	bdl	bdl	99,5	pXRF	High	bronze	Corroded
37	SEALIP/MY/HLTP1/2	Halin HLTP1	ring fragment	bdl	bdl	0,4	bdl	bdl	bdl	bdl	bdl	bdl	bdl	0,0	0,1	1,4	bdl	bdl	bdl	bdl	0,1	97,1	bdl	bdl	0,1	bdl	0,1	0,0	bdl	bdl	bdl	bdl	bdl	bdl	bdl	99,3	pXRF	Low	leaded copper	Hammered/annealed
38	SEALIP/MY/MLW/1	Maliwan	fragment	bdl	bdl	0,1	7,6	bdl	bdl	bdl	bdl	bdl	bdl	0,0	0,1	13,4	bdl	0,5	bdl	bdl	bdl	78,1	0,1	bdl	bdl	bdl	bdl	bdl	0,1	bdl	bdl	bdl	bdl	bdl	bdl	100,0	pXRF	Low	leaded bronze	As cast
39	SEALIP/MY/MLW/2	Maliwan	fragment	bdl	bdl	0,7	19,4	bdl	bdl	bdl	bdl	bdl	bdl	bdl	0,1	3,5	bdl	0,6	0,0	bdl	bdl	75,0	0,1	0,1	0,4	bdl	bdl	bdl	0,1	bdl	bdl	bdl	bdl	bdl	bdl	100,1	pXRF	Medium	leaded bronze	As cast
40	SEALIP/MY/MLW/3	Maliwan	fragment	bdl	bdl	bdl	0,1	bdl	bdl	bdl	bdl	bdl	bdl	0,0	0,7	0,0	bdl	0,0	bdl	bdl	bdl	98,4	bdl	bdl	0,1	bdl	bdl	bdl	bdl	bdl	0,8	bdl	bdl	bdl	bdl	100,0	pXRF	Medium	copper	As cast
41	SEALIP/MY/BAW/1	Baw Mountain, Kyaukse	Cu mineral	72,4	4,6	0,2	bdl	bdl	bdl	bdl	bdl	bdl	bdl	bdl	bdl	0,1	bdl	0,1	bdl	bdl	bdl	3,3	bdl	bdl	0,3	0,1	bdl	bdl	bdl	bdl	6,4	bdl	bdl	12,3	bdl	99,7	pXRF		Mineral	
42	SEALIP/MY/BAW/2	Baw Mountain, Kyaukse	Cu mineral	60,8	2,4	0,5	bdl	bdl	bdl	bdl	bdl	bdl	bdl	bdl	bdl	0,9	bdl	0,6	bdl	bdl	bdl	5,4	bdl	bdl	0,7	bdl	bdl	bdl	bdl	bdl	0,3	3,0	bdl	bdl	24,9	bdl	99,7	pXRF		Mineral	
43	SEALIP/MY/BAW/3	Baw Mountain, Kyaukse	Cu mineral	55,5	0,1	0,3	bdl	bdl	bdl	bdl	bdl	bdl	bdl	bdl	bdl	bdl	bdl	0,2	bdl	bdl	0,5	1,4	bdl	bdl	1,5	bdl	bdl	bdl	bdl	0,3	5,8	bdl	bdl	33,5	bdl	99,1	pXRF		Mineral	
44	SEALIP/MY/BWD/1	Bawdwin	Cu mineral	bdl	bdl	bdl	0,1	bdl	bdl	bdl	bdl	bdl	bdl	bdl	bdl	42,9	bdl	3,6	bdl	bdl	0,2	37,0	0,5	0,3	0,1	0,1	bdl	bdl	bdl	bdl	13,2	bdl	bdl	1,3	bdl	99,3	pXRF		leaded copper	
45	SEALIP/MY/BWD/2	Bawdwin	Cu mineral																																				Mineral	
46	SEALIP/MY/KAW/1	Kawlin	Cu mineral	7,4	bdl	bdl	bdl	bdl	bdl	bdl	bdl	bdl	bdl	bdl	bdl	bdl	bdl	0,1	bdl	bdl	bdl	27,0	bdl	bdl	26,0	bdl	bdl	bdl	bdl	bdl	32,2	bdl	bdl	6,7	bdl	99,3	pXRF		Mineral	
47	SEALIP/MY/KAW/2	Kawlin	Cu mineral	bdl	bdl	0,2	bdl	bdl	bdl	bdl	bdl	bdl	bdl	bdl	bdl	bdl	bdl	2,1	bdl	bdl	bdl	26,7	bdl	bdl	22,8	0,2	bdl	bdl	bdl	bdl	29,4	bdl	bdl	14,9	bdl	96,4	pXRF		Mineral	
48	SEALIP/MY/KAW/3	Kawlin	Cu mineral	15,3	bdl	bdl	bdl	bdl	0,1	bdl	bdl	bdl	bdl	bdl	bdl	bdl	bdl	0,1	bdl	bdl	bdl	18,3	bdl	bdl	21,1	1,5	bdl	bdl	bdl	bdl	23,1	bdl	bdl	19,8	bdl	99,3	pXRF		Mineral	
49	SEALIP/MY/MIN/1	Mingan	Cu mineral	68,2	bdl	bdl	bdl	bdl	bdl	bdl	bdl	bdl	bdl	bdl	bdl	bdl	bdl	bdl	bdl	bdl	bdl	0,6	bdl	bdl	0,7	bdl	bdl	bdl	bdl	1,5	bdl	bdl	bdl	28,7	bdl	99,7	pXRF		Mineral	
50	SEALIP/MY/MIN/2	Mingan	Cu mineral	53,1	bdl	bdl	bdl	bdl	bdl	bdl	bdl	0,5	bdl	bdl	bdl	bdl	bdl	bdl	bdl	bdl	bdl	9,6	bdl	bdl	3,7	0,6	bdl	bdl	1,4	7,1	bdl	bdl	bdl	20,3	1,7	97,9	pXRF		Mineral	
51	SEALIP/MY/MIN/3	Mingan	Cu mineral	64,9	bdl	bdl	bdl	bdl	bdl	bdl	bdl	bdl	0,2	bdl	bdl	bdl	bdl	bdl	bdl	bdl	bdl	9,4	bdl	bdl	0,6	0,1	bdl	bdl	0,1	6,4	0,1	bdl	bdl	17,9	bdl	99,6	pXRF		Mineral	
52	SEALIP/MY/NTL/1	Nant Twin village	Cu mineral	66,1	bdl	1,9	bdl	bdl	bdl	bdl	bdl	bdl	bdl	bdl	bdl	bdl	bdl	bdl	bdl	bdl	bdl	17,8	bdl	bdl	bdl	bdl	bdl	bdl	bdl	0,3	0,2	bdl	bdl	13,2	bdl	99,5	pXRF		Mineral	
53	SEALIP/MY/NTL/2	Nant Twin village	Cu mineral	58,9	bdl	0,1	bdl	bdl	bdl	bdl	bdl	bdl	bdl	bdl	bdl	0,1	bdl	0,1	bdl	bdl	0,8	15,2	bdl	bdl	0,2	bdl	bdl	bdl	bdl	0,2	0,2	bdl	bdl	24,0	bdl	99,8	pXRF		Mineral	
54	SEALIP/MY/NTL/3	Nant Twin village	Cu mineral	73,0	1,3	0,4	bdl	bdl	bdl	bdl	bdl	bdl	bdl	bdl	bdl	0,1	bdl	bdl	bdl	bdl	0,1	8,7	bdl	bdl	0,1	bdl	bdl	bdl	bdl	0,2	0,2	bdl	bdl	15,8	bdl	99,8	pXRF		Mineral	
55	SEALIP/MY/POHT/1	Pala Dauk Hter Taung	Cu mineral																																				Mineral	
56	SEALIP/MY/POHT/2	Pala Dauk Hter Taung	Cu mineral																																				Mineral	
57	SEALIP/MY/POHT/3	Pala Dauk Hter Taung	Cu mineral																																				Mineral	
58	SEALIP/MY/ST/1	Sabad Taung	Cu mineral																																				Mineral	
59	SEALIP/MY/ST/2	Sabad Taung	Cu mineral																																				Mineral	
60	SEALIP/MY/ST/3	Sabad Taung	Cu mineral																																				Mineral	
61	SEALIP/MY/TKN/1	Thabeik Kyinn	Cu mineral	46,7	0,1	bdl	bdl	bdl	bdl	bdl	bdl	bdl	bdl	bdl	bdl	bdl	bdl	bdl	bdl	bdl	bdl	34,6	bdl	bdl	6,7	bdl	bdl	bdl	bdl	1,9	0,5	bdl	bdl	7,9	bdl	98,4	pXRF		Mineral	
62	SEALIP/MY/TKN/2	Thabeik Kyinn	Cu mineral	55,0	0,4	bdl	bdl	bdl	bdl	bdl	bdl	bdl	bdl	bdl	bdl	bdl	bdl	bdl	bdl	bdl	bdl	29,1	bdl	bdl	6,4	bdl	bdl	bdl	bdl	1,1	0,1	bdl	bdl	6,5	bdl	98,5	pXRF		Mineral	
63	SEALIP/MY/TKN/3	Thabeik Kyinn	Cu mineral	35,6	bdl	bdl	bdl	bdl	bdl	bdl	bdl	bdl	bdl	bdl	bdl	bdl	bdl	bdl	bdl	bdl	bdl	45,8	bdl	bdl	2,9	bdl	bdl	bdl	bdl	1,7	0,1	0,7	bdl	8,1	2,3	97,1	pXRF		Mineral	
64	SEALIP/MY/YTCM/1	Yang Tse Copper	Cu ingot																																				pure copper	

Elemental & OM:

The Halin samples exhibit only three alloy classes (Table 3), using the conventional alloying cutoff of 1 wt. %, with bronze predominating (21), followed by copper (14) and lastly leaded copper (2). Notwithstanding the majority of medium-high corrosion levels (9+13 vs 15 'low') likely obscuring original tin and lead contents, and thus reducing the potential to identify modality in the elemental data, our samples are clearly regionally atypical in that the Iron Age samples are almost all unleaded. This is mainly visible in the HL28 assemblage, which consists in part of wire bundles of a near-pure copper (97-99 wt. % Cu, Sn & Pb not detected), likely representing raw, at most part-refined, product from the smelter, which could have served as highly frangible commodity money (Dussubieux & Pryce 2016), but also of small bronze and copper bells and rattles that would usually be leaded alloys in the MSEA Iron Age, so as to improve castability in a decorative object. The only definitely leaded Halin artefacts are a leaded copper ring from an Iron Age HL29-1 context, and a leaded copper ring fragment from Bagan period HLTP1. Of the Maliwan artefacts, two are leaded bronze and one is copper but the lack of typology does not allow us to assess the suitability of alloy to usage.

In terms of working techniques, the study artefacts are predominantly as cast (29), followed by hammered/annealed (5), hammered (1) and annealed (1), with the remainder (4) too corroded for microstructures to be visible (Figures 6-8). As our majority metal artefact class is that of Iron Age raw copper wires, it is striking that they are all cast, as opposed to drawn or hammered. The Iron Age raw copper pseudo-spearheads were also left as cast, which is commensurate with our interpretation of them as ingots or commodity money, and not weapons or tools. We note that the Bronze Age axes from HL29 and HL29-1 were also as cast or too corroded to tell, whether they were produced in copper or bronze, which suggests they were never thermomechanically-treated for use as tools or weapons, nor work-hardened through use, and were thus possibly produced explicitly for funerary rites (as per Bronze Age Ban Non Wat axes, Pryce 2011). Surprisingly, the only artefacts to present evidence of thermal and/or mechanical treatments are an Iron Age copper bell or rattle from HL28 and a selection of Bronze Age bronze bangles and rings from HL29-1, as well as two Bagan period leaded copper rings from HL29-1 and HLTP-1. The three Maliwan artefacts were as cast but as they are fragmentary we cannot evaluate their original use.

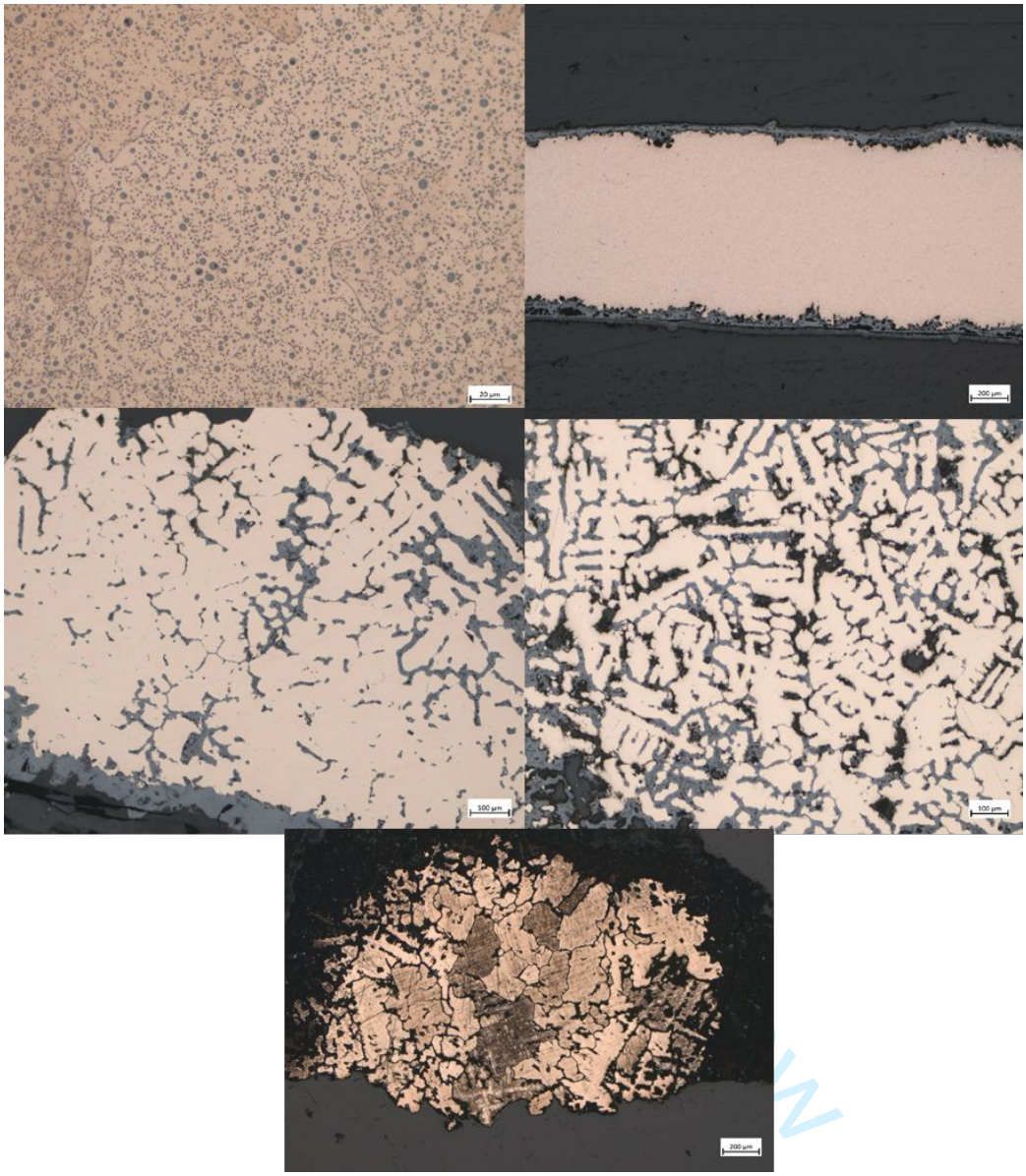

Figure 6: Optical micrographs. Top-left, as cast wire bundle (HL28/2) with round copper sulphide inclusions, top-right, wire bundle (HL28/5), bottom-left bronze cast bell/rattle (HL28/12) and bottom-right bronze as cast bangle (HL29-1/1). Bottom, a bronze ring with an as cast microstructure (HL29-1/7).

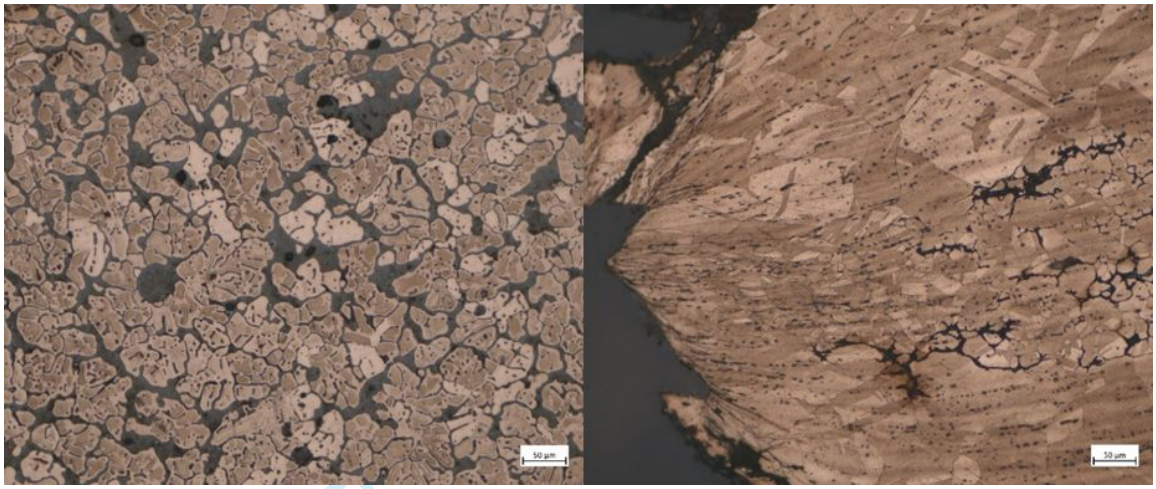

Figure 7: Optical micrographs, after etching. Left, a leaded-copper sample (NYG3/1) with an as cast structure. Right, a copper ring sample (HL29-1/8) which has been hammered and annealed.

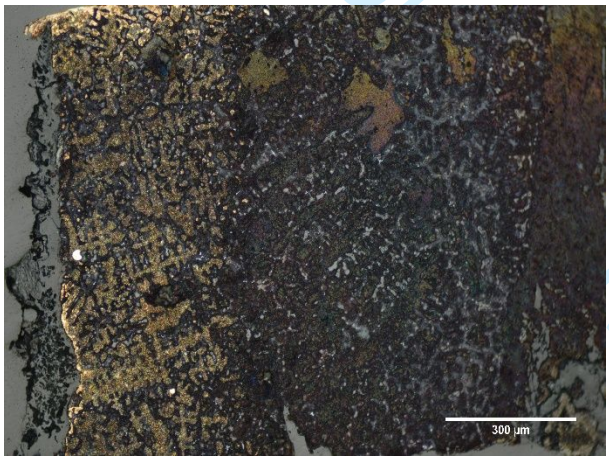

Figure 8: HL28/18 almost entirely composed of corrosion products but with an identifiably as-cast structure.

The Halin elemental results exhibit a low variability when compared with other Myanmar copper-base metal datasets, which reveal six alloy types: two Bronze Age fragments from the Oakaie area approach the threshold of 'arsenical bronze'; one Iron Age bangle from Kokkokhahla composed of arsenical copper; 18 Bronze and Iron Age ornament and tool fragments made from bronze, 17 Iron Age wires and pseudo-spearheads made from copper; one Iron Age high-tin bronze bowl fragment from Supan; one Bronze Age socketed small spearhead or large arrowhead from Nyaung'gan in leaded copper (Pryce *et al.* 2018a: Table 2). As per Halin, there is a clear tendency for Iron Age copper and Bronze Age bronze but again, this is likely to be by virtue of the older artefacts being definite finished products whereas the later wire bundles and pseudo-spearheads appear to constitute a specific aspect of regional funerary tradition, potentially deposits of commodity money (Dussubieux & Pryce 2016).

The lower number of alloy classes at Halin is due to the absence of high-tin bronzes, which are an exotic class in MSEA, likely representing mid-late 1st millennium BC exchange systems with South Asia (Bennett & Glover 2012; Pryce & Bellina 2018). There is only one other high-tin bronze

identified in Myanmar (SEALIP/MY/SP/1 in Pryce *et al.* 2018a) and, given the extensive monumental and textual evidence for Indian influence at Halin, it is probable that such alloys exist there but haven't been excavated and/or identified yet. The other minor alloying constituent apparently absent from Halin is that of arsenic, which we will come back to in light of lead isotope data.

Lead Isotope Analysis:

Table 4: Full raw lead isotope data for the present study samples.

	SEALIP ID	Lab ID	Material type	206Pb/204Pb	err (2σ)	207Pb/204Pb	err (2σ)	208Pb/204Pb	err (2σ)	207Pb/206Pb	err (2σ)	206Pb/207Pb	err (2σ)	208Pb/206Pb	err (2σ)
1	SEALIP/MY/BAW/1	1907566	Mineral	18,428	0,002	15,764	0,002	38,805	0,006	0,856	0,00003	1,1683	0,00003	2,106	0,0001
2	SEALIP/MY/BAW/2	1907567	Mineral	18,425	0,002	15,768	0,001	38,814	0,004	0,856	0,00003	1,1679	0,00003	2,107	0,0006
3	SEALIP/MY/BAW/3	1907568	Mineral	18,433	0,002	15,757	0,001	38,796	0,004	0,855	0,00002	1,1690	0,00002	2,105	0,0010
4	SEALIP/MY/BWD/1	1907569	Mineral	18,385	0,002	15,793	0,002	38,767	0,004	0,859	0,00002	1,1635	0,00002	2,109	0,0001
5	SEALIP/MY/BWD/2	1907570	Mineral	18,391	0,002	15,797	0,002	38,787	0,005	0,859	0,00002	1,1636	0,00002	2,109	0,0001
6	SEALIP/MY/KAW/1	1907571	Mineral	18,306	0,002	15,646	0,002	38,904	0,006	0,855	0,00004	1,1700	0,00004	2,125	0,0002
7	SEALIP/MY/KAW/2	1907572	Mineral	18,305	0,002	15,646	0,002	38,900	0,006	0,855	0,00003	1,1700	0,00003	2,125	0,0001
8	SEALIP/MY/KAW/3	1907573	Mineral	18,322	0,001	15,652	0,001	38,921	0,004	0,854	0,00003	1,1706	0,00003	2,124	0,0001
9	SEALIP/MY/MIN/1	1907560	Mineral	18,833	0,003	15,704	0,003	39,445	0,008	0,834	0,00003	1,1986	0,00003	2,094	0,0001
10	SEALIP/MY/MIN/2	1907561	Mineral	19,099	0,002	15,719	0,002	41,699	0,005	0,823	0,00003	1,2144	0,00003	2,183	0,0001
11	SEALIP/MY/MIN/3	1907562	Mineral	19,260	0,002	15,725	0,002	42,711	0,005	0,817	0,00003	1,2241	0,00003	2,218	0,0001
12	SEALIP/MY/NTL/1	1907563	Mineral	19,189	0,002	15,763	0,002	39,175	0,005	0,822	0,00003	1,2167	0,00003	2,042	0,0001
13	SEALIP/MY/NTL/2	1907564	Mineral	19,186	0,002	15,764	0,002	39,133	0,006	0,822	0,00004	1,2153	0,00004	2,040	0,0001
14	SEALIP/MY/NTL/3	1907565	Mineral	19,226	0,012	15,763	0,011	39,172	0,030	0,820	0,00013	1,2190	0,00013	2,037	0,0005
15	SEALIP/MY/PDHT/1	1804225	Mineral	18,414	0,001	15,605	0,001	38,522	0,003	0,848	0,00002	1,1799	0,00002	2,092	0,0001
16	SEALIP/MY/PDHT/2	1804226	Mineral	18,356	0,003	15,615	0,002	38,326	0,006	0,851	0,00003	1,1757	0,00003	2,088	0,0001
17	SEALIP/MY/PDHT/3	1804227	Mineral	18,795	0,001	15,592	0,001	38,160	0,004	0,829	0,00002	1,2061	0,00002	2,030	0,0001
18	SEALIP/MY/ST/1	1804222	Mineral	28,219	0,002	16,258	0,002	40,422	0,005	0,576	0,00002	1,7360	0,00002	1,433	0,0001
19	SEALIP/MY/ST/2	1804223	Mineral	21,635	0,001	15,885	0,001	42,281	0,004	0,734	0,00002	1,3618	0,00002	1,955	0,0001
20	SEALIP/MY/ST/3	1804224	Mineral	21,204	0,001	15,889	0,001	41,796	0,004	0,749	0,00001	1,3344	0,00001	1,971	0,0001
21	SEALIP/MY/TKN/1	1907574	Mineral	18,552	0,003	15,746	0,003	38,999	0,007	0,849	0,00003	1,1775	0,00003	2,102	0,0001
22	SEALIP/MY/TKN/2	1907575	Mineral	18,356	0,003	15,725	0,002	38,759	0,007	0,857	0,00004	1,1667	0,00004	2,112	0,0001
23	SEALIP/MY/TKN/3	1907576	Mineral	18,350	0,002	15,757	0,002	38,673	0,005	0,859	0,00003	1,1646	0,00003	2,108	0,0001
24	SEALIP/MY/YTCM/1	1907577	Mineral equivalent	17,885	0,004	15,596	0,005	37,853	0,012	0,873	0,00008	1,1461	0,00008	2,117	0,0002
25	SEALIP/MY/HL28/1	1804228	Consumption artefact	18,501	0,009	15,569	0,009	38,643	0,021	0,841	0,00007	1,1884	0,00007	2,089	0,0001
26	SEALIP/MY/HL28/2	1804229	Consumption artefact	18,430	0,002	15,616	0,002	38,634	0,009	0,847	0,00010	1,1803	0,00012	2,096	0,0002
27	SEALIP/MY/HL28/3	1804230	Consumption artefact	18,589	0,002	15,614	0,002	38,811	0,009	0,840	0,00010	1,1906	0,00012	2,088	0,0002
28	SEALIP/MY/HL28/4	1804231	Consumption artefact	18,596	0,002	15,618	0,001	38,826	0,004	0,840	0,00002	1,1906	0,00002	2,088	0,0001
29	SEALIP/MY/HL28/5	1804232	Consumption artefact	18,589	0,001	15,616	0,001	38,809	0,004	0,840	0,00001	1,1904	0,00001	2,088	0,0001
30	SEALIP/MY/HL28/6	1804233	Consumption artefact	18,580	0,001	15,618	0,001	38,799	0,003	0,840	0,00001	1,1898	0,00001	2,088	0,0001
31	SEALIP/MY/HL28/7	1804234	Consumption artefact	18,608	0,001	15,616	0,002	38,829	0,005	0,839	0,00002	1,1918	0,00002	2,087	0,0001
32	SEALIP/MY/HL28/8	1804235	Consumption artefact	18,597	0,002	15,618	0,002	38,825	0,009	0,840	0,00010	1,1908	0,00012	2,088	0,0002
33	SEALIP/MY/HL28/9	1804236	Consumption artefact	18,611	0,002	15,617	0,001	38,839	0,005	0,839	0,00001	1,1920	0,00001	2,087	0,0001
34	SEALIP/MY/HL28/10	1804237	Production artefact	18,292	0,001	15,703	0,001	38,542	0,003	0,859	0,00001	1,1647	0,00001	2,107	0,0001
35	SEALIP/MY/HL28/11	1804238	Consumption artefact	18,593	0,002	15,618	0,002	38,814	0,005	0,840	0,00002	1,1904	0,00002	2,088	0,0001
36	SEALIP/MY/HL28/12	1804239	Consumption artefact	18,687	0,002	15,627	0,002	38,532	0,006	0,836	0,00002	1,1958	0,00002	2,062	0,0001
37	SEALIP/MY/HL28/13	1901264	Consumption artefact	17,984	0,001	15,598	0,001	37,925	0,004	0,868	0,00002	1,1523	0,00002	2,109	0,0001
38	SEALIP/MY/HL28/14	1901265	Consumption artefact	18,120	0,001	15,605	0,001	38,103	0,004	0,862	0,00002	1,1605	0,00002	2,103	0,0001
39	SEALIP/MY/HL28/15	1901266	Consumption artefact	18,542	0,008	15,700	0,006	38,691	0,017	0,847	0,00002	1,1805	0,00002	2,087	0,0001
40	SEALIP/MY/HL28/16	1901267	Consumption artefact	18,531	0,002	15,669	0,002	38,664	0,005	0,846	0,00002	1,1820	0,00002	2,086	0,0001
41	SEALIP/MY/HL28/17	1901268	Consumption artefact	19,080	0,002	15,697	0,002	39,201	0,005	0,823	0,00002	1,2148	0,00002	2,055	0,0001
42	SEALIP/MY/HL28/18	1901269	Consumption artefact	18,565	0,005	15,700	0,003	38,636	0,009	0,846	0,00005	1,1819	0,00005	2,081	0,0001
43	SEALIP/MY/HL29/1	1901270	Consumption artefact	18,583	0,002	15,607	0,002	38,787	0,004	0,840	0,00003	1,1900	0,00003	2,087	0,0001
44	SEALIP/MY/HL29/2	1804240	Consumption artefact	18,573	0,002	15,616	0,001	38,776	0,005	0,841	0,00002	1,1896	0,00002	2,088	0,0001
45	SEALIP/MY/HL29/3	1804241	Consumption artefact	18,573	0,002	15,616	0,001	38,776	0,005	0,841	0,00002	1,1896	0,00002	2,088	0,0001
46	SEALIP/MY/HL29/4	1804242	Consumption artefact	19,192	0,001	15,771	0,001	39,196	0,002	0,822	0,00001	1,2171	0,00001	2,042	0,0001
47	SEALIP/MY/HL29/5	1804243	Consumption artefact	18,718	0,001	15,704	0,001	39,010	0,003	0,839	0,00001	1,1921	0,00001	2,084	0,0001
48	SEALIP/MY/HL29/6	1907640	Consumption artefact	18,399	0,004	15,620	0,004	38,460	0,009	0,849	0,00004	1,1772	0,00004	2,090	0,0002
49	SEALIP/MY/HL29/7	1907641	Consumption artefact	18,842	0,002	15,689	0,002	38,786	0,006	0,833	0,00004	1,2003	0,00004	2,059	0,0001
50	SEALIP/MY/HL29/8	1907642	Consumption artefact	18,060	0,002	15,541	0,002	38,037	0,005	0,861	0,00003	1,1615	0,00003	2,106	0,0001
51	SEALIP/MY/HL29-1/1	1804244	Consumption artefact	18,331	0,001	15,718	0,001	38,645	0,004	0,857	0,00001	1,1663	0,00001	2,108	0,0001
52	SEALIP/MY/HL29-1/2	1804245	Consumption artefact	18,332	0,001	15,725	0,001	38,659	0,004	0,858	0,00001	1,1659	0,00001	2,109	0,0001
53	SEALIP/MY/HL29-1/3	1804246	Consumption artefact	18,343	0,001	15,727	0,002	38,671	0,005	0,857	0,00001	1,1663	0,00001	2,108	0,0001
54	SEALIP/MY/HL29-1/4	1804247	Consumption artefact	18,326	0,001	15,720	0,001	38,644	0,005	0,858	0,00001	1,1657	0,00001	2,109	0,0001
55	SEALIP/MY/HL29-1/5	1804248	Consumption artefact	18,469	0,003	15,660	0,003	38,645	0,008	0,848	0,00003	1,1794	0,00003	2,092	0,0001
56	SEALIP/MY/HL29-1/6	1804249	Consumption artefact	19,024	0,001	15,748	0,001	39,085	0,004	0,828	0,00002	1,2081	0,00002	2,054	0,0001
57	SEALIP/MY/HL29-1/7	1804250	Consumption artefact	18,376	0,002	15,712	0,002	38,670	0,006	0,855	0,00002	1,1696	0,00002	2,104	0,0001
58	SEALIP/MY/HL29-1/8	1907638	Consumption artefact	18,393	0,002	15,794	0,002	38,771	0,005	0,859	0,00002	1,1639	0,00002	2,108	0,0001
59	SEALIP/MY/HL30-1/1	1907639	Consumption artefact	18,324	0,002	15,719	0,002	38,665	0,005	0,858	0,00003	1,1650	0,00003	2,110	0,0001
60	SEALIP/MY/HLTP1/1	1907643	Consumption artefact	18,596	0,002	15,748	0,002	38,840	0,005	0,847	0,00002	1,1802	0,00002	2,089	0,0001
61	SEALIP/MY/HLTP1/2	1907644	Consumption artefact	18,357	0,002	15,738	0,002	38,602	0,006	0,858	0,00005	1,1658	0,00005	2,103	0,0002
62	SEALIP/MY/MLW/1	1804394	Consumption artefact	18,425	0,001	15,705	0,001	38,981	0,004	0,852	0,00001	1,1731	0,00001	2,116	0,0001
63	SEALIP/MY/MLW/2	1804395	Consumption artefact	17,784	0,001	15,576	0,001	38,472	0,004	0,876	0,00000	1,1417	0,00000	2,164	0,0001
64	SEALIP/MY/MLW/3	1804396	Consumption artefact	18,357	0,002	15,770	0,003	38,653	0,008	0,859	0,00001	1,1640	0,00001	2,106	0,0002

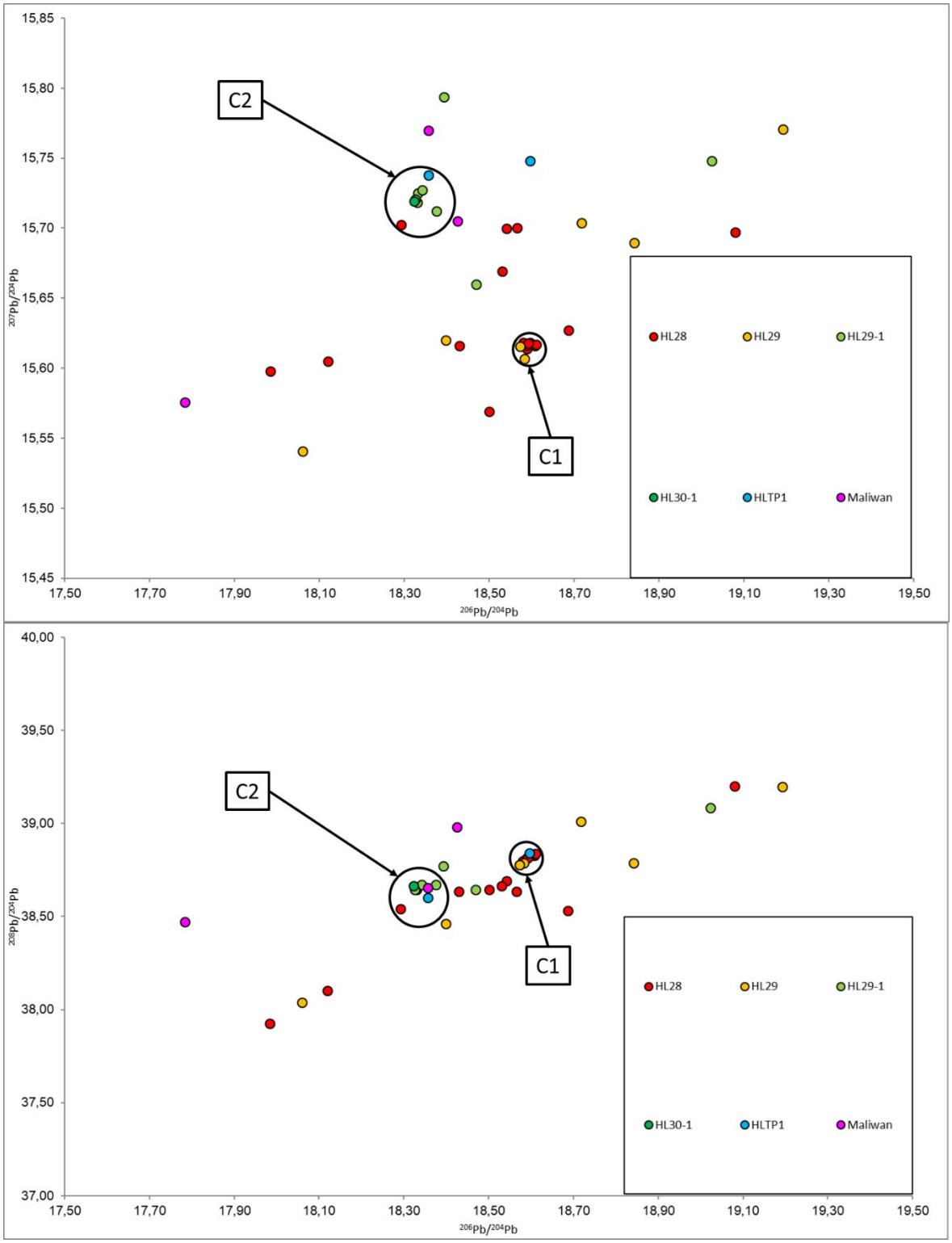

Figure 9: Lead isotope ratios for all Halin and Maliwan metal artefacts. C1 and C2 represent two clusters we consider identifiable within the new copper-base artefact data. Error bars are smaller than symbols.

Our presentation and interpretation of these data proceeds in stages, from new Myanmar artefact data, all Myanmar artefact data, the addition of Myanmar mineral data, comparison with regional (MSEA and Yunnan) production, and finally Bronze Age consumption data to assess potential evidence for proto-SSR interactions. This layering is intended to make our interpretative process more transparent, as is our use of simple double biplots that capture all possible isotope variation, and the provision of full tabulated raw data (Table 4). To remind the reader, for artefacts to have lead isotope consistency, they must plot together on *both* graphs.

All our new data plot within known ranges for Southeast Asian artefacts. Within the data cloud, only two clusters appear at this stage, C1 and C2 (Figure 9). C1 comprises SEALIP/MY/HL28/3-9+11 and SEALIP/MY/HL29/1-3 but not SEALIP/MY/HLTP1/1, which does not have a compatible $^{207}Pb/^{204}Pb$ ratio. C2 comprises SEALIP/MY/HL29-1/1-4+7, SEALIP/MY/HL30-1/1, SEALIP/MY/HL28/10 and SEALIP/MY/HLTP1/2 but not SEALIP/MY/HL29-1/8 or SEALIP/MY/MLW/3, which do not have compatible $^{207}Pb/^{204}Pb$ ratios. Thus, from the new data we can distinguish two possible shared sources of raw copper or recycled bronze, C1 composed of Iron Age copper wires and copper pseudo spearheads, and C2 composed of Bronze Age bronze bangles, Iron Age bronze casting spillage and a Bagan period bronze ring. The remaining data are somewhat dispersed but can be compared to previous Myanmar artefact data (Figure 10).

The clustering of these data indicates that C1 also includes SEALIP/MY/MT/1 and SEALIP/MY/NGO1-3 & 5-10, Iron Age raw copper pseudo-spearhead and wires, respectively. As per our previous study (Pryce *et al.* 2018a), the proliferation of unalloyed copper suggests C1 represents an as yet unlocated primary (smelting) production centre. Similarly, C2 is expanded with the addition of SEALIP/MY/OAI/2, SEALIP/MY/OAI3/2-4, SEALIP/MY/MHT/3 and SEALIP/MY/SP/1; in order, a Bronze Age leaded[1] bronze platy fragment, Bronze Age bronze bracelet and ring fragments, a Bronze Age bronze ring fragment, and an Iron Age high-tin bronze bowl, respectively, which suggests C2 could represent a secondary (foundry) production signature. We now also distinguish C3, comprised of SEALIP/MY/OAI1/1 and SEALIP/MY/HL28/15 & 18; a Bronze Age bronze axe and Iron Age bronze bells/rattles. C3 could potentially include SEALIP/MY/MHT/1, a Bronze Age bronze fragment, but there is ca. 5% divergence in $^{208}Pb/^{204}Pb$ ratios. Given that all the C3 samples are alloyed, we tentatively, given low sample numbers, suggest the signature represents a secondary production centre.

Regarding the few Myanmar artefacts with significant arsenic contents, the Kokkokhahla samples were never submitted for lead isotope analysis, as their weak context did not justify the expense. However, the two Oakaie samples (SEALIP/MY/OAI/1 & SEALIP/MY/OAI3/3) plot relatively close together for $^{206}Pb/^{204}Pb$ and $^{207}Pb/^{204}Pb$ but differ by ca. 2.5% on $^{208}Pb/^{204}Pb$ ratios. Given these samples are more 'urogenic', having a higher proportion of lead decayed from ^{238}U, this could increase the variability of their constituent lead derived from ^{232}Th decay, 'thorogenic'. The other samples plotting in this area, SEALIP/MY/MOH/1 & SEALIP/MY/HL29/4, do not contain measurable quantities of arsenic. Among the remaining data there are hints of further consistency but insufficient sample numbers to propose tentative groups, certainly without reference to potential copper production signatures.

[1] A borderline case, with 1.3 wt. % Pb in a highly corroded matrix.

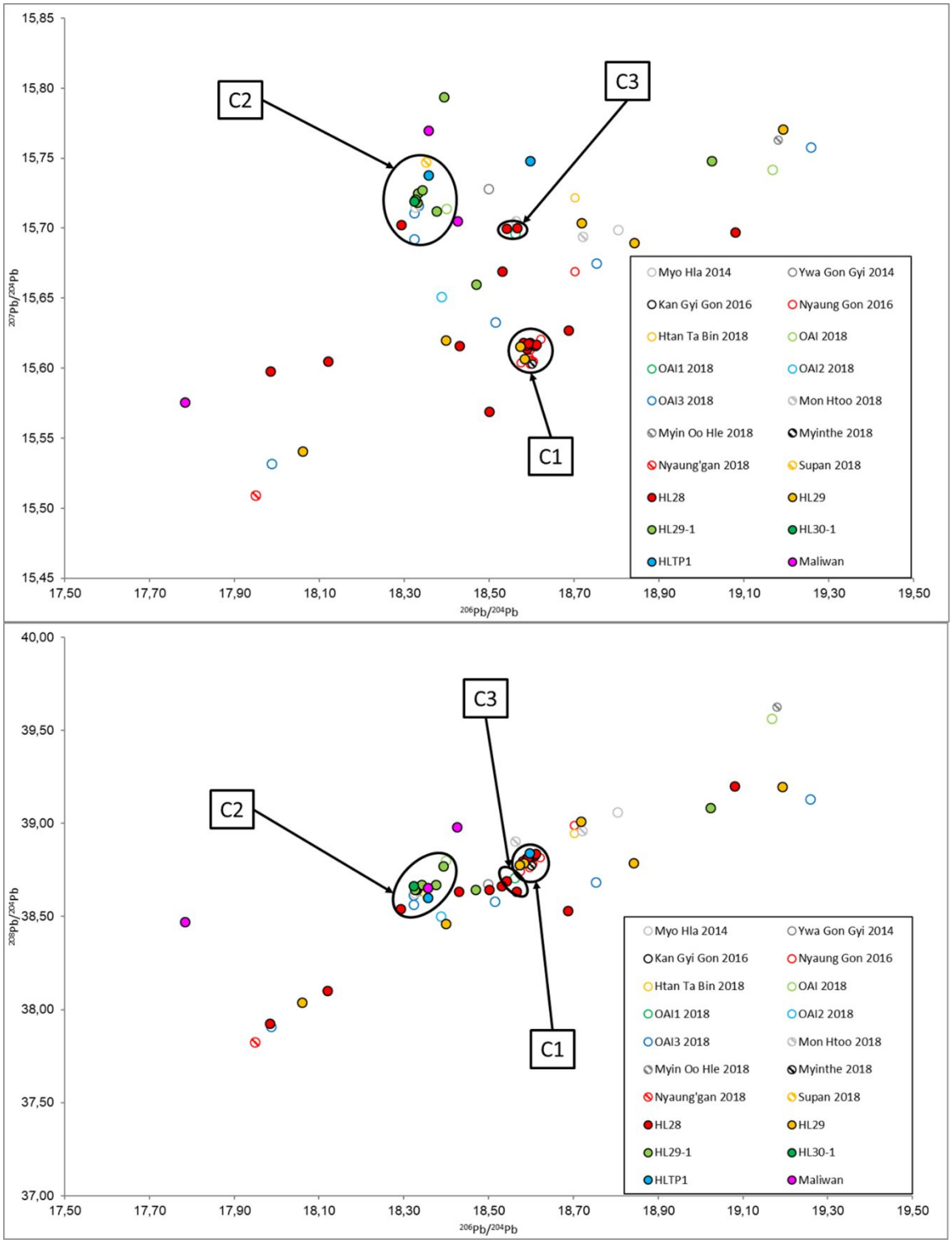

Figure 10: Lead isotope ratios for all Myanmar metal artefacts. C3 represents a cluster we consider identifiable once previously published Myanma data are included. Error bars are smaller than symbols. Published data from (Dussubieux & Pryce 2016; Pryce et al. *2018a; 2014).*

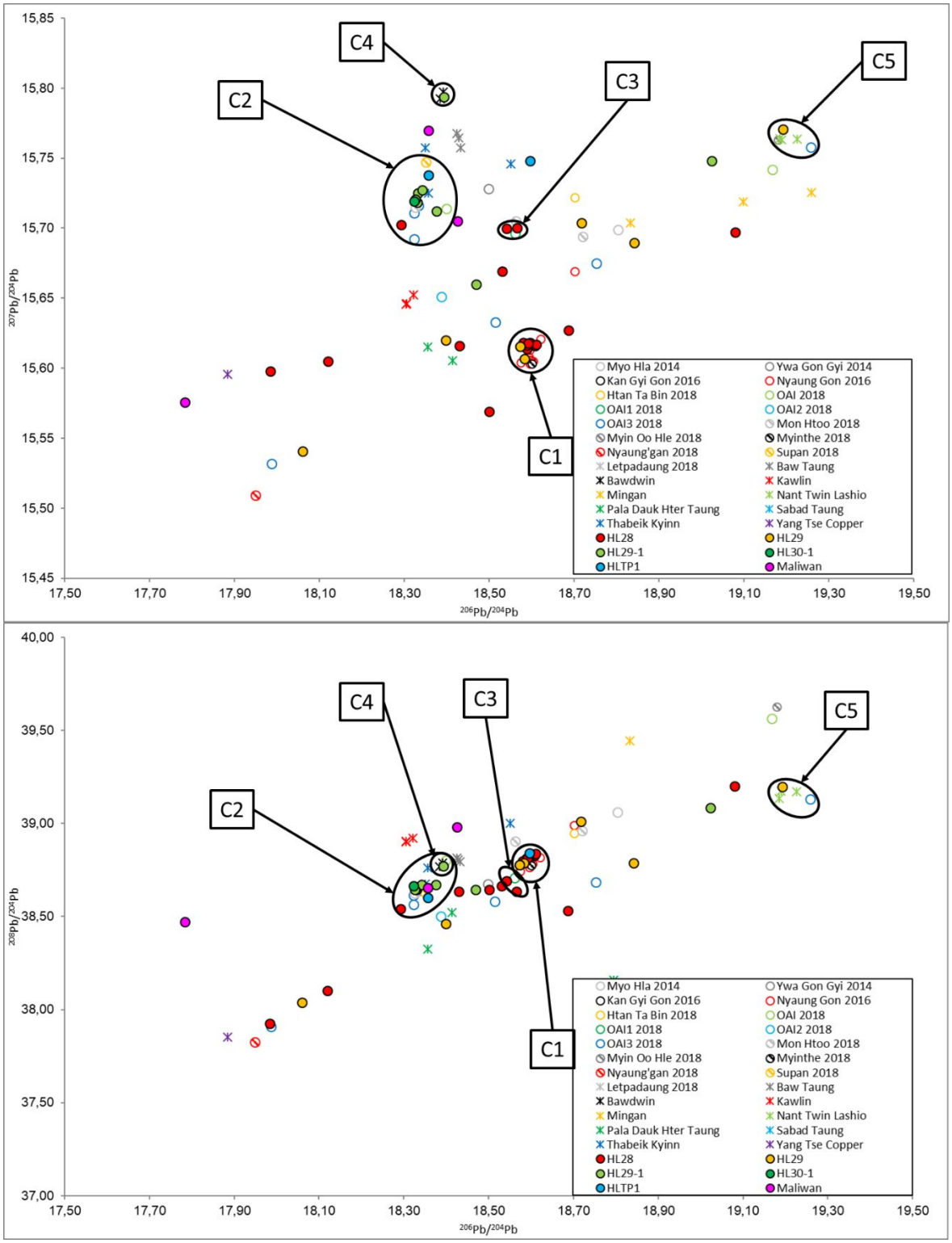

Figure 11: All Myanmar artefact and mineral LI data, representing all four stable isotope ratios. Letpadaung and Sabad Taung samples plot far to the left and right, respectively, and two Mingan samples plot off scale for $^{208}Pb/^{204}Pb$ ratios,

so the axes are constrained for greater legibility. C4 and C5 represent two clusters we consider identifiable when Myanma mineral data are included. Symbols are larger than error bars.

As stated in the introduction, our mineral samples do not necessarily come from regions known or even suspected of having ancient metal production. They were analysed in order to gain an appreciation of lead isotope variation in north-central Myanmar copper mineralisations, in the absence of published geological data. As per the rest of MSEA, Figure 11 shows there is a significant dispersion in these mineral signatures; so much so that we have excluded some far outliers from the graphs as the other results would be hard to read. In light of the new Myanmar artefact data, our (Pryce *et al.* 2018a) interpretation of Letpadaung mine being unrelated to ancient copper production holds (cf. Moore & Pauk 2001). The Yang Tse Copper sample[2] differs considerably from that of Letpadaung despite their physical separation of just over 5 km, suggesting the two mineralisations are of different geological formations, as seen at Phu Lon in northern Thailand (Pryce *et al.* 2011b). Nevertheless, neither of the modern Monywa mines are consistent with ancient metal samples, with the vaguely possible exception of SEALIP/MY/HL28/13, an Iron Age bronze bell.

Of the other mineralisations, sampled from copper minerals rather than modern ingots, it can be seen that both Kawlin and Baw Mountain have very tight and distinct signatures, which do not correspond to any metal artefacts (Figures 3 & 13). Pala Dauk Hter Taung's signature is more dispersed in its $^{206}Pb/^{204}Pb$ ratios but two of the samples appear compatible with SEALIP/MY/HL29/6, a Bronze Age bronze axe. However, we strongly discount the reliability of this link due to the absence of archaeological evidence for early exploitation (or even habitation) in that locality. The Mingan samples have substantial urogenic and thorogenic variation and are inconsistent with any metal samples. Thabeik Kyinn has more dispersion than the aforementioned Kawlin and Baw Mountain mineralisations, but considerably less than the Mingan and Pala Dauk Hter Taung samples. Of note, two of its samples fall within the C2 cluster defined above, which is interesting as this mineralisation is located only ca. 50 km from Halin, some of whose metal samples are also C2 compatible. Ancient production is not known at Thabeik Kyinn but these results suggest it should be checked.

Finally, there are two clusters, C4 and C5, that are extremely intriguing in terms of primary copper production centre potential. The native leaded copper and malachite samples from Bawdwin, a lead/silver mine known to be operated up to 500 years ago (LaTouche & Brown 1909), plot closely together (C4) and are highly consistent with a leaded copper ring from HL29-1 (SEALIP/MY/HL29-1/8). HL29-1 is primarily a Bronze Age cemetery but this ring was found in context #1018, which is a jar burial dating to the Bagan period (Pryce *et al.* in press). This association suggests, albeit on the evidence of one archaeological find, that Bawdwin metal production could be twice as ancient as previously thought, up to 1000 years old. This proposition is supported by C5, which although having a more urogenic lead isotope signature, represents copper minerals from Nant Twin in association with artefact signatures from OAI3 (SEALIP/MY/OAI3/7, a possible bronze cutting tool) and HL29 (SEALIP/MY/HL29/4, a bronze axe). The difference is that these artefacts are both dated to the Bronze Age, which could thus push Shan State copper production back another two

[2] Which like the Letpadaung sample is a modern ingot and thus represents a pooled signature of that mine's minerals.

millennia to ca. 1000 BC. This would be the first explicit protohistoric link between the Shan Hills region and the Irrawaddy basin, and hints at wider regional connections.

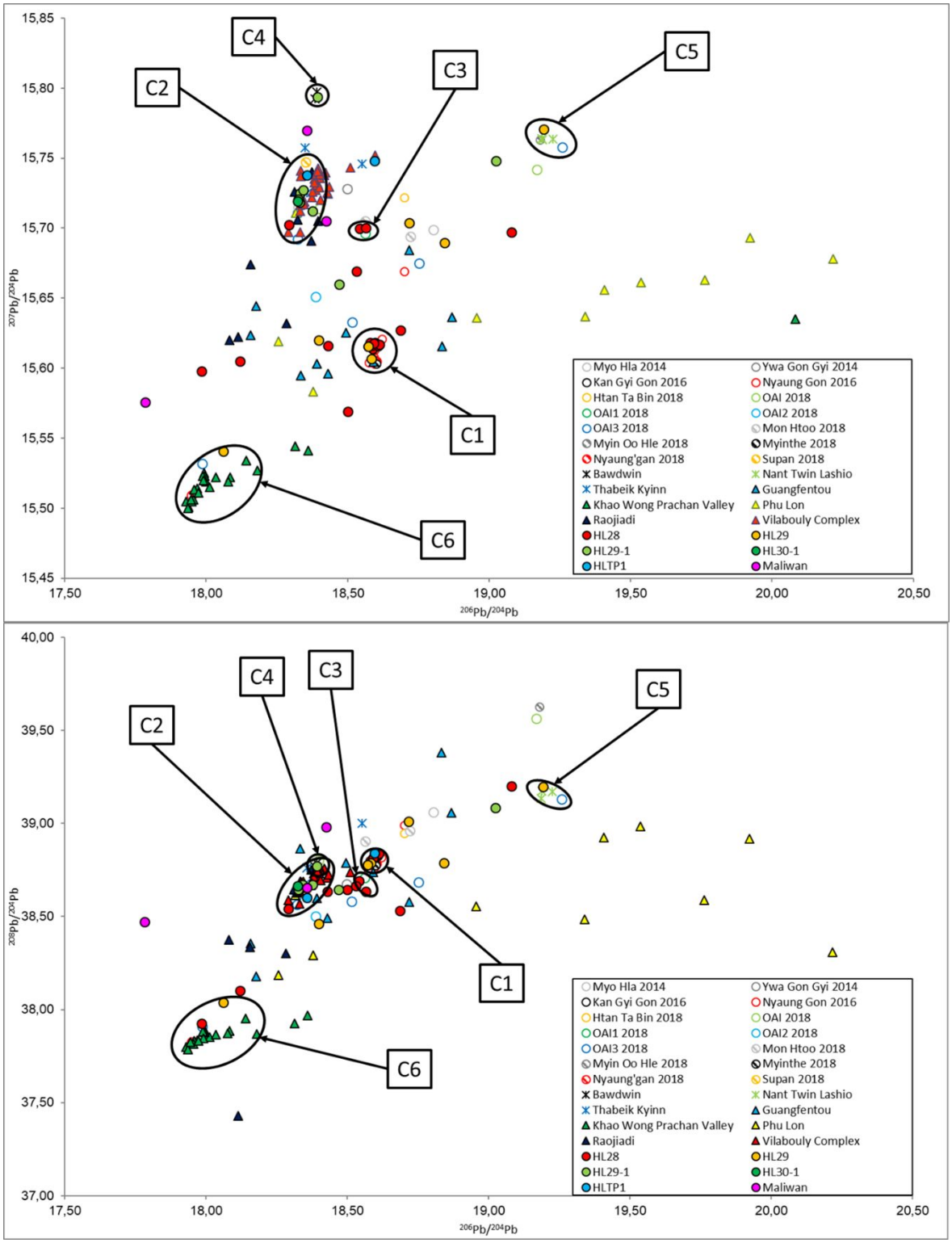

Figure 12: All Myanmar artefact plus mineral LI data deemed potentially relevant in the previous section, representing all four stable isotope ratios, plotted against published copper production systems in Thailand (Khao Wong Prachan Valley and Phu Lon), Laos (Vilabouly Complex), Yunnan (Guangfentou) and Sichuan (Raojiadi) (Chen et al. *2020; Pryce*

et al. *2022b; Zou* et al. *2019). C6 is a cluster we consider identifiable once regional copper production data are included. Error bars are smaller than symbols.*

Nevertheless, it is clear that the majority of the Myanmar metal samples are not consistent with the studied minerals, and we can thus look towards other, proven, prehistoric copper production systems in MSEA and southwest China (Figures 3 & 12). Within the former these are limited to the Khao Wong Prachan Valley (KWPV) in central Thailand (Pigott *et al.* 1997), Phi Lon (PL) in northern Thailand (Pigott & Weisgerber 1998) and the Vilabouly Complex (VC) in central Laos (Pigott & Pryce 2022; Tucci *et al.* 2014), all of which have been geochemically characterised within SEALIP/BROGLASEA (Cadet *et al.* 2019; Pryce *et al.* 2011c; 2011b; 2014). Within the latter, there is no doubt that there are likely to be a great many metal production loci in this strongly metallogenic region but we can only go by what has been identified and published: Guangfentou in Yunnan (Zou *et al.* 2019) and Raojiadi in Sichuan (Chen *et al.* 2020).

Guangfentou, Phu Lon and Raojiadi all have rather dispersed isotopic signatures, doubtless representing multiple mineralisations at the same mine (as at Phu Lon, Kamvong & Zaw 2009), or the processing of ores from multiple mines (as proposed for Guangfentou by Zou *et al.* 2019) but Figure 12 clearly indicates that C1, which has a very tight signature, is not compatible with the known copper production sites, and thus remains an unknown. However, C2 is highly consistent with the Vilabouly Complex in central Laos, a primary rather than secondary copper signature as suggested above. A potential 1300+ geodesic kilometre Bronze Age exchange system was identified previously with Oakaie/Nyaung'gan artefacts (Pryce *et al.* 2018a) but with the Halin material it now extends through the Iron Age and as far as the Bagan Period. Of course, old artefacts could have been recycled over time but, in our opinion, it is unlikely the original isotopic signature would hold after perhaps centuries of reuse: mixing, alloying and recycling (see e.g., Bray *et al.* 2015; Liu *et al.* 2020).

C3, as tight as C1 but not as dense, and representing Bronze and Iron Age consumption remains without consistency. Neither are C4 and C5 compatible with the other known production signatures, suggesting our linking them to Bawdwin and Nant Twin Lashio mineralisations holds for the time being. At this stage we believe we can add C6 to our list of possible groups, with consistency seen between the Khao Wong Prachan Valley copper production signature (Figure 8). This ca. 1000 geodesic kilometre exchange route was already detected with a Bronze Age bronze bracelet from Oakaie 3 (Pryce *et al.* 2018a), which we can now reinforce with SEALIP/MY/HL29/8, a bronze spearhead. It is pertinent that C6 does not seem to extend into the Iron Age as, after many years of uncertainty, the latest radiometric dating from the Khao Wong Prachan Valley suggests that metal production there did not persist beyond the Bronze Age (Higham *et al.* 2020). SEALIP/MY/HL28/13 & 14 are not C6 members as they are incompatible in their $^{207}Pb/^{204}Pb$ ratios. We do not consider SEALIP/MY/NYG/1 a C6 member, despite its high isotopic consistency, as it is a leaded alloy and C6 is a copper signature.

Having now assessed the Halin (and Maliwan) data with respect to: 1. themselves, 2. all Myanmar artefacts, 3. Myanmar minerals, and 4. MSEA and southwestern Chinese production systems, the next logical step would be 5. MSEA and southern Chinese consumption data. Our recent investigations of northern MSEA/southern Chinese exchange systems have attempted this stage manually, with reasonable results for the existence of late 2nd through 1st millennium BC networks running from Yunnan to Vietnam, Thailand and Myanmar (Pryce *et al.* 2022a; 2022b). Our substantial new Myanmar dataset, which covers over two millennia, offers the possibility to

assess further chronological contiguity with the historically attested SSR ca. 3rd c. BC (Figure 2, Yang 2004). Manual processing of Myanmar data with regards to the 'late 2nd/early 1st millennium BC interaction arc between Mainland Southeast Asia and Southwest China' identified in Pryce et al. (2022b) indicates:

- The present study's group C1 is compatible with SEALIP/CH/HBS/4, a 800-600 BC (Mid Bronze Age) flat copper fragment from Hebosuo on Lake Dian in Yunnan. This does not necessarily mean the C1 source is in the Dian area but that its product was accessible to communities in north-central Myanmar and Yunnan. As C1 samples are mostly mid-late 1st millennium BC, we can thus draw our proto-SSR network closer to the above-depicted historical SSR.
- C2, which is highly consistent with the Vilabouly Complex copper production signature, is also compatible with SEALIP/TH/BC/1 & 4, a bronze socketed spearhead and O-section bangle from Bronze Age Ban Chiang in northeast Thailand. A great many MSEA artefacts are consistent with this production signature and its output spans the Bronze and Iron Ages, thus linking to the historical SSR.
- C3 is not consistent with previously identified groups outside of Myanmar.
- Neither is C4 but as our only dated artefact in this group is dated to the Bagan period, early 2nd millennium AD, we have very few comparative regional data.
- The urogenic C5 could include potentially include SEALIP/TH/BNW/6, a 1000-900 BC copper axe from Ban Non Wat in northeast Thailand.
- As mentioned above, C6 is compatible with copper production from the Khao Wong Prachan Valley in central Thailand, a volume of isospace far less densely occupied than that of the Vilabouly Complex. C6 is consistent with SEALIP/TH/BNW/5, 7 & 8, a bronze axe and copper-base chisel and axe, respectively, from 1000-900 BC Ban Non Wat. There are no Iron Age or later data consistent with this group.

Not previously identified potential groupings include:

- SEALIP/MY/HL28/14, an Iron Age bronze bell, is compatible with SEALIP/TH/NPW/11, a late 2nd millennium BC Early Bronze Age bronze axe from Non Pa Wai in central Thailand, thus spanning the Bronze and Iron Ages and potentially abutting SSR networks.
- SEALIP/MY/HL29-1/5, a Bronze Age bronze axe, is consistent with SEALIP/TH/BC/2 & 3, bronze O-section bangles from Bronze Age Ban Chiang, thus not adjoining the historical SSR period.

Therefore, of the eight potential groups, three offer chronological contiguity with the SSR. Manual processing of the above datasets is not too problematic but their presentation already becomes difficult due to the density of data points: hence the lack of a figure provided here. These issues are massively compounded if we attempt to add the full regional datasets for Bronze and Iron Age and Historical samples. The resulting mass of overlapping multi-coloured symbols over three ratios makes the identification of individual samples and groups very difficult. 'Zooming in' only obscures potential clusters and disguises the overall diversity of the dataset. Likewise, one can process one site versus another one at a time, but this discounts the possibility of clusters only being detectable across multiple sites. Furthermore, sites are not always the appropriate scale of analysis, if we are interested in a particular period, alloy or typology for example. While the lead author has long prided himself in using simple biplots of raw data (e.g. Pryce *et al.* 2011b: Figure

7), easily intelligible to the non-specialist reader, we have reached a point when a data processing evolution is required to more objectively evaluate the combined datasets for proto-SSR evidence.

Discussion on the potential for a Bronze Age SSR

Thus far, and in all but one previous SEALIP-BROGLASEA publication, attributions of 'consistency' between LI signatures for copper/lead-base metal consumption or between those of consumption and production, were decided by Mk1 Eyeballing of the data cloud. Subjectivity does not necessarily imply these interpretations were liberal. Indeed, our previous application of an 'objective' measure, Kernel Density Estimates (Pryce *et al.* 2011b), gave such broad compatibility, at 10% confidence increments, that the lead author was deeply dissatisfied by their historical likelihood. Wary of the LI archaeology interpretative pitfalls of yesteryear in the Mediterranean arena (summarised in Pollard 2009), Pryce resorted to excessive conservatism in Southeast Asia: requiring that a metal artefact plot *within* the data cloud of a well-defined production signature before suggesting consistency, or giving only effusive estimates of potential proximity between consumption signatures.

To address this, we assumed that any two samples should be considered provisionally consistent and potentially sharing the same supply route: using the same raw material source, a market place or a mediator, if the difference between their lead isotope (LI) ratios is within the interval of total variance between the LI ratios of an assemblage of artefacts, archaeologically-reasoned to represent a single primary copper production signature. To define our LI ratio thresholds, we choose the slag and ingot assemblages from four sites in two areas: Non Pa Wai and Nil Kham Haeng in the Khao Wong Prachan Valley (KWPV) of central Thailand, and Puen Baolo and Thong Na Nguak in the Vilabouly Complex (VC) of central Laos. All four sites are well-documented primary copper production loci with both technological and geochemical characterisations (Cadet *et al.* 2019; 2022; Natapintu 1988; Pigott *et al.* 1997; Pryce *et al.* 2010; 2011c; 2011b). Assemblages of slag, which represents an anthropogenic and pooled LI signature of minerals (ore, gangue and flux), ceramic (crucible, tuyère and furnace) and fuel ash, from these sites produced coherent and easily distinguishable LI production fields. To these fields may be added the LI signatures of raw copper artefacts, identified as ingots, excavated at the respective loci, which corresponded very closely to the associated slag fields. Given the congruence of time, location and technology, it is reasonable to assume these ingots were smelted on site from local minerals. These combined, slag and ingot, LI signatures plot closely[3] but not exactly in the same isospace, and these margins can be calculated easily.

[3] The two outliers consist of a low-tin bronze axe, one of the earliest copper-base artefacts known in Southeast Asia, and interpreted as an import (Pryce *et al.* 2011c), and a slag fragment that is more consistent with minerals from Phu Lon in northern Thailand. This latter sample is one of two regional examples of slag and/or minerals apparently being transported between primary copper production loci, and not a labelling error as the batches were processed months apart (Pryce *et al.* 2011b; Pryce 2014; Pryce *et al.* 2014). The data from these two outliers were thus eliminated from our calculations but for sound archaeological/archaeometric reasons, rather than them not fitting our preconceptions.

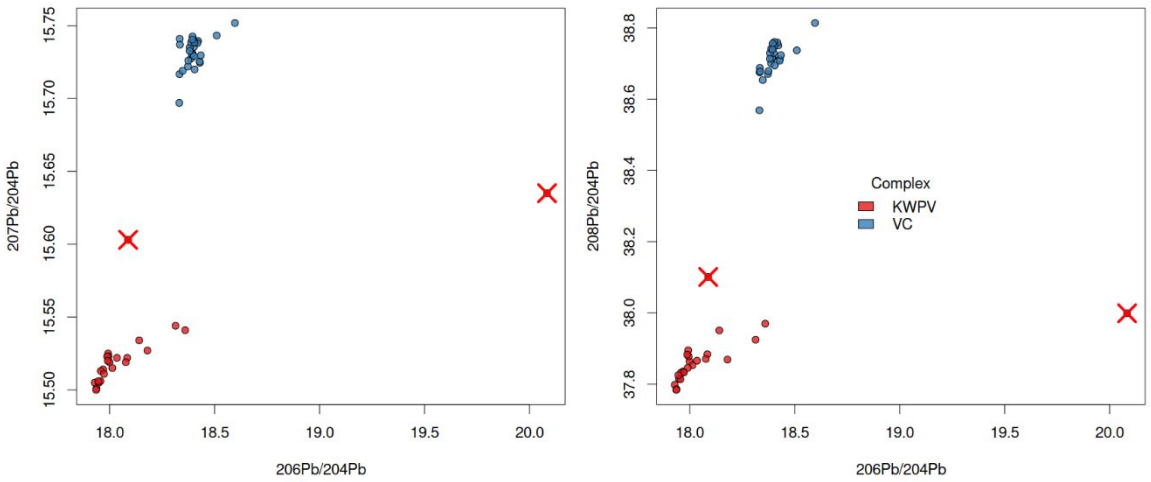

Figure 13: Biplots showing the relatively high, at a regional scale, consistency in LI ratios of slag and copper-base metal artefacts from the Khao Wong Prachan Valley (Non Pa Wai and Nil Kham Haeng) and the Vilabouly Complex (Puen Baolo and Thong Na Nguak). The two NPW outliers, a bronze axe and a slag fragment, are represented by a red cross.

We generated a distribution of difference in the three LI ratios: $^{208}Pb/^{204}Pb$, $^{207}Pb/^{204}Pb$ and $^{206}Pb/^{204}Pb$, between every pair of samples from the KWPV and, separately, VC groups (Figure 13). In mathematical terms, for two samples A and B and with LI ratios $R_i^A < R_i^B$ if $R_i^A < R_i^B$ then $D_i(A,B) = 1 - \frac{R_i^A}{R_i^B}$. Thus. if ratio I for sample A is 80 and ratio I for sample B is 100, B is 20% larger than A. Using the relation between these ratios allows us to account for the fact that LI ratios do not vary linearly, and samples with higher LI ratios can have larger differences in their ratio compositions while still exhibiting consistency.

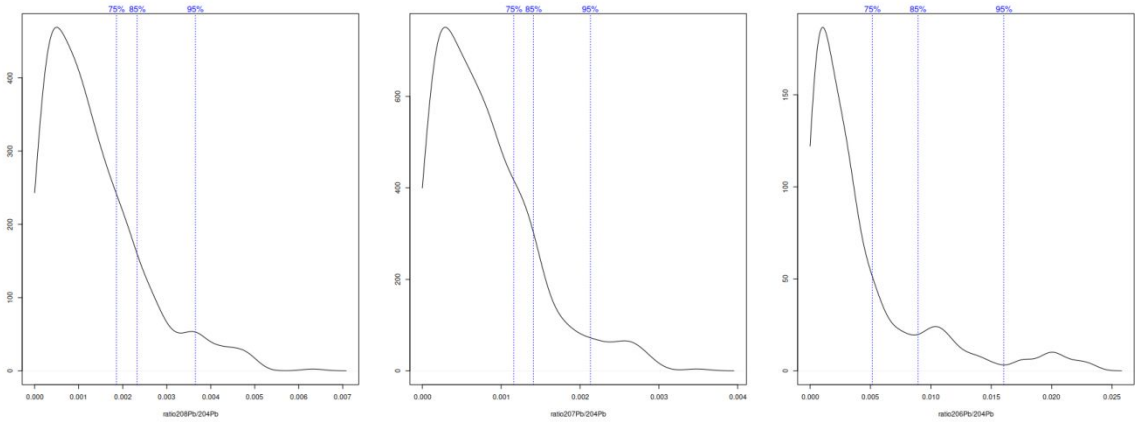

Figure 14: Distribution of distances between KWPV and VC samples for each lead isotope ratio. Vertical dashed blue lines represent the values for the 75,85 and 95 percentiles.

In Figure 14, we see the maximum difference for our regional production-defined ratios are: 0.7% for $^{208}Pb/^{204}Pb$, 0.4% for $^{207}Pb/^{204}Pb$, and 2.6% for $^{206}Pb/^{204}Pb$. Thus any two random samples with *all three* ratio differences below these thresholds would be considered *provisionally* consistent. However, during testing we found that using 100% thresholds was giving excess attributed

connectivity in the wider dataset. The reason can be seen in the non-parametric distributions in Figure 14, with large areas under the curve for low variation, and disproportionately smaller areas under the curve with higher variation. We therefore experimented with variations from 75% to 95%. The 75% threshold was too strict, eliminating potential consistency attribution from samples that would on an archaeological basis be highly expected to be consistent; ergo typologically, technologically and chronologically compatible artefacts from nearby sites. We settled on applying a 95% threshold, which eliminated the unworkable levels of connectivity but retained previous inter-assemblage consistency attributions made by traditional subjective interpretation and highlighted several new consistencies to be evaluated from an archaeological perspective. A 95% threshold gives the following absolute inter-sample differences for the three ratios: $^{206}Pb/^{204}Pb$ of 1.603%; $^{207}Pb/^{204}Pb$ of 0.213%; and $^{208}Pb/^{204}Pb$ of 0.365%.

We then computed the same measure between all pairs of Myanmar archaeological copper-base consumption samples and all regional Bronze Age copper-base consumption samples; including the southern Chinese assemblages for which suitable LI data are available[4]:

Yunnan – Haimenkou (HMK), Chenggong (CGG), Dabona (DAB), Dali (DL), Lijiang (LG), Lijiashan (LJ), Shizhaishan (SZH), Wanjiaba (WJB), Yangfutou (YGT) (Cui & Wu 2008);

Guangxi – Andengyang (ADY) and Yuanlongpo (YLG) (Anon. 2020).

Following the complex networks community detection approach from Radivojević & Grujić (2018), but focusing on lead isotope rather than elemental data, as Southeast Asia's geological diversity is more amenable to such an approach than Southeast Europe (Killick *et al.* 2020), we conducted complex network analysis in two steps (as outlined in methods). First we used the LI data to estimate the number of groups with high densities of consistency. These groups represent artefacts sharing consistent isotopic signatures and thus potentially sharing same supply routes/networks: sources of raw materials, market places, producers, merchants, mediators etc; theoretically copper for unleaded copper or unleaded bronze, or lead for leaded copper or leaded bronze. In the second step, we linked sites / geographic areas where these artefacts were found, with the number of shared consistent artefacts as a measure of potential relatedness between two sites/areas, creating a network between them and, still following the approach from Radivojević & Grujić (2018), extracting communities using the Leiden Algorithm (Traag *et al.* 2019). Since Radivojević & Grujić (2018) used the Louvain algorithm, which exhibited satisfactory computing prowess and robustness, a novel and improved method appeared, Leiden algorithm, which guaranteed faster computing and enhanced precision. While both algorithms present excellent results when applied to the same dataset (Grujić & Radivojević *forthcoming*), we opted for the most recent one (Leiden). The Leiden algorithm operates by partitioning the network into clusters of spatial areas that maximize the number of links between areas within the same cluster (or modules), while minimizing the number of links between areas not in the same cluster. In other words, it extracts communities of areas that share consistent artefacts and splits into different communities of areas sharing fewer elements.[5] This community detection or modularity

[4] Erring on the side of inclusivity for Chinese sites where the dating broadly equates to the Bronze Age in MSEA terms.

[5] All the computation was done using R Programming language (R Core Team 2021) and are available online as a git repository: https://github.com/simoncarrignon/bronze-age-ssr. All network operations have been

approach allowed us to model communities of places that may have had interacting populations; whether by means of direct or indirect material culture exchanges, complete or incomplete technological transmissions, or the actual movement of people – as individuals, groups or en masse. While evaluation of these options requires detailed assessment of chronology, typology, alloy type, production methods and socioeconomic ascribed values, our approach does give us a means of rationalising a large and unwieldy database that is otherwise underexploited.

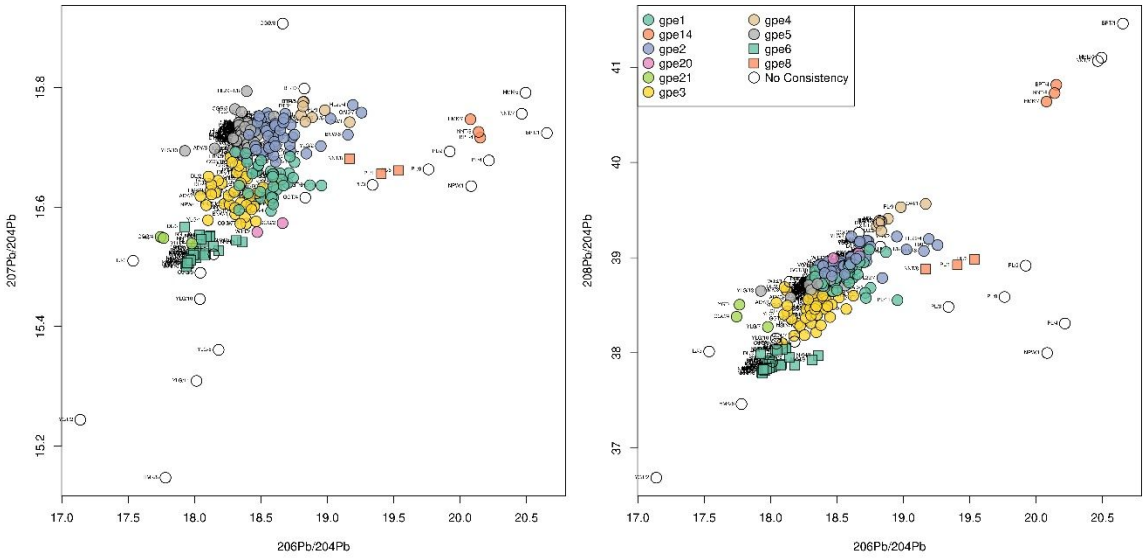

Figure 15: Biplots of LI data from regional Bronze Age assemblages, as processed by our defined consistency thresholds to identify groups of artefacts.

From a regional dataset of 281 Bronze Age (or southern Chinese equivalent) samples, a total of 29 'groups' (GPE, sample level patterning) were computed using the Leiden algorithm (Figure 15). Nineteen of those consisted of only one sample (no consistency), and of the multi-member groups, GPE20 consists of only two members, CH/CGG/2 & CH/WJB/2, but presents no anomalies as the sites represented are ca. 115 km distant and contact might be expected. GPE14 has three members, SEALIP/TH/BPT/4, SEALIP/TH/NNT/9 & CH/HMK/7, of which the latter is ca. 1100 km distant but would not surprise regional archaeologists given the Mekong River covers much of the route. GPE21 comprises three members, CH/CGG/4, CH/YGT/1 & CH/YLG/7, of which the first two sites are ca. 60 km apart but the latter ca. 600 km – we do not feel qualified to comment on the probability of this group but note that the Pearl River and its tributaries make up much of the route. GPE8 consists of three highly radiogenic samples (SEALIP/TH/PL/1, SEALIP/TH/PL/6 & SEALIP/TH/NNT/8) from northern Thailand, for which consistency is not surprising from an archaeological perspective.

---

done using igraph package (Csárdi & Nepusz 2006). The communities have been detected using the Leiden algorithm (Traag et al 2019).

Of the remaining large multi-member groups:

- GPE1 consists of 39 samples from Myanmar, Thailand, Vietnam and Yunnan;
- GPE2 consists of 52 samples from Laos, Myanmar, Thailand, Vietnam, Yunnan and Guangxi;
- GPE3 consists of 40 samples from Myanmar, Thailand, Vietnam, Yunnan and Guangxi;
- GPE4 consists of 8 samples from Myanmar, Thailand, Vietnam and Yunnan;
- GPE5 consists of 79 samples from Laos, Myanmar, Thailand, Vietnam, Yunnan and Guangxi;
- GPE6 consists of 34 samples from Myanmar, Thailand and Yunnan.

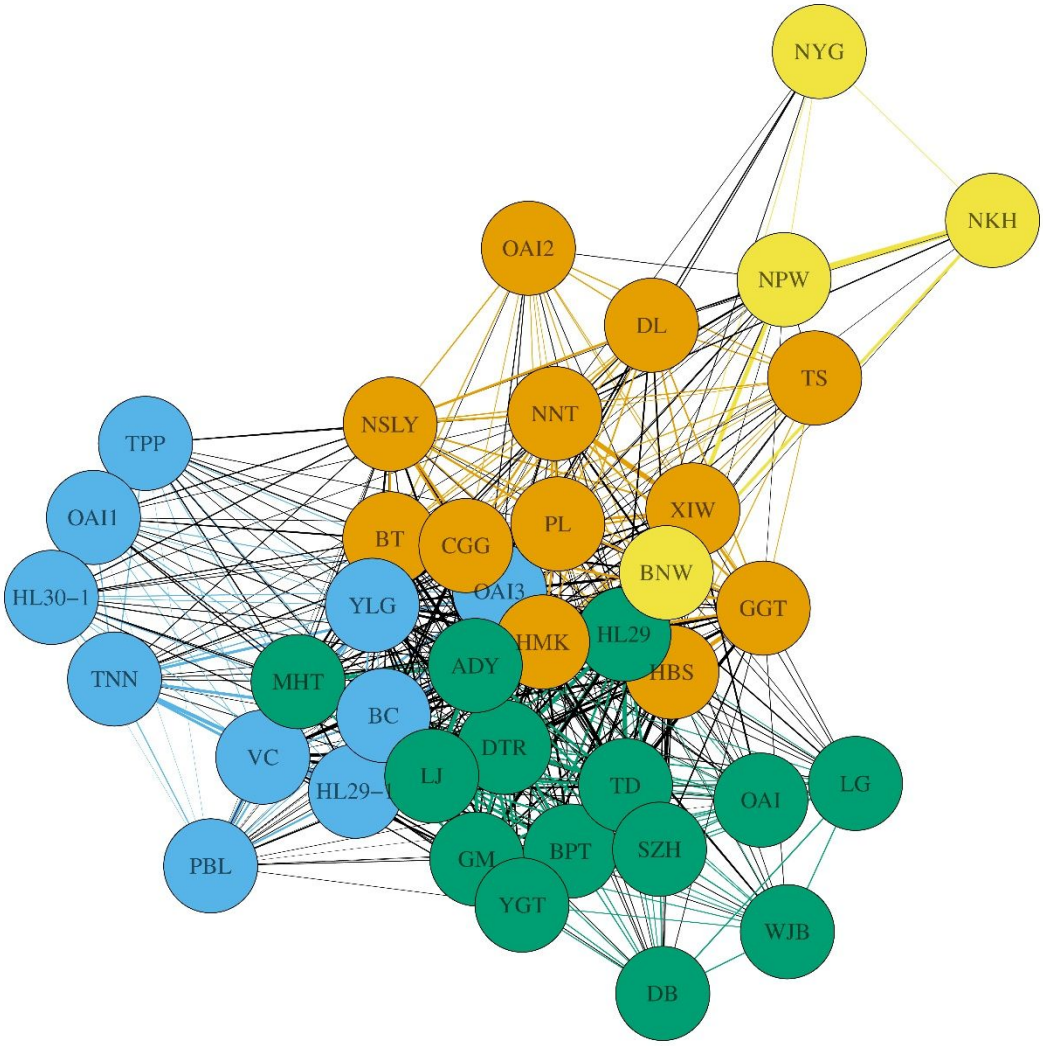

Figure 16: Network of sites based on shared artefacts from the same family, each node colour represent a different community detected by the Leuven community detection algorithm. The edges between nodes from within the same community are coloured using the colour of the community. The edges that link nodes from different communities are black.

Following from groups (samples), we moved on to detecting communities (or modules), which allowed us to assess the presence and degree of connectivity between groups (and hence the sites and areas they originated from). Our schematic representation is non-geographic but shows the three main communities of sites with metal assemblages comprised of artefacts with algorithmically-consistent LI signatures (Figure 16). The lines drawn between the sites shows that two sites share at least one sample from the same group. The thickness of those lines is a function of the number of artefacts from similar groups shared by two sites, normalised by the total number of samples a site has.

- The yellow community is comprised of central and southern northeast Thai and north-central Myanma sites;
- The blue community is comprised of northern northeast Thai, central and northern Lao, north-central Myanma and central Guangxi sites;
- The orange community is comprised of northern northeast and southern Thai, northern Vietnamese, north-central Myanma and central and western Yunnan sites.
- The green community is comprised of north-central Myanmar, northern northeast Thai, northern Vietnamese, central Guangxi, central and western Yunnan

In order to understand the implications of these computations, it is necessary to add the geographical component (Figure 17). The dark grey lines equate to a geolocalised projection of Figure 1, the historically reconstructed 7th-13th c. AD SSR, and the other colours represent our communities. What is immediately apparent is the *extent* of the connectedness of communities, which showcase the Bronze Age metal exchange network. It covers parts of all Mainland Southeast Asia and well into Yunnan and Guangxi, with the exception of Cambodia and central/southern Vietnam, for which there are no late 2nd/early 1st millennium BC metals data. However, we acknowledge that we do not have metal networks extending into northeastern India or beyond Yunnan/Guangxi further north into China, which is critical as the historic SSR served to supply the imperial capital at Xi'an. The lack of an Indian connection at this juncture may be real, as current archaeological data indicate such interactions effloresced from the mid-1st millennium BC (Bellina 2014; Bellina *et al.* 2019; Dussubieux & Pryce 2016) but these cultural exchanges could well have precedents. As concerns China, there is a dearth of archaeometallurgical data from Guangxi, Guangdong and Sichuan, the other provinces close to MSEA, though prehistoric metal assemblages there are plentiful. We acknowledge our lack of familiarity with Chinese archaeology and geology – though we hope interested Chinese colleagues pursue the idea (as they now are for general Neolithic and Bronze Age research, see Ma *et al.* 2022; Yao *et al.* 2020). In summary, we postulate that the geographical extent of our Bronze Age metal exchange network is equivalent to the historical SSR routes from Yunnan and possibly Guangxi, south into Vietnam, Laos, Thailand and Myanmar.

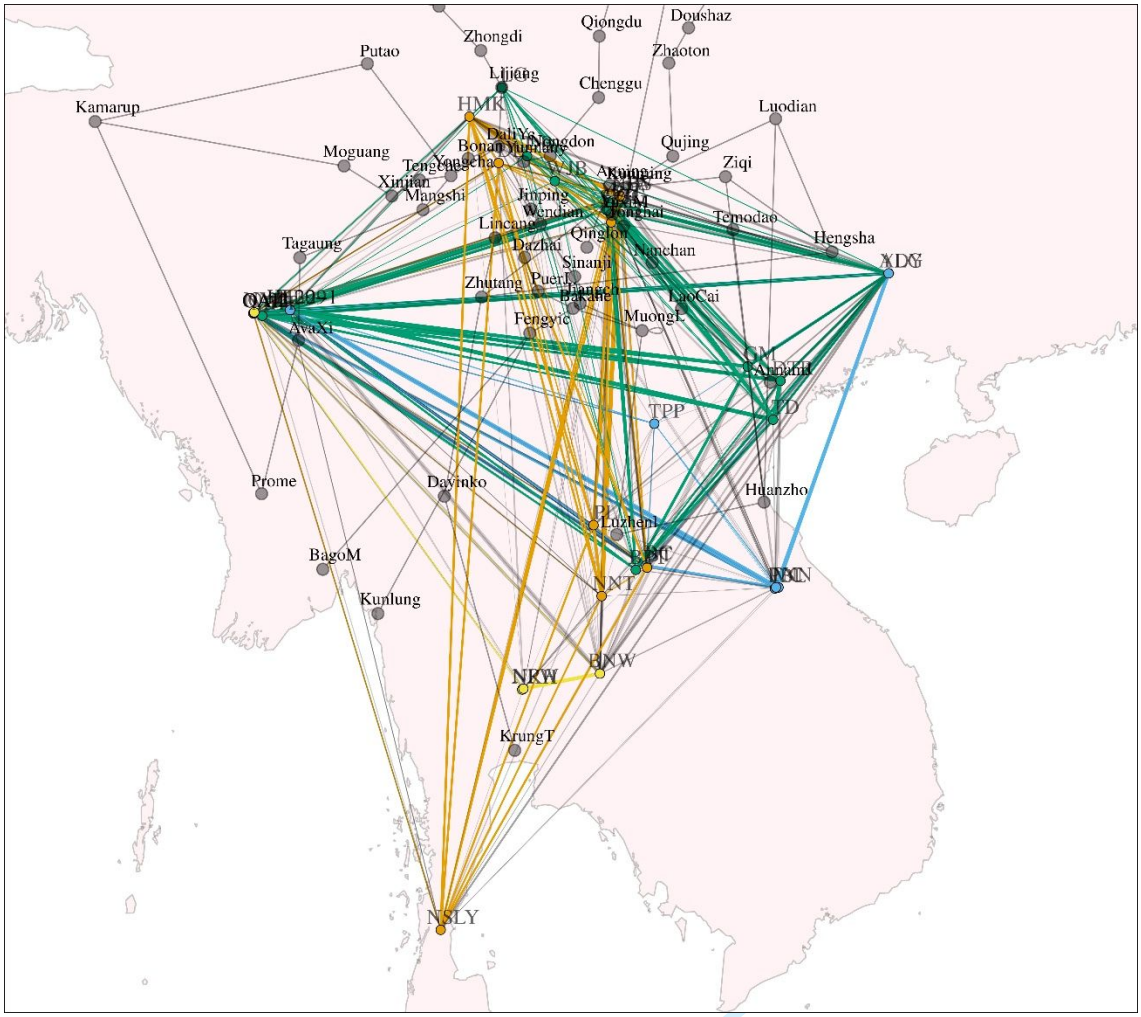

Figure 17: Map showing the reconstructed Nanzhao-Dali period SSR (from Figure 1), overlain with our calculated Myanmar multi-period and regional Bronze Age assemblage communities, using the same colour codes as for Figure 16.

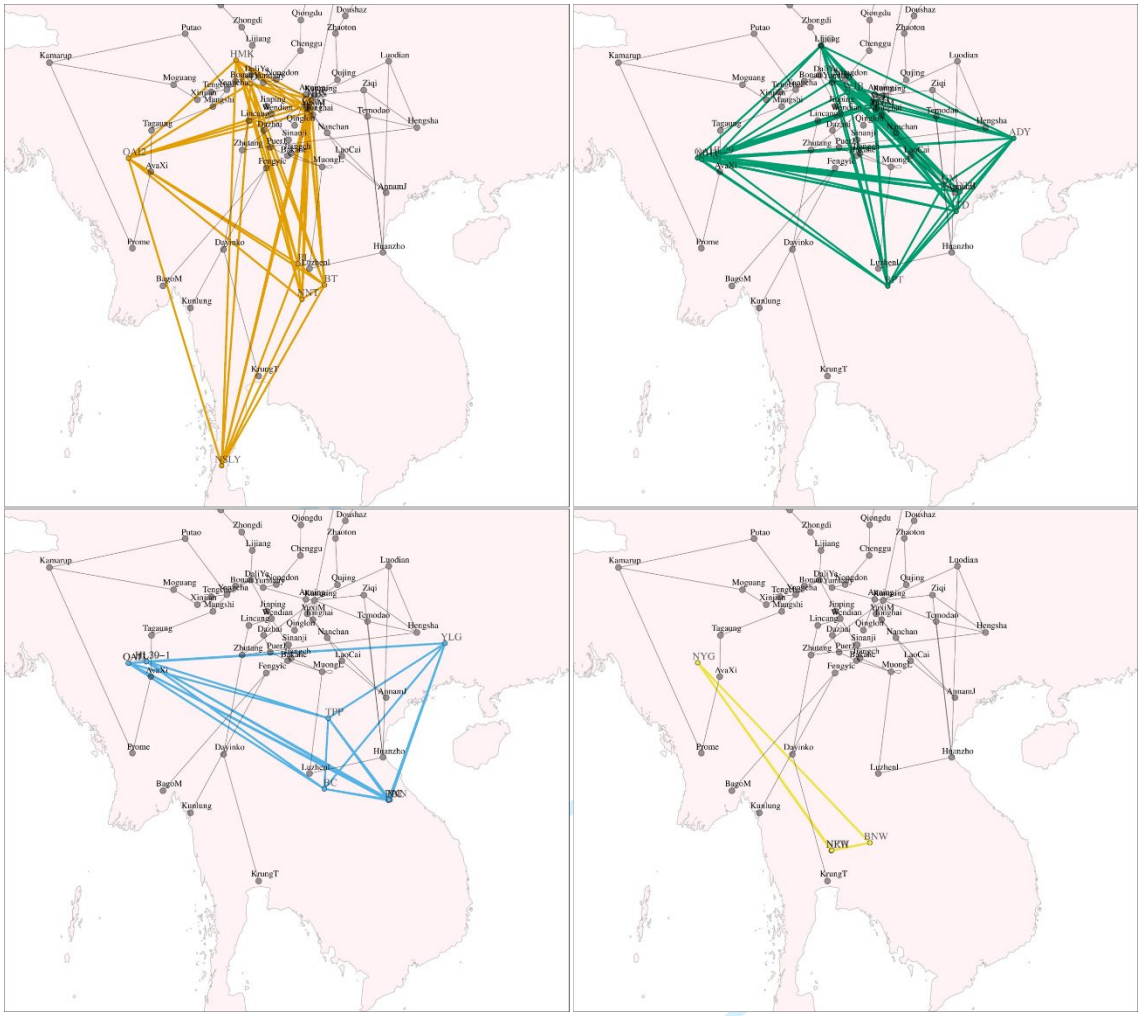

Figure 18: Maps detailing each calculated Bronze Age assemblage community. From top left, an unknown but Kunming-centred copper consumption network (orange), an unknown southern China-centred copper consumption network (green), the Vilabouly Complex copper production network (blue), and the Khao Wong Prachan Valley copper production network (yellow).

This does not imply, however, that the nature of those networks is equivalent. Firstly, we note that the reconstructed historical SSR in Figure 1 shows both places (sites and/or regions) *and* routes; often seen as following riverine lines of communication. Our reconstructed Bronze Age metal network shows only places, with geodesic lines representing isotopic consistency rather than transport. The routes via which Bronze Age metal (and potentially metal technologies) were moved by people is unclear but could be montane, riverine, marine, or a combination of those (see Pryce 2018). Indeed, when we break down the networks by community (Figure 18), we see quite distinct patterning that may represent overlapping networks, either contemporary or sequential within our available chronological resolution.

The orange network equates to an unknown primary or secondary copper production signature; thus we cannot be certain in which direction the metal was moving. That said, the major community concentration is in western and central Yunnan, from which it extends 600-800 km

southwest to Oakaie in north-central Myanmar. Rivers probably account for these putative exchange networks, the Daying or Nanting and Irrawaddy/Chindwin into Myanmar, with portions of montane portage likely. These are historic SSR routes. The occurrence of the Yunnan-centred distribution community 850-1100 km south at Non Nok Tha, Phu Lon and Ban Tong in northern northeast Thailand is harder to explain as these data are not fully published and scrutinised, but a pathway including the Lancang/Mekong River via southern Yunnan is not implausible and also lies on a historic SSR route. As we have previously stated, community detection is but a guide and we discount the likelihood of Tham Than Nam Lot Yai in southern Thailand participating in this network but it is not impossible.

The green network also equates to an unknown primary or secondary copper production signature. However, Hebuoso and Shangxihe, near Kunming, sit at what appears to be the apex of this distribution, which extends ca. 350 km northwest to Lijiang, ca. 600 km east to Andengyang in Guangxi, ca. 500 km southeast to Dai Trach, Gò Mun and Thành Dên in northern Vietnam, ca. 750 km southwest to Halin in north-central Myanmar and ca. 800 km south to Ban Phak Top in northern northeast Thailand. Again, rivers probably account for much of these passages, the Pearl River to Guangxi, the Red River to Vietnam and the aforementioned to Myanmar and possibly Thailand, including montane portage. These are also historic SSR routes.

The blue community equates to the central Lao Vilabouly Complex primary copper production signature, suggesting that metal (raw, semi-finished or finished product) were transported north, south and west over scales ranging from 300 km geodesic (Ban Non Wat) to 450 km geodesic (Tham Pà Ping) to 1100 km geodesic (Tham Than Nam Lot Yai) and 1300 km geodesic (Oakaie), also by the 10th or possibly 11th c. BC. We consider it unlikely that VC copper was exchanged ca. 770 km north to Yuanlongpo but the community identification does not interpret for us and can be used to check future typo-technological associations between these areas (Ciarla 2007). For the northeast Thai sites (and Ban Non Wat has VC signature metal by the Iron Age, Pryce *et al.* 2014), river routes do seem most likely, using the Mekong and its tributaries. However, for the southern Thai and north-central Myanma assemblages it is again unknown; though marine transport is likely for the south, and even a cross-peninsular transportation and mounting the Irrawaddy River could explain the western distribution. There is no indication that VC metal was exchanged into northern Vietnam or Yunnan but Tham Pà Ping does approach the current Lao:Viet border.

The yellow community equates to the central Thai Khao Wong Prachan Valley primary copper production signature, suggesting that raw metal, semi-finished or finished goods were transported east to the relatively nearby site of Ban Non Wat at ca. 180 km distance, but also to Halin and Oakaie, ca. 1000 km to the NNE by the 10th c. BC. Despite being the largest known sites for prehistoric copper production in MSEA (Pigott & Pryce 2022; Pigott *et al.* 1997; Pryce *et al.* 2010), it has long been noted that the distribution for this copper, as reconstructed by lead isotope-based provenance studies, seems to have been limited (see Pryce *et al.* 2011b; 2014 for possible explanations) and has never been detected in Iron Age consumption assemblages. Given the lack of intermediary sites with KWPV-compatible metal assemblages, the route between central Thailand and north-central Myanmar is unknown, but is probably considerably longer than the geodesic track and may have involved multiple actors. There is no indication that KWPV metal moved north to be consumed in northern northeast Thailand, Laos, Vietnam, Guangxi and Yunnan.

While neither the yellow nor blue communities map onto historic SSR routes they are certainly coeval with the orange and green communities, which do so map. Indeed, one might have to look at historic Maritime Silk Road pathways to explain part of the yellow and blue community distributions; the MSR also being suspected of greater antiquity than historical data allow for (Bellina 2014; Dussubieux & Bellina 2018). It is notable that while varying our threshold from 75-95% did impact the number of groups of artefacts detected, the communities of sites remained stable, which hints our reconstructions may have some resilience.

Finally, we wish to give consideration to the respective social exchange mechanisms represented by the Bronze Age metal network and the historical SSR. The SSR represented in Figure 1, for the Nanzhao-Dali period, 7th-13th c. AD, was ultimately a means of supplying required commodities, horses, tea, precious metals, from frontier regions to the imperial state capital at Xi'an. It was a tribute and/or profit-driven phenomenon of a powerful and hierarchical central state (Yang 2008). As Yang (2008) also notes, this was not the origin of the historical period SSR in the 3rd-2nd c. BC, which was a process motivated by Han military ambitions to seek a direct path to central Asia. From what can be reconstructed of Early Bronze Age MSEA metallurgy, copper/bronze production and consumption behaviours were not solely motivated by market forces for commodities (Pryce 2009; Pryce *et al.* 2010; White & Hamilton 2019; White & Pigott 1996). In late 2nd-early/mid-1st millennium BC MSEA, and in particular the most studied MSEA regions of north-central Myanmar and northeast and central Thailand, copper-base metal has a weak but not invisible correlation with hierarchical behaviours. Instead metal was made and used by and within small, probably independent, communities, both at the few (KWPV, VC and PL) primary production sites (Cadet *et al.* 2022; Pigott 2019; Pryce *et al.* 2010; 2011c; 2011a), and also at the more widespread secondary production and consumptions sites (Hamilton & White 2019; White 2019). There is even solid lead isotope evidence for the movement of copper-base metals *and production materials* (slag and/or ore) between primary productions centres, strongly suggesting an at least partial basis of gifting in metal exchange (as per SEALIP/TH/NPW/1, excluded from our threshold calculation Pryce *et al.* 2011b; 2014). With the probable exception of Ban Non Wat in southern northeast Thailand (Higham 2011; 2022), and possibly those of Khok Charoen in central Thailand and Oakaie/Halin in north-central Thailand (Pradier 2022), the appearance and adoption of copper-base metal does not seem to be coeval with noticeable shifts away from pre-existing Neolithic modes of life (Higham 2021; Higham & Cawte 2021; Pradier 2022; Pradier *et al.* 2019; Pryce *et al.* 2018b; in press; White 2019).

Notwithstanding our unwillingness to push our argument into unfamiliar archaeometallurgical territory, namely the provinces of Sichuan, Guangxi, Guangdong and Guizhou, perhaps the termination of our reconstructed networks (Figures 17 & 18) in Yunnan is indicative of the socio-political reality of late 2nd-early-mid 1st millennium BC southern China. If the Han conquest of the Dian kingdom in the 2nd c. BC was intended to subdue a 'frontier' territory and population, then perhaps the relatively integrated southern metal networks simply did not exist into central China 800-900 years prior. That is not to say no contact or interaction, but not of the intensity that saw KWPV and VC metals move over 1000 km geodesic from the very outset of the Myanmar Bronze Age (Pryce *et al.* 2018a), as well as the Yunnan-centred distributions evidenced in this paper. That the Vietnamese Bronze Age does not fit the general MSEA pattern, recalls the 3rd c. BC SSR network as reconstructed in Figure 2. In conclusion, we do not argue for a literal prehistoric incarnation of the historic SSR with all its associated economic and political associations. Rather we posit that the long-dated pre-existence of widespread connectivity of reasonable intensity, via

rivers and possibly across mountain ranges, would have allowed the SSR to flourish once the Han state achieved control of Yunnan.

Acknowledgments

We offer our particular thanks to Daw Kalayar Myat Myat Htwe, who has longstanding interests in Myanmar archaeometallurgy and who helped us obtain the geological samples for this study, and also Daw Cherry Thin, who allowed us access to previously excavated material in the Halin National Musem. The freshly excavated samples came from the fieldwork of the *Mission Archéologique Française au Myanmar*, which was funded by the *Commission Consultative de Fouilles* of the *Ministère de l'Europe et des Affaires Etrangères* during the period 2013-2020. The analytical data in this paper derive from the *Agence National de Recherche*-funded project 'BROGLASEA' (https://anr.fr/Project-ANR-16-CE27-0011). The statistical processing of BROGLASEA data was conducted under the auspices of the *Fondation Fyssen*-funded project, 'Network Analysis for Archaeometallurgy, and Beyond' (NAAMB). We also thank the National Institute for Mathematical and Biological Synthesis (NIMBioS) for the IT support. We wish to thank the two anonymous reviewers for their constructive criticism.

References

Aebischer, S., C. Cloquet, J. Carignan, C. Maurice & R. Pienitz, 2015. Disruption of the geochemical metal cycle during mining: Multiple isotope studies of lake sediments from Schefferville, subarctic Québec, *Chemical Geology* 412, 167–78.

Anon., 2020. *Wuming Matou Xianqinmu [The Pre-Qin Tombs in Matou, Wuming]*. Beijing: Wenwu chubanshe.

Bellina, B., 2003. Beads, social change and interaction between India and Southeast Asia, *Antiquity* 77(296), 285–97.

Bellina, B., 2014. Maritime Silk Roads' Ornament Industries: Socio-political Practices and Cultural Transfers in the South China Sea, *Cambridge Archaeological Journal* 24, 345–77.

Bellina, B., A. Favereau & L. Dussubieux, 2019. Southeast Asian early Maritime Silk Road trading polities' hinterland and the sea-nomads of the Isthmus of Kra, *Journal of Anthropological Archaeology* 54, 102–20.

Bellina, B., M.S. Win, K.M.M. Htwe, H.M. Thu, C. Castillo, C. Colonna, L. Dussubieux, A. Favereau, E. Miyama, B. Pradier, T.O. Pryce, S. Srikanlaya & E. Trivière, 2018. Myanmar's earliest Maritime Silk Road port-settlements revealed, *Antiquity* 92(366), .

Bellina, B.H.M. & I.C. Glover, 2004. The archaeology of early contacts with India and the Mediterranean World from the fourth century BC to the fourth century AD, in *Southeast Asia, from the Prehistory to History*. I.C. Glover&P. Bellwood. London: Routledge/Curzon Press, 68–89.

Bennett, A. & I. Glover, 2012. The high-tin bronzes of Thailand, in *Proceedings of the 5th Forbes Symposium on Ancient Asian Bronzes*, eds. P. Jett, B. McCarthy & J.G. Douglas. Washington D.C.: Smithsonian, 101–14.

Bray, P.J., A. Cuénod, C. Gosden, P. Hommel, R. Liu & A.M. Pollard, 2015. Form and flow: the 'karmic cycle' of copper, *Journal of Archaeological Science* 56, 202–9.

Cadet, M., T.O. Pryce, P. Dillmann, T. Sayavongkhamdy, V. Souksavatdy, T. Luangkhoth & N. Chang, 2022. Technological reconstruction of the late prehistoric primary copper production of the Vilabouly Complex (central Laos), *Archaeological and Anthropological Sciences* 14(8), 141.

Cadet, M., T. Sayavongkhamdy, V. Souksavatdy, T. Luangkhoth, P. Dillmann, C. Cloquet, J. Vernet, P. Piccardo, N. Chang, J. Edgar, E. Foy & T.O. Pryce, 2019. Laos' central role in Southeast Asian copper exchange networks: A multi-method study of bronzes from the Vilabouly Complex, *Journal of Archaeological Science* 109, 104988.

Chen, D., Y. Yang, J. Du, X. Tang & W. Luo, 2020. Alloy ratio and raw material sourcing of Warring States Period bronze bracelets in Huili County, Southwest China by pXRF and MC-ICP-MS, *Heritage Science* 8(1), 69.

Ciarla, R., 2007. Rethinking Yuanlongpo: the case for technological links between the Lingnan (PRC) and central Thailand in the Bronze Age, *East and West* 57, 305–28.

Claudius, P., 1406. *Geographia [Translated by Jacobus Angeli]*. Rome.

Cloquet, C., J. Carignan & G. Libourel, 2006. Atmospheric pollutant dispersion around an urban area using trace metal concentrations and Pb isotopic compositions in epiphytic lichens, *Atmospheric Environment* 40(3), 574–87.

Csárdi, G. & T. Nepusz, 2006. The igraph software package for complex network research, *InterJournal, complex systems* 1695, 1–9.

Cui, J. & X. Wu, 2008. The archaeological research of lead isotopes: examples of bronzes from Yunnan, China, and Vietnam, *Wenwu*.

Dussubieux, L. & B. Bellina, 2018. Glass ornament production and trade polities in the Upper-Thai Peninsula during the Early Iron Age, *Archaeological Research in Asia* 13, 25–36.

Dussubieux, L. & T.O. Pryce, 2016. Myanmar's role in Iron Age interaction networks linking Southeast Asia and India: Recent glass and copper-base metal exchange research from the Mission Archéologique Française au Myanmar, *Journal of Archaeological Science: Reports* 5, 598–614.

Favereau, A., T.O. Pryce, T.T. Win, L. Champion, T.T. Win, K.M.M. Htwe, A.A. Mar, B. Pradier & A. Willis, 2018. Étude du mobilier céramique de deux cimetières de la fin du deuxième au début du premier millénaire avant notre ère en Haute Birmanie : technologie, typologie et chronologie, *Bulletin de l'Ecole française d'Extrême-Orient* 104, 33–61.

Fuxi, G., 2009. Ancient glass research along the Silk Road, in *Origin and Evolution of Ancient Chinese Glass*, eds. G. Fuxi, R. Brill & T. Shoutun. Singapore: World Scientific, 1–40.

Georjon, C., U.A.A. Kyaw, D.T.T. Win, D.T.T. Win, B. Pradier, A. Willis, P. Petchey, Y. Iizuka, E. Gonthier, J. Pelegrin, B. Bellina & T.O. Pryce, 2021. Late Neolithic to Early-Mid Bronze Age semi-precious stone bead production and consumption at Oakaie and Nyaung'gan in central-northern Myanmar, *Archaeological Research in Asia* 25, 100240.

Grujić, J. & M. Radivojević, forthcoming. Community Detection, in *Oxford Handbook of Archaeological Network Research*, eds. T. Brughmans, B. Mills, J. Munson & M.A. Peeples. Oxford: Oxford University Press.

Hamilton, E.G. & J.C. White, 2019. The archaeometallurgy of prehistoric northern northeast Thailand in regional context, in *Ban Chiang, Northeast Thailand, Volume 2C: The Metal Remains in Regional Context*, eds. J.C. White & E.G. Hamilton. Philadelphia, P.A.: University of Pennsylvania Press, 65–121.

Higham, C., 2011. The Bronze Age of Southeast Asia: New Insight on Social Change from Ban Non Wat, *Cambridge Archaeological Journal* 21(3), 365–89.

Higham, C., 2022. Stasis or stimulus? Exotic materials and social display in Southeast Asia: Response to Pfaffenberger, *Advances in Archaeomaterials* 3(1), 34–43.

Higham, C.F., 2017. First farmers in Mainland Southeast Asia, *Journal of Indo-Pacific Archaeology* 41, 13–21.

Higham, C.F.W., 2021. The later prehistory of Southeast Asia and southern China: the impact of exchange, farming and metallurgy, *Asian Archaeology* 4(2), 63–93.

Higham, C.F.W. & H. Cawte, 2021. Bronze Metallurgy in Southeast Asia with Particular Reference to Northeast Thailand, *Journal of World Prehistory* 34(1), 1–46.

Higham, C.F.W., K. Douka & T.F.G. Higham, 2015. A New Chronology for the Bronze Age of Northeastern Thailand and Its Implications for Southeast Asian Prehistory, *PLOS One* 10, e0137542.

Higham, T.F.G., A.D. Weiss, C.F.W. Higham, C.B. Ramsey, J. d'Alpoim Guedes, S. Hanson, S.A. Weber, F. Rispoli, R. Ciarla, T.O. Pryce & V.C. Pigott, 2020. A prehistoric copper-production centre in central Thailand: its dating and wider implications, *Antiquity* 94(376), 948–65.

Huang, Q., 2020. Ancient Glass Technology in South and Southwest China, in *Development History of Ancient Chinese Glass Technology* (Series on Archaeology and History of Science in China Volume 3). : World Scientific, 509–57.

Hudson, B. & N. Lwin, 2012. Earthernware from a firing site in Myanmar (Burma) dates to more than 4500 years ago, *Bulletin of the Indo-Pacific Prehistory Association* 32(0), 19–22.

Hung, H.-C., Y. Iizuka, P. Bellwood, K.D. Nguyene, B. Bellina, P. Silapanth, E. Dizon, R. Santiago, I. Datani & J.H. Manton, 2007. Ancient jades map 3,000 years of prehistoric exchange in Southeast Asia, *Proceedings of the National Academy of Sciences* 104(50), 19745–50.

Jiang, J., G. Lu, Q. Wang & S. Wei, 2021. The analysis and identification of charred suspected tea remains unearthed from Warring State Period Tomb, *Scientific Reports* 11(1), 16557.

Kamvong, T. & K. Zaw, 2009. The origin and evolution of skarn-forming fluids from the Phu Lon deposit, northern Loei Fold Belt, Thailand: Evidence from fluid inclusion and sulfur isotope studies, *Journal of Asian Earth Sciences* 34, 624–33.

Killick, D.J., J.A. Stephens & T.R. Fenn, 2020. Geological constraints on the use of lead isotopes for provenance in archaeometallurgy, *Archaeometry* 62(S1), 86–105.

LaTouche, T.D. & J.C. Brown, 1909. The Silver-Lead Mines of Bawdwin, Northern Shan States, *RGSI* 27(3), 235–63.

Li, Y., C. Zhang, W.T.T. Taylor, L. Chen, R.K. Flad, N. Boivin, H. Liu, Y. You, J. Wang, M. Ren, T. Xi, Y. Han, R. Wen & J. Ma, 2020. Early evidence for mounted horseback riding in northwest China, *Proceedings of the National Academy of Sciences* 117(47), 29569–76.

Linduff, K.M. & J. Mei, 2009. Metallurgy in Ancient Eastern Asia: Retrospect and Prospects, *Journal of World Prehistory* 22, 265–81.

Liu, R., A.M. Pollard, Q. Cao, C. Liu, V. Sainsbury, P. Howarth, P. Bray, L. Huan, B. Yao, Y. Fu & J. Tang, 2020. Social hierarchy and the choice of metal recycling at Anyang, the last capital of Bronze Age Shang China, *Scientific Reports* 10(1), 18794.

Lu, H., J. Zhang, Y. Yang, X. Yang, B. Xu, W. Yang, T. Tong, S. Jin, C. Shen, H. Rao, X. Li, H. Lu, D.Q. Fuller, L. Wang, C. Wang, D. Xu & N. Wu, 2016. Earliest tea as evidence for one branch of the Silk Road across the Tibetan Plateau, *Scientific Reports* 6, 18955.

Ma, M., Y. Lu, G. Dong, L. Ren, R. Min, L. Kang, Z. Zhu, X. Li, B. Li, Z. Yang, N. Cili, R. Liu, Y. Gao & F. Chen, 2022. Understanding the transport networks complex between South Asia, Southeast Asia and China during the late Neolithic and Bronze Age, *The Holocene* 09596836221131698.

Manhes, G., C.J. Allègre, B. Dupré & B. Hamelin, 1980. Lead isotope study of basic-ultrabasic layered complexes: Speculations about the age of the earth and primitive mantle characteristics, *Earth and Planetary Science Letters* 47(3), 370–82.

Moore, E. & P. Pauk, 2001. Nyaung-gan: A preliminary note on a Bronze Age cemetery near Mandalay, Myanmar (Burma), *Asian Perspectives* 40, 35–47.

Natapintu, S., 1988. Current Research on ancient copper-base metallurgy in Thailand, in *Prehistoric Studies: The Stone and Metal Ages in Thailand*, eds. P. Charoenwongsa & B. Bronson. Bangkok: The Thai Antiquity Working Group, 107–24.

Pautreau, J.-P., Ch. Maitay & A.A. Kyaw, 2010. Level of Neolithic occupation and 14C dating at Ywa Gon Gyi, Samon valley (Myanmar), *Aséanie* 25, 11–22.

Pigott, V.C., 2019. Prehistoric copper mining and smelting in Southeast Asia: evidence from Thailand and Laos, in *Ban Chiang, Northeast Thailand, Volume 2C: The Metal Remains in Regional Context*, eds. J.C. White & E.G. Hamilton. Philadelphia, P.A.: University of Pennsylvania Press, 5–56.

Pigott, V.C. & T.O. Pryce, 2022. Prehistoric Copper Production and Exchange in Southeast Asia, in *The Oxford Handbook of Early Southeast Asia*, eds. C.F.W. Higham & N.C. Kim. Oxford: Oxford University Press, 430–57.

Pigott, V.C. & G. Weisgerber, 1998. Mining archaeology in geological context. The prehistoric copper mining complex at Phu Lon, Nong Khai Province, northeast Thailand, in *Metallurgica Antiqua: In Honour of Hans-Gert Bachmann and Robert Maddin*, eds. T. Rehren, A. Hauptmann & J.D. Muhly. Bochum: Deutsches Bergbau-Museum Bochum, pp. 135-161, 135–61.

Pigott, V.C., A. Weiss & S. Natapintu, 1997. Archaeology of copper production: Excavations in the Khao Wong Prachan Valley, central Thailand, in *South-East Asian Archaeology 1992. Proceedings of the Fourth International Conference of the European Association of South-East Asian Archaeologists. Rome, 28th September - 4th October 1992*, eds. R. Ciarla & F. Rispoli. Rome: Istituto Italiano per l'Africa e l'Oriente, pp 119-157, 119–57.

Pollard, A.M., 2009. What a long, strange Trip it's been: Lead Isotopes and Archaeology, in *From Mine to Microscope: Advances in the Study of Ancient Technology*, eds. A.J. Shortland, I. Freestone, T. Rehren & M.S. Tite. Oxford: Oxbow Books, 181–89.

Polo, M., 1918. *The Travels of Marco Polo*. London: J.M. Dent & Sons.

Pradier, B., 2022. *Archéologie Funéraire de La Fin de La Préhistoire de La Région Centrale Du Myanmar (Birmanie)*, Université de Paris-Nanterre.

Pradier, B., U. Aung Aung Kyaw, D. Tin Tin Win, A. Willis, A. Favereau, F. Valentin & T.O. Pryce, 2019. Pratiques funéraires et dynamique spatiale à Oakaie 1, une nécropole à la transition du Néolithique à l'Âge du Bronze au Myanmar (Birmanie) / Funerary practices and spatial dynamic at Oakaie 1, a burial ground at the transition of the Neolithic and Bronze Age in Myanmar (Burma), *Société Préhistorique française* 116(3), 539–60.

Pryce, T., M. Cadet, F. Allard, N. Kim, T.H. Hiep, L.T.M. Dung, W. Lam & E. Foy, 2022a. Copper-base metal supply during the northern Vietnamese Bronze and Iron Ages: metallographic, elemental, and lead isotope data from Dai Trach, Thành Dên, Gò Mun, and Xuân Lâp, *Archaeological and Anthropological Sciences* 14(1), 16.

Pryce, T.O., 2009. *Prehistoric Copper Production and Technological Reproduction in the Khao Wong Prachan Valley of Central Thailand*, University College London.

Pryce, T.O., 2011. The excavation of Ban Non Wat: The Bronze Age, in *XIX Technical Analysis of Bronze Age Ban Non Wat Copper-Base Artefacts*, eds. C.F.W. Higham & A. Kijngam. Bangkok: The Fine Arts Department, 489–98.

Pryce, T.O., 2014. Metallurgy in Southeast Asia, (ed.)Selin, H. *Encyclopaedia of the History of Science, Technology, and Medicine in Non-Western Cultures* 3, 1–17.

Pryce, T.O., 2018. Initiating discourse on the (multi?) directionality of the Mainland Southeast Asian Bronze Age transition., in *Proceedings of the Ninth International Conference on the Beginings of the Use of Metals and Alloys BUMA-IX: Messages from the History of Metals to the Future Metal Age*. Busan, South Korea: Jea-Young Choi & Jank-Sik Park, 160–75.

Pryce, T.O., S. Baron, B.H.M. Bellina, P.S. Bellwood, N. Chang, P. Chattopadhyay, E. Dizon, I.C. Glover, E. Hamilton, C.F.W. Higham, A.A. Kyaw, V. Laychour, S. Natapintu, V. Nguyen, J.-P. Pautreau, E. Pernicka, V.C. Pigott, M. Pollard, C. Pottier, A. Reinecke, T. Sayavongkhamdy, V. Souksavatdy & J. White, 2014. More questions than answers: the Southeast Asian Lead Isotope Project 2009–2012, *Journal of Archaeological Science* 42, 273–94.

Pryce, T.O. & B. Bellina, 2018. High-tin bronze bowls and copper drums: Non-ferrous archaeometallurgical evidence for Khao Sek's involvement and role in regional exchange systems, *Archaeological Research in Asia* 13, 50–58.

Pryce, T.O., A.H. Bevan, R. Ciarla, F. Rispoli, J.L. Malakie, B. Hassett & C. Castillo, 2011a. Intensive archaeological survey in tropical environments: methodological and metallurgical insights from Khao Sai On, central Thailand, *Asian Perspectives* 50, 53–69.

Pryce, T.O., M. Brauns, N. Chang, E. Pernicka, M. Pollard, C. Ramsey, T. Rehren, V. Souksavatdy & T. Sayavongkhamdy, 2011b. Isotopic and technological variation in prehistoric primary Southeast Asian copper production, *Journal of Archaeological Science* 38, 3309–22.

Pryce, T.O., K.M.M. Htwe, M. Georgakopoulou, T. Martin, E. Vega, T. Rehren, T.T. Win, T.T. Win, P. Petchey, J. Innanchai & B. Pradier, 2018a. Metallurgical traditions and metal exchange networks in late prehistoric central Myanmar, c. 1000 BC to c. AD 500, *Archaeological and Anthropological Sciences* 10(5), 1087–1109.

Pryce, T.O., A.A. Kyaw, M.M. Kyaw, T.T. Win, T.T. Win, K.H. Win, M.M. Mon, M.M. Aye, S.H. Htay, A.A. Mar, B. Bellina, R.A. Bentley, L. Champion, C. Colonna, A.J. Cook, A. Favereau, D.Q. Fuller, C. Georjon, C.F.W. Higham, K.M.M. Htwe, Y. Iizuka, J. Innanchai, C. Le Meur, X. Peixoto, P. Petchey, R. Pinhasi, B. Pradier, F. Valentin, A. Willis & A. Zazzo, 2018b. A first absolute chronology for Late Neolithic to Early Bronze Age Myanmar: New data from the 2014-2016 seasons of the Mission Archéologique Française au Myanmar at Nyaung'gan and Oakaie, *Antiquity* (92), 690–708.

Pryce, T.O., W. Lam, M. Cadet, Z. Jiang, W. Yang & A. Yao, 2022b. A late 2nd/early 1st millennium BC interaction arc between Mainland Southeast Asia and Southwest China: Archaeometallurgical data from Hebosuo and Shangxihe, Yunnan, *Journal of Archaeological Science* 143, 105612.

Pryce, T.O., V.C. Pigott, M. Martinón-Torres & T. Rehren, 2010. Prehistoric Copper Production and Technological Reproduction in the Khao Wong Prachan Valley of Central Thailand., *Archaeological and Anthropological Sciences* 2, 237–64.

Pryce, T.O., M. Pollard, M. Martinòn-Torres, V.C. Pigott & E. Pernicka, 2011c. Southeast Asia's first isotopically-defined prehistoric copper production system: When did extractive metallurgy begin in the Khao Wong Prachan Valley of central Thailand?, *Archaeometry* 53, 146–63.

Pryce, T.O., B. Pradier, A. Favereau, U. Saw Naing Oo, C. Le Meur, D. Kay Thwe Oo, U. Arkar Aye, D. Thu Thu Win, K.A. Langowska, K. Hanus, Y. Iizuka, C. Georjon, Y. Zhuang, C.C. Castillo, D.Q. Fuller, D. Hlaing Sabai Win, L. Champion, U. Myo Minh Oo, U. Min Naing Oo, U. Zeyar Phyo, D. Khin Thidar Lin, U. Phyo Wai Mg, K. Atiphat Paibool, K. Varis Domethong, C.F.W. Higham & T.F.G. Higham, in press. Honing the Mainland Southeast Asian late prehistoric and early historic chronology: an 94 14C determination, up to four millennia, sequence from Halin in central-northern Myanmar, *Antiquity*.

R Core Team, 2021.

Radivojević, M. & J. Grujić, 2018. Community structure of copper supply networks in the prehistoric Balkans: An independent evaluation of the archaeological record from the 7th to the 4th millennium BC, *Journal of Complex Networks* 6(1), 106–24.

Rispoli, F., 2007. The Incised & Impressed Pottery Style of Mainland Southeast Asia Following the Paths of Neolithization, *East and West* 57, 235–304.

Sarjeant, C., 2014. *Contextualising the Neolithic Occupation of Southern Vietnam* (Terra Australis 42). Canberra: ANU Press.

Thirlwall, M.F., 2002. Multicollector ICP-MS analysis of Pb isotopes using a 207Pb - 204Pb double spike demonstrates up to 400 ppm/amu systematic errors in Tl-normalization, *Chemical Geology* 184(3–4), 255–79.

Traag, V.A., L. Waltman & N.J. van Eck, 2019. From Louvain to Leiden: guaranteeing well-connected communities, *Scientific Reports* 9(1), 5233.

Tucci, A., T. Sayavongkhamdy, N. Chang & V. Souksavatdy, 2014. Ancient Copper Mining in Laos: Heterarchies, Incipient States or Post-State Anarchists?, *Journal of Anthropology and Archaeology* 2, 1–15.

Venunan, P., S. Ploymukda, B. Boripon, P. Kwansakul, K. Suteerattanapirom & T.O. Pryce, 2022. A royal wreck? Morpho-technological, elemental and lead isotope analysis of ingots from the Bang Kachai II shipwreck, Thailand, *Journal of Archaeological Science: Reports* 42, 103414.

von Richthofen, F.F., 1877. *China: Ergebnisse Eigner Reisen Und Darauf Gegründeter Studien*. Berlin: Verlag von Dietrich Reimer.

Wan, X., 2013. *The Horse in Pre-Imperial China*, University of Pennsylvania.

White, J.C., 2019. Providing a Regional Socioeconomic Context for Prehistoric Metallurgy in Thailand, in *Ban Chiang, Northeast Thailand, Volume 2C: The Metal Remains in Regional Context*, eds. J.C. White & E.G. Hamilton. Philadelphia, P.A.: University of Pennsylvania Press, 1–4.

White, J.C. & E.G. Hamilton, 2019. Conclusions: Placing Metals in Social Contexts in Prehistoric Thailand, in *Ban Chiang, Northeast Thailand, Volume 2C: The Metal Remains in Regional Context*, eds. J.C. White & E.G. Hamilton. Philadelphia, P.A.: University of Pennsylvania Press, 155–83.

White, J.C. & V.C. Pigott, 1996. From Community Craft to Regional Specialisation: Intensification of Copper Production in Pre-State Thailand, in *Craft Specialization and Social Evolution: In Memory of V. Gordon Childe*, ed. B. Wailes. Philadelphia: University Museum Publications., 151–75.

Yang, B., 2004. Horses, Silver, and Cowries: Yunnan in Global Perspective, *Journal of World History* 15(3), 281–322.

Yang, B., 2008. *Between Winds and Clouds. The Making of Yunnan. Second Century BCE to Twentieth Century CE*. New York: Colombia University Press.

Yao, A., V. Darré, J. Zhilong, W. Lam & Y. Wei, 2020. Bridging the time gap in the Bronze Age of Southeast Asia and Southwest China, *Archaeological Research in Asia* 22, 100189.

Zou, G., J. Cui, X. Liu, X. Li & R. Min, 2019. Investigation of early Bronze Age civilizations in Yunnan: a scientific analysis of metallurgical relics found at the Guangfentou ruins in Jiangchuan, *Archaeological and Anthropological Sciences* 11(1), 15–31.

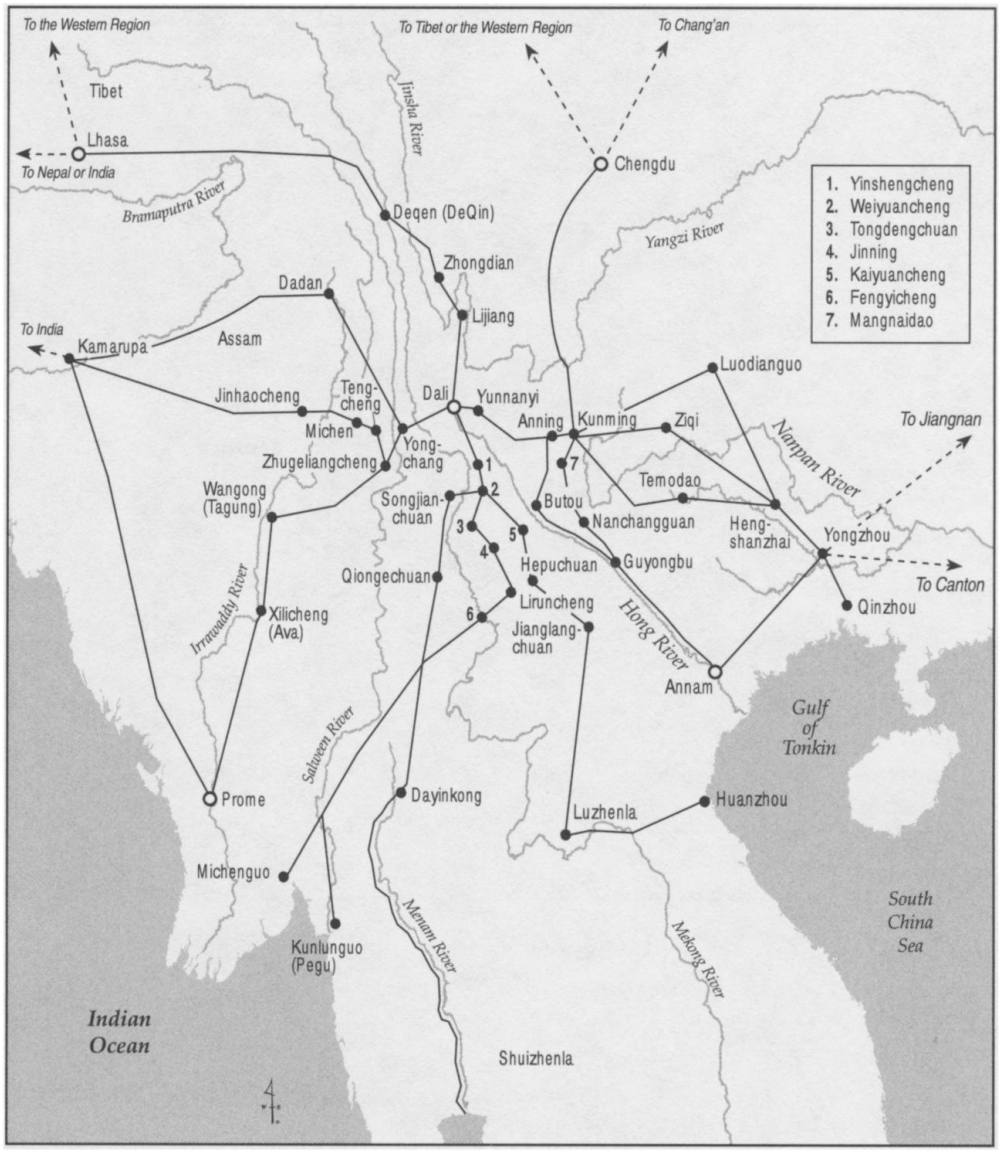

Figure 1: The SSR during the Nanzhao-Dali period, 7th-13th c. AD, reproduced with permission from (Yang 2004: Map 2).

274x314mm (120 x 120 DPI)

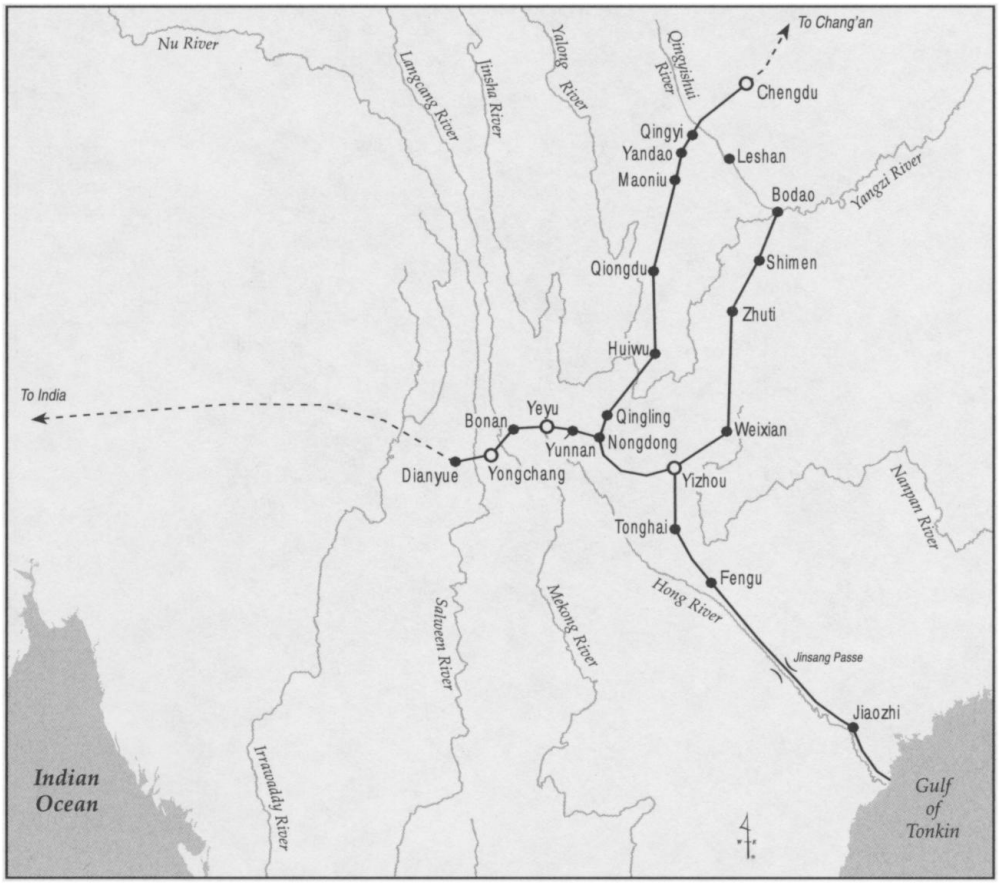

Figure 2: The SSR before the 3rd c. BC, reproduced with permission from (Yang 2004: Map 1), with the exclusion of Mainland Southeast Asia due to lack of textual sources.

275x242mm (120 x 120 DPI)

Figure 3: Excavations yielding copper-base artefacts for the present study, with respect to Halin village, the National Museum, and the southern part of the Pyu city wall (white line approximation).

458x329mm (72 x 72 DPI)

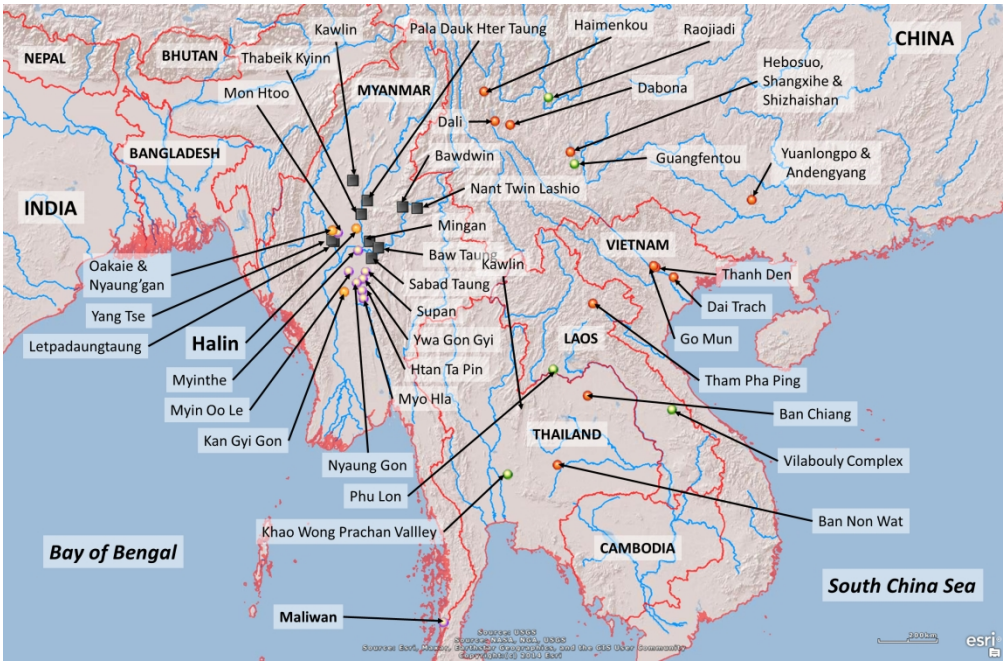

Figure 4: Map showing the present study sites/locations, terrain, major rivers and national boundaries. Black squares represent sampled mineralisations, pink circles represent Myanmar Iron Age consumption sites (excavated by the MAFM under the direction of J.-P. Pautreau), orange circles represent Myanmar Bronze Age – Bagan period consumption sites excavated by the MAFM (under the direction of the lead author), and red circles other consumption sites cited in the paper. Green circles represent the documented prehistoric copper producing centres with lead isotope characterisations.

445x293mm (150 x 150 DPI)

Figure 5: The study's archaeological artefacts. Please note missing image for SEALIP/MY/HLTP1/2.

592x317mm (150 x 150 DPI)

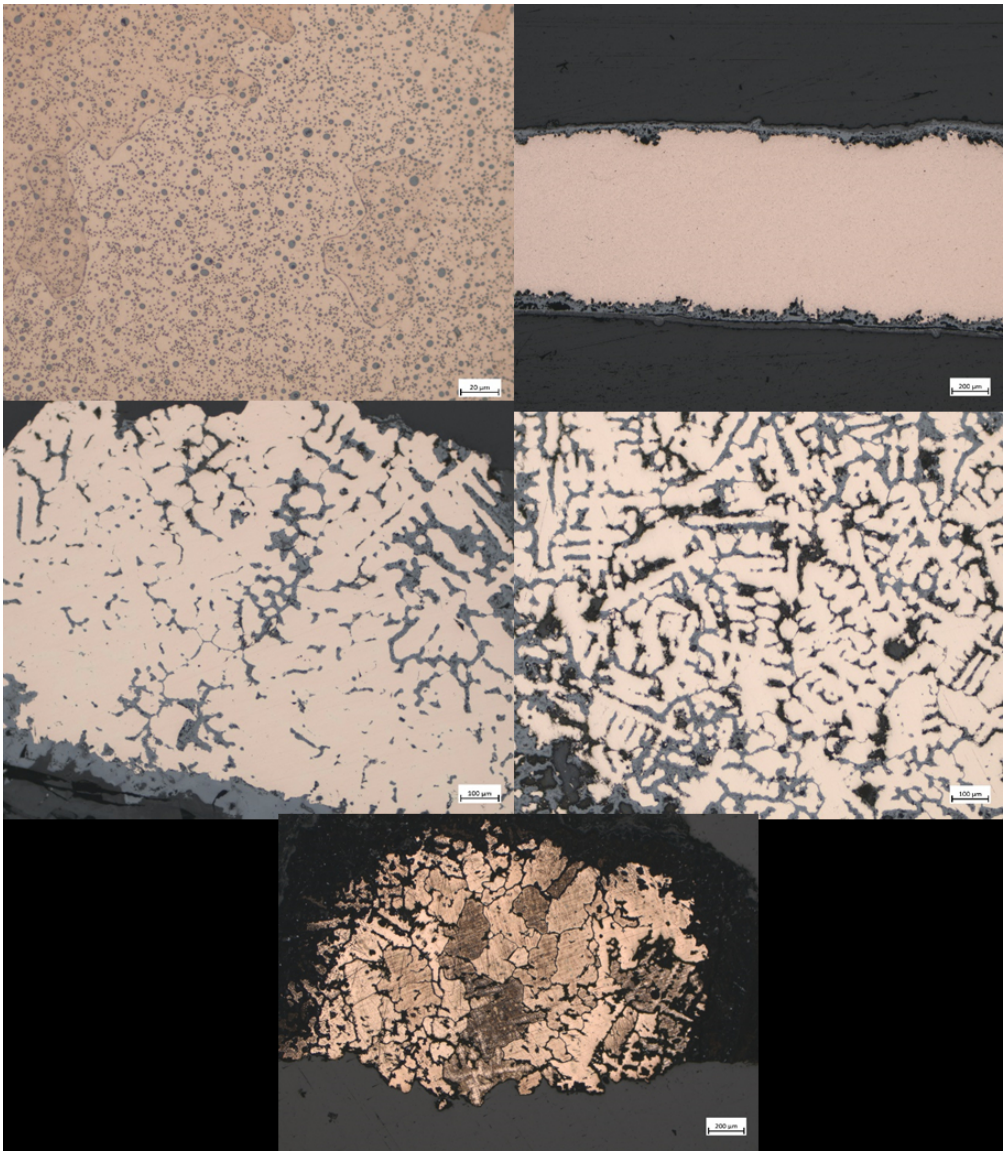

Figure 6: Optical micrographs. Top-left, as cast wire bundle (HL28/2) with round copper sulphide inclusions, top-right, wire bundle (HL28/5), bottom-left bronze cast bell/rattle (HL28/12) and bottom-right bronze as cast bangle (HL29-1/1). Bottom, a bronze ring with an as cast microstructure (HL29-1/7).

153x176mm (150 x 150 DPI)

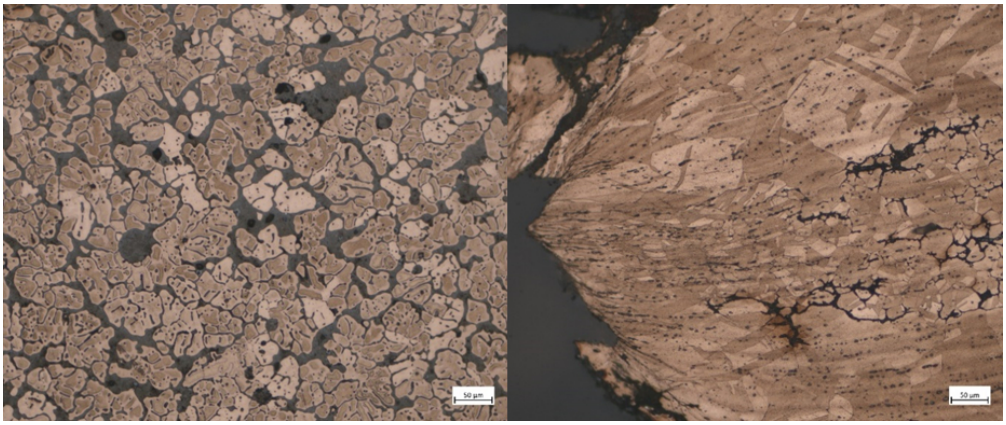

Figure 7: Optical micrographs, after etching. Left, a leaded-copper sample (NYG3/1) with an as cast structure. Right, a copper ring sample (HL29-1/8) which has been hammered and annealed.

156x65mm (150 x 150 DPI)

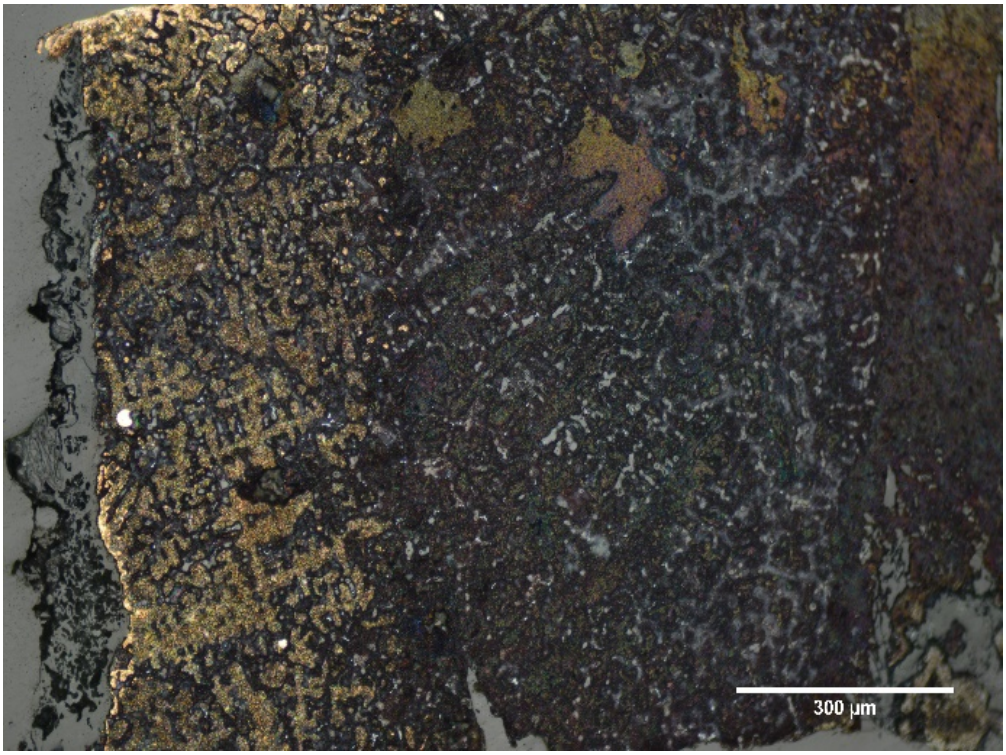

Figure 8: HL28/18 almost entirely composed of corrosion products but with an identifiably as-cast structure.

79x59mm (220 x 220 DPI)

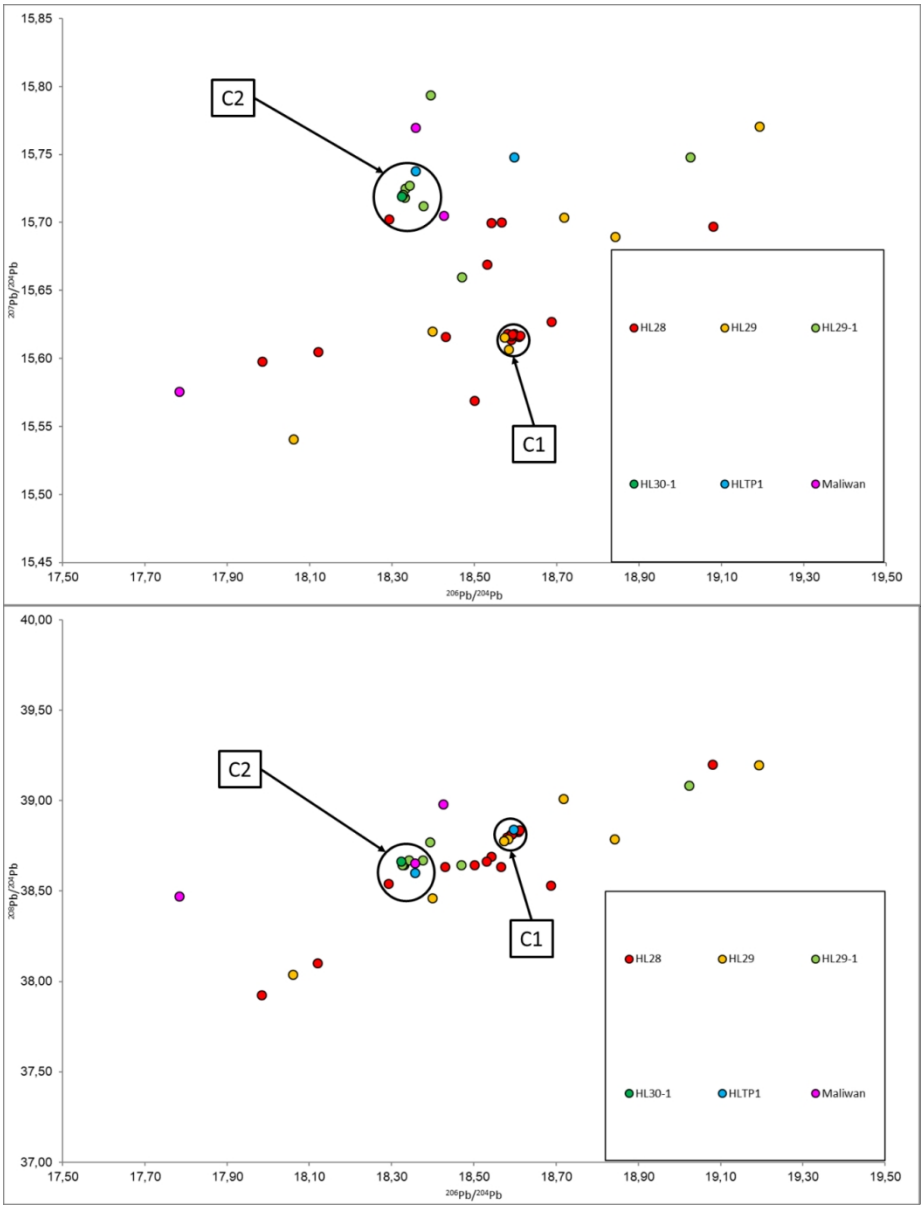

Figure 9: Lead isotope ratios for all Halin and Maliwan metal artefacts. C1 and C2 represent two clusters we consider identifiable within the new copper-base artefact data. Error bars are smaller than symbols.

155x202mm (220 x 220 DPI)

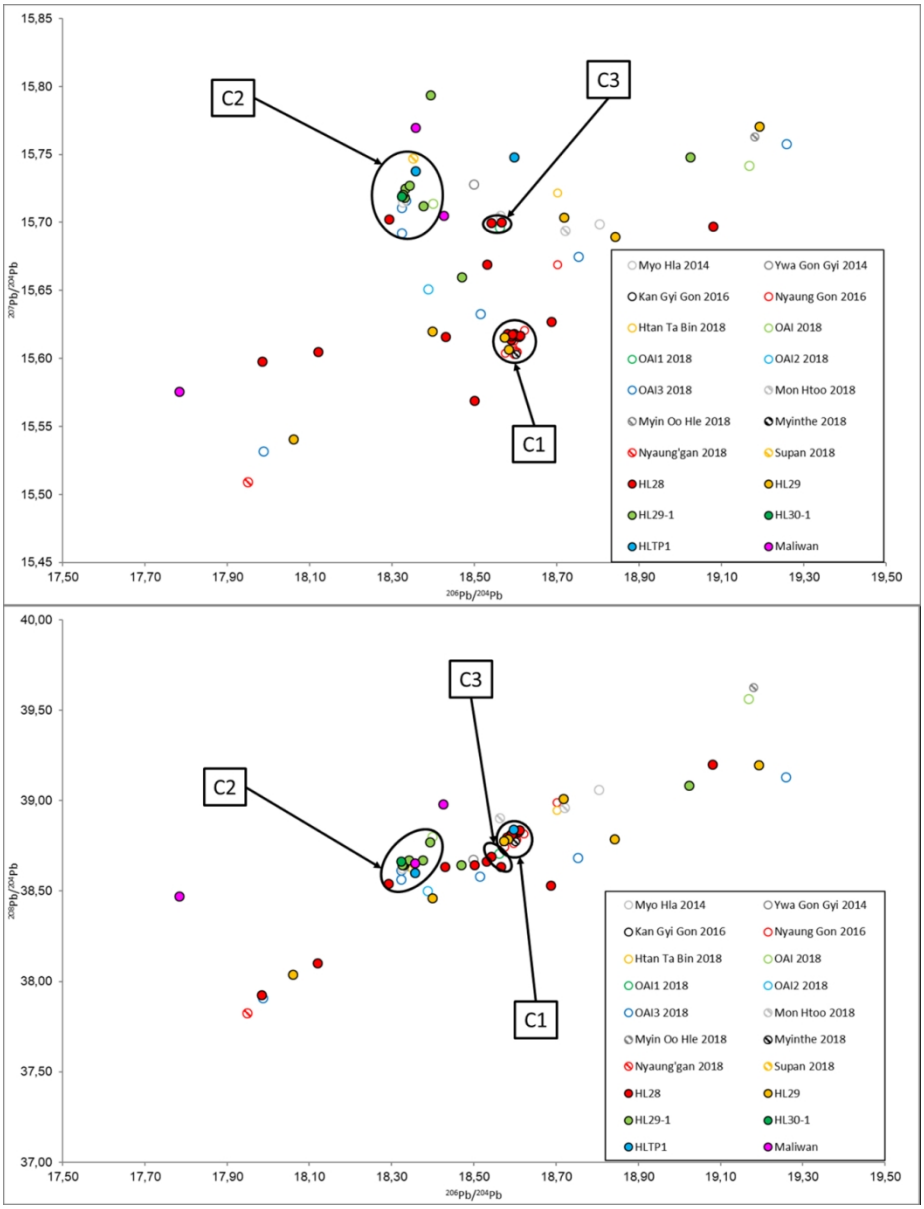

Figure 10: Lead isotope ratios for all Myanmar metal artefacts. C3 represents a cluster we consider identifiable once previously published Myanma data are included. Error bars are smaller than symbols. Published data from (Dussubieux & Pryce 2016; Pryce et al. 2018a; 2014).

154x201mm (220 x 220 DPI)

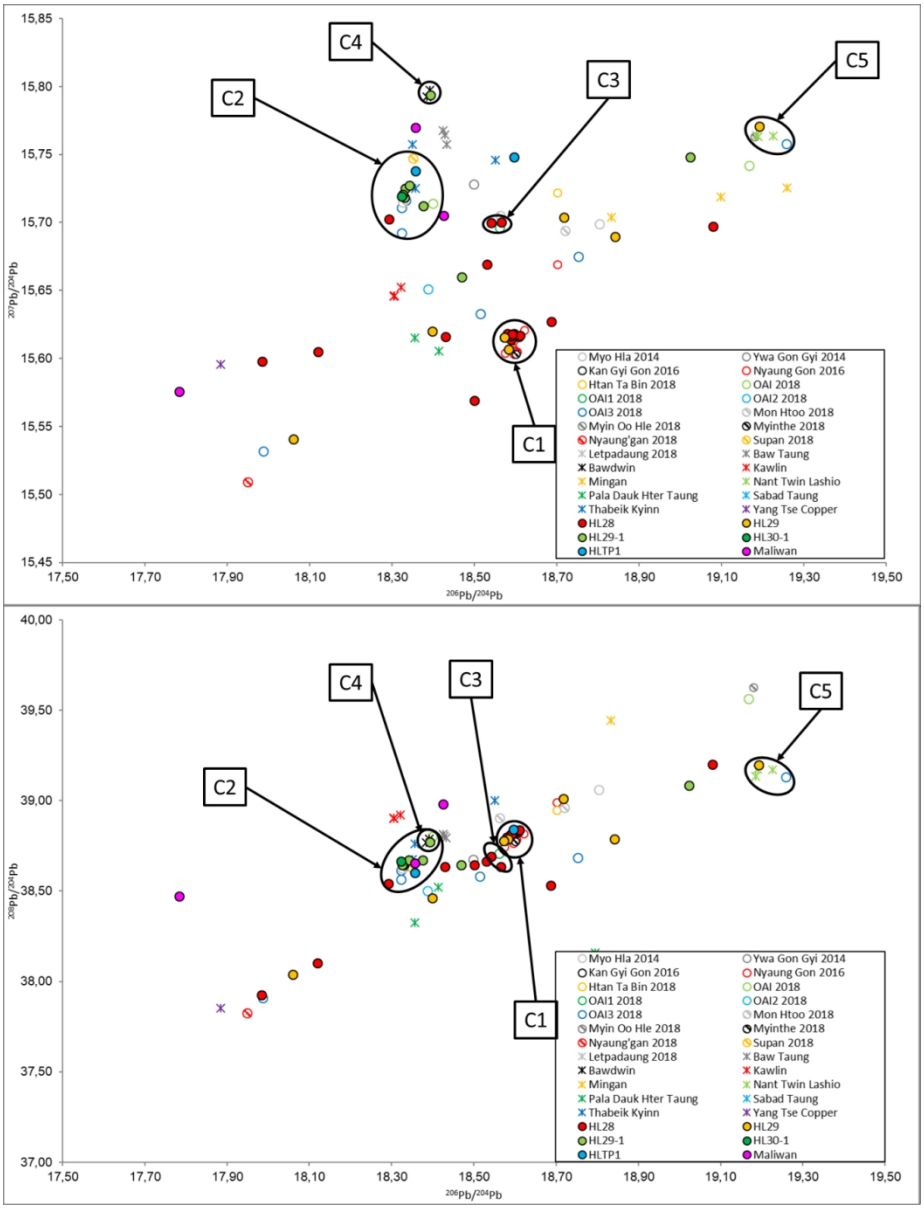

Figure 11: All Myanmar artefact and mineral LI data, representing all four stable isotope ratios. Letpadaung and Sabad Taung samples plot far to the left and right, respectively, and two Mingan samples plot off scale for 208Pb/204Pb ratios, so the axes are constrained for greater legibility. C4 and C5 represent two clusters we consider identifiable when Myanma mineral data are included. Symbols are larger than error bars.

155x202mm (220 x 220 DPI)

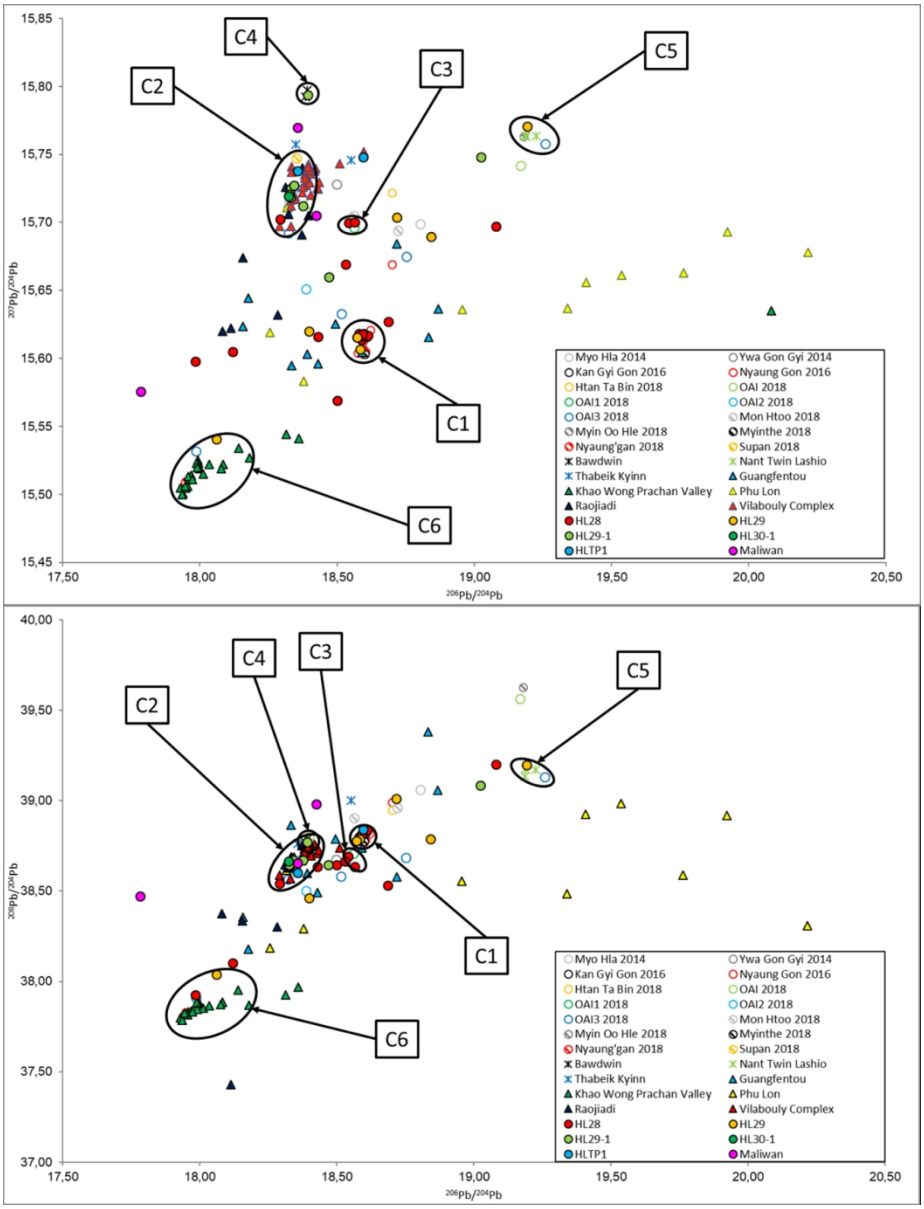

Figure 12: All Myanmar artefact plus mineral LI data deemed potentially relevant in the previous section, representing all four stable isotope ratios, plotted against published copper production systems in Thailand (Khao Wong Prachan Valley and Phu Lon), Laos (Vilabouly Complex), Yunnan (Guangfentou) and Sichuan (Raojiadi) (Chen et al. 2020; Pryce et al. 2022b; Zou et al. 2019). C6 is a cluster we consider identifiable once regional copper production data are included. Error bars are smaller than symbols.

154x201mm (220 x 220 DPI)

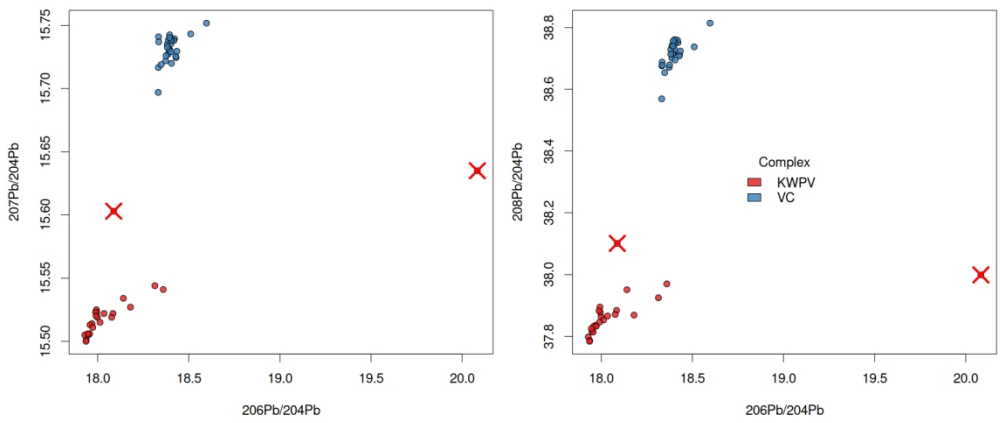

Figure 13: Biplots showing the relatively high, at a regional scale, consistency in LI ratios of slag and copper-base metal artefacts from the Khao Wong Prachan Valley (Non Pa Wai and Nil Kham Haeng) and the Vilabouly Complex (Puen Baolo and Thong Na Nguak). The two NPW outliers, a bronze axe and a slag fragment, are represented by a red cross.

447x192mm (96 x 96 DPI)

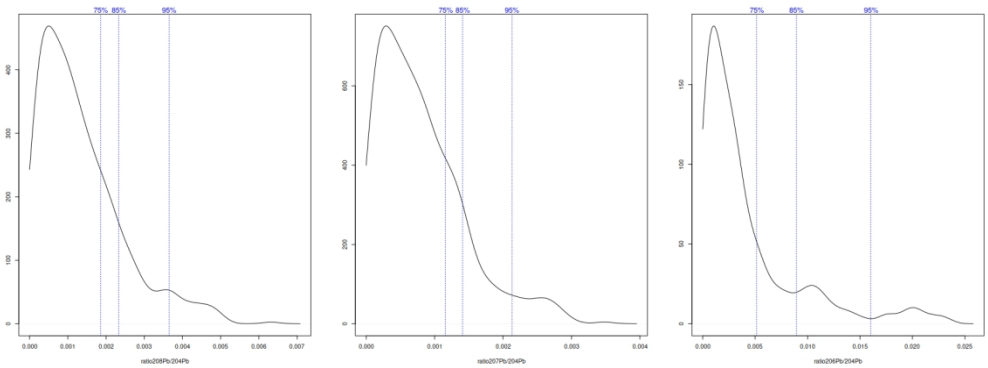

Figure 14: Distribution of distances between KWPV and VC samples for each lead isotope ratio. Vertical dashed blue lines represent the values for the 75,85 and 95 percentiles.

467x173mm (96 x 96 DPI)

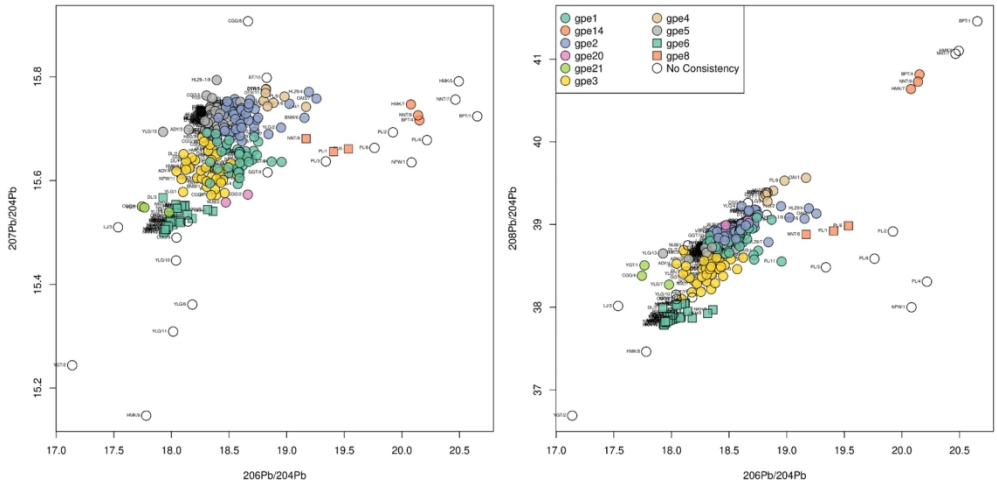

Figure 15: Biplots of LI data from regional Bronze Age assemblages, as processed by our defined consistency thresholds to identify groups of artefacts.

279x139mm (150 x 150 DPI)

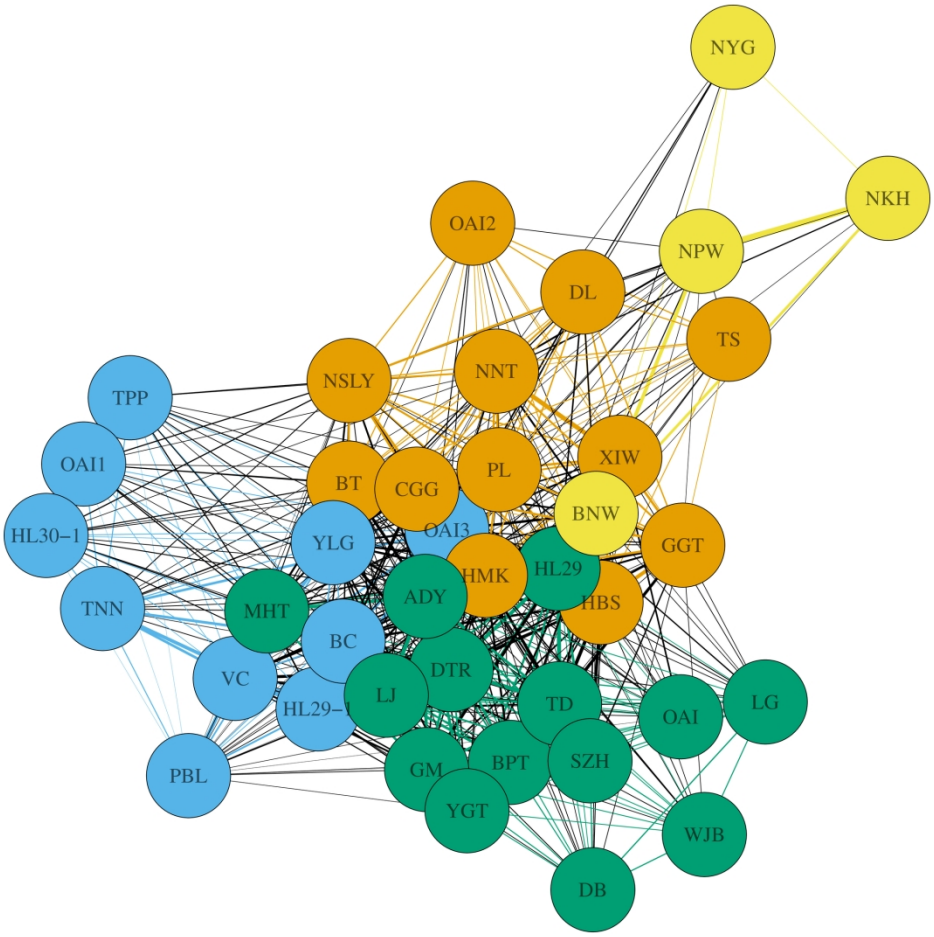

Figure 16: Network of sites based on shared artefacts from the same family, each node colour represent a different community detected by the Leuven community detection algorithm. The edges between nodes from within the same community are coloured using the colour of the community. The edges that link nodes from different communities are black.

203x203mm (300 x 300 DPI)

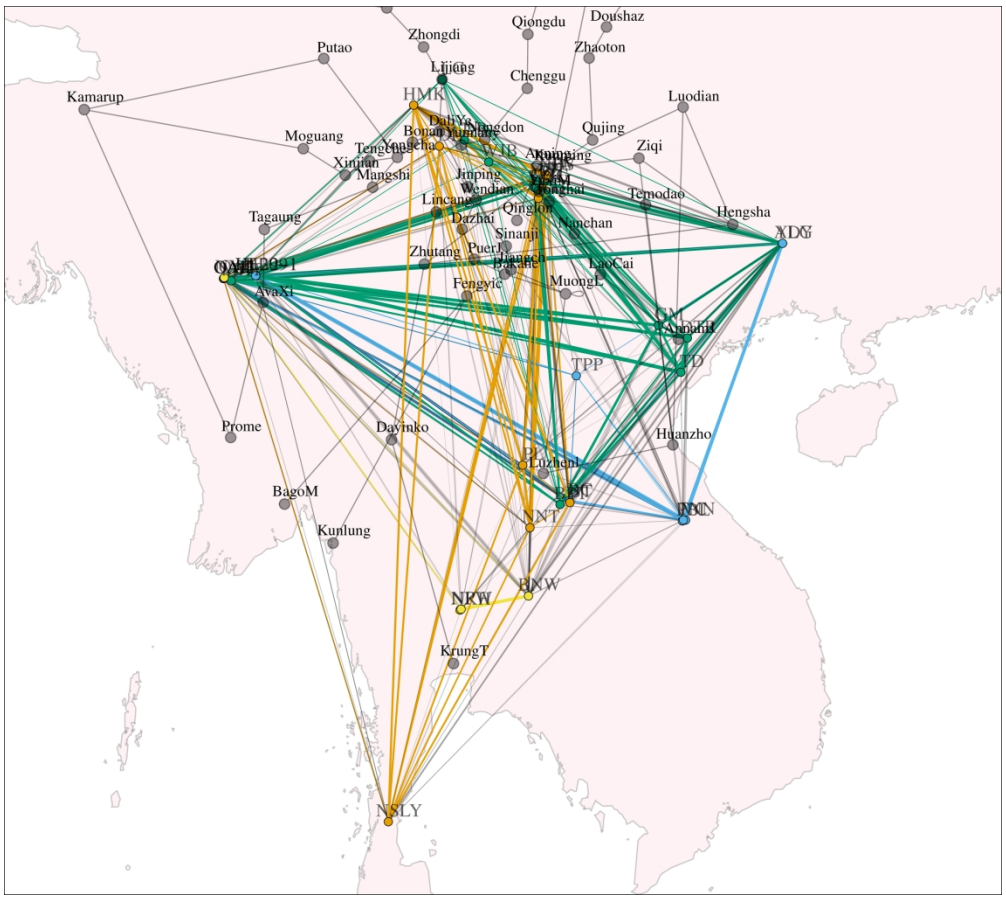

Figure 17: Map showing the reconstructed Nanzhao-Dali period SSR (from Figure 1), overlain with our calculated Myanmar multi-period and regional Bronze Age assemblage communities, using the same colour codes as for Figure 16.

228x203mm (300 x 300 DPI)

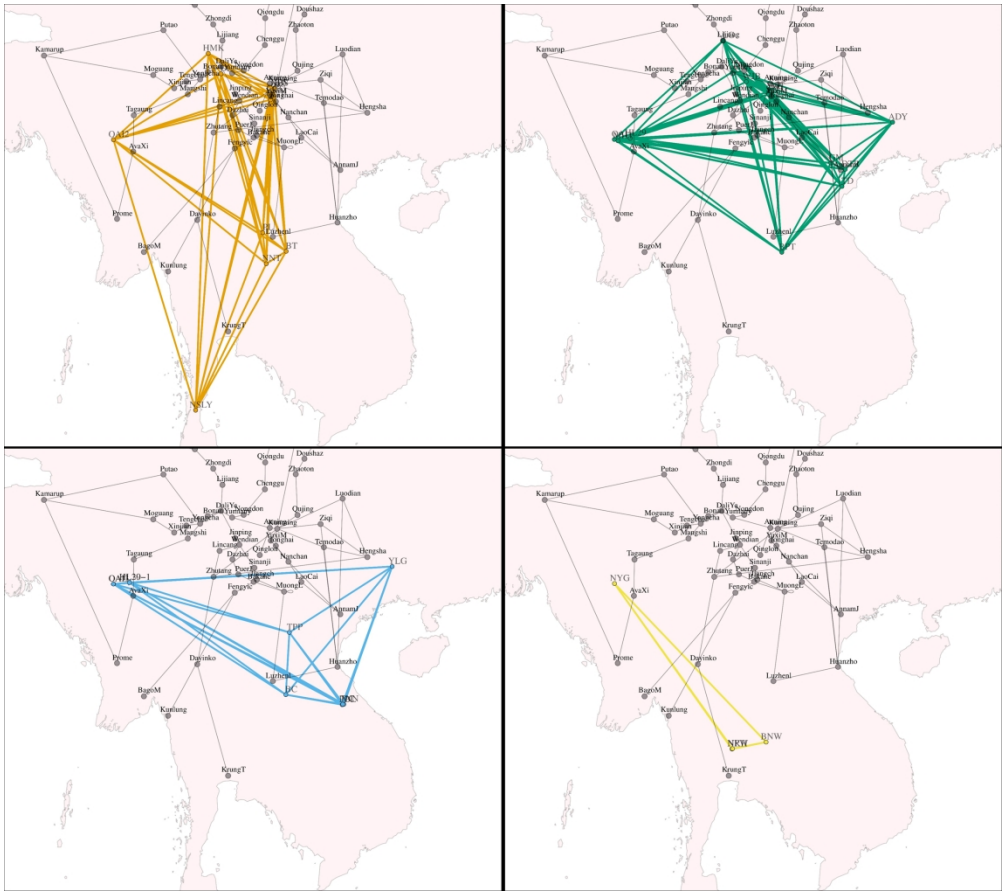

Figure 18: Maps detailing each calculated Bronze Age assemblage community. From top left, an unknown but Kunming-centred copper consumption network (orange), an unknown southern China-centred copper consumption network (green), the Vilabouly Complex copper production network (blue), and the Khao Wong Prachan Valley copper production network (yellow).

429x381mm (150 x 150 DPI)

	SEALIP ID	Site	Sample type	Artefact
1	SEALIP/MY/BAW/1	Baw Mountain, Kyaukse	Mineral	Cu mineral
2	SEALIP/MY/BAW/2	Baw Mountain, Kyaukse	Mineral	Cu mineral
3	SEALIP/MY/BAW/3	Baw Mountain, Kyaukse	Mineral	Cu mineral
4	SEALIP/MY/BWD/1	Bawdwin	Mineral	Cu mineral
5	SEALIP/MY/BWD/2	Bawdwin	Mineral	Cu mineral
6	SEALIP/MY/KAW/1	Kawlin	Mineral	Cu mineral
7	SEALIP/MY/KAW/2	Kawlin	Mineral	Cu mineral
8	SEALIP/MY/KAW/3	Kawlin	Mineral	Cu mineral
9	SEALIP/MY/MIN/1	Mingan	Mineral	Cu mineral
10	SEALIP/MY/MIN/2	Mingan	Mineral	Cu mineral
11	SEALIP/MY/MIN/3	Mingan	Mineral	Cu mineral
12	SEALIP/MY/NTL/1	Nant Twin village	Mineral	Cu mineral
13	SEALIP/MY/NTL/2	Nant Twin village	Mineral	Cu mineral
14	SEALIP/MY/NTL/3	Nant Twin village	Mineral	Cu mineral
15	SEALIP/MY/PDHT/1	Pala Dauk Hter Taung	Mineral	Cu mineral
16	SEALIP/MY/PDHT/2	Pala Dauk Hter Taung	Mineral	Cu mineral
17	SEALIP/MY/PDHT/3	Pala Dauk Hter Taung	Mineral	Cu mineral
18	SEALIP/MY/ST/1	Sabad Taung	Mineral	Cu mineral
19	SEALIP/MY/ST/2	Sabad Taung	Mineral	Cu mineral
20	SEALIP/MY/ST/3	Sabad Taung	Mineral	Cu mineral
21	SEALIP/MY/TKN/1	Thabeik Kyinn	Mineral	Cu mineral
22	SEALIP/MY/TKN/2	Thabeik Kyinn	Mineral	Cu mineral
23	SEALIP/MY/TKN/3	Thabeik Kyinn	Mineral	Cu mineral
24	SEALIP/MY/YTCM/1	Yang Tse Copper	Mineral equivalent	Cu ingot
25	SEALIP/MY/HL28/1	Halin HL28	Consumption artefact	wire bundle
26	SEALIP/MY/HL28/2	Halin HL28	Consumption artefact	wire bundle
27	SEALIP/MY/HL28/3	Halin HL28	Consumption artefact	wire bundle
28	SEALIP/MY/HL28/4	Halin HL28	Consumption artefact	wire bundle multi
29	SEALIP/MY/HL28/5	Halin HL28	Consumption artefact	wire bundle multi
30	SEALIP/MY/HL28/6	Halin HL28	Consumption artefact	wire bundle multi
31	SEALIP/MY/HL28/7	Halin HL28	Consumption artefact	wire bundle
32	SEALIP/MY/HL28/8	Halin HL28	Consumption artefact	wire bundle
33	SEALIP/MY/HL28/9	Halin HL28	Consumption artefact	wire bundle
34	SEALIP/MY/HL28/10	Halin HL28	Production artefact	possible casting spillage
35	SEALIP/MY/HL28/11	Halin HL28	Consumption artefact	wire bundle
36	SEALIP/MY/HL28/12	Halin HL28	Consumption artefact	large bell/rattle
37	SEALIP/MY/HL28/13	Halin HL28	Consumption artefact	small bell/rattle
38	SEALIP/MY/HL28/14	Halin HL28	Consumption artefact	small bell/rattle
39	SEALIP/MY/HL28/15	Halin HL28	Consumption artefact	small bell/rattle
40	SEALIP/MY/HL28/16	Halin HL28	Consumption artefact	small bell/rattle
41	SEALIP/MY/HL28/17	Halin HL28	Consumption artefact	small bell/rattle
42	SEALIP/MY/HL28/18	Halin HL28	Consumption artefact	small bell/rattle
43	SEALIP/MY/HL29/1	Halin HL29	Consumption artefact	pseudo spear head
44	SEALIP/MY/HL29/2	Halin HL29	Consumption artefact	pseudo spear head
45	SEALIP/MY/HL29/3	Halin HL29	Consumption artefact	pseudo spear head
46	SEALIP/MY/HL29/4	Halin HL29	Consumption artefact	axe
47	SEALIP/MY/HL29/5	Halin HL29	Consumption artefact	axe
48	SEALIP/MY/HL29/6	Halin HL29	Consumption artefact	asymmetric curved axe
49	SEALIP/MY/HL29/7	Halin HL29	Consumption artefact	spearhead
50	SEALIP/MY/HL29/8	Halin HL29	Consumption artefact	spearhead
51	SEALIP/MY/HL29-1/1	Halin HL29-1	Consumption artefact	bangle
52	SEALIP/MY/HL29-1/2	Halin HL29-1	Consumption artefact	bangle
53	SEALIP/MY/HL29-1/3	Halin HL29-1	Consumption artefact	bangle
54	SEALIP/MY/HL29-1/4	Halin HL29-1	Consumption artefact	bangle (double line)

55	SEALIP/MY/HL29-1/5	Halin HL29-1	Consumption artefact	axe
56	SEALIP/MY/HL29-1/6	Halin HL29-1	Consumption artefact	flat ring
57	SEALIP/MY/HL29-1/7	Halin HL29-1	Consumption artefact	ring
58	SEALIP/MY/HL29-1/8	Halin HL29-1	Consumption artefact	spiral square section ring
60	SEALIP/MY/HL30-1/1	Halin HL30-1	Consumption artefact	ring
61	SEALIP/MY/HLTP1/1	Halin HLTP1	Consumption artefact	platy fragment
62	SEALIP/MY/HLTP1/2	Halin HLTP1	Consumption artefact	ring fragment
63	SEALIP/MY/MLW/1	Maliwan	Consumption artefact	fragment
64	SEALIP/MY/MLW/2	Maliwan	Consumption artefact	fragment
65	SEALIP/MY/MLW/3	Maliwan	Consumption artefact	fragment

* only MAFM-excavated samples have radiometric dating

Context	Catalogue	Reference	Period *	Mass
surface collection			geological	-
surface collection			geological	-
surface collection			geological	-
surface collection			geological	-
surface collection			geological	-
surface collection			geological	-
surface collection			geological	-
surface collection			geological	-
surface collection			geological	-
surface collection			geological	-
surface collection			geological	-
surface collection			geological	-
surface collection			geological	-
surface collection			geological	-
surface collection			geological	-
surface collection			geological	-
surface collection			geological	-
surface collection			geological	-
surface collection			geological	-
surface collection			geological	-
surface collection			geological	-
surface collection			geological	-
surface collection			geological	-
surface collection			geological	-
surface collection			geological	-
surface collection			geological	-
surface collection			geological	-
surface collection			geological	-
personal collection			modern	-
MoC excavation	2013/2/3-A		IA	8.05
MoC excavation	2013/2/3-B		IA	9.75
MoC excavation	2013/2/3-C		IA	7.85
MoC excavation	2013/2/3-D		IA	7.95
MoC excavation	2013/2/3-D		IA	-
MoC excavation	2013/2/3-D		IA	-
MoC excavation	2013/2/3-E		IA	10.1
MoC excavation	2013/2/3-F		IA	3.9
MoC excavation	2013/2/3-G		IA	6.55
MoC excavation	2013/2/3-H		IA	9.5
MoC excavation	2013/2/3-I		IA	7.9
MoC excavation	2/4/2014		IA	189.65
MoC excavation	2013/2/5-A		IA	39.6
MoC excavation	2013/2/5-B		IA	25.15
MoC excavation	2013/2/5-C		IA	15
MoC excavation	2013/2/5-D		IA	19.4
MoC excavation	2013/2/5-E		IA	18.15
MoC excavation	2013/2/5-F		IA	16.95
MoC excavation	2013/2/1		?	18.6
MoC excavation	2013/2/2		?	20.25
MoC excavation	2013/2/8		?	13.45
MoC excavation	2013/2/6		?	243.8
MoC excavation	2013/2/7		?	243.15
HL29 Burial 14	2006	2016/2/38	?	243
HL29 Burial 8 Skeleton 11	2001	2016/2/34	?	216
HL29 Burial 6 Skeleton 14	2005	2016/2/39	?	230
B12, Context 1043	1540		BA	2.45
B12, Context 1043, A	1541a		BA	4.9
B12, Context 1043, B	1541b		BA	4.5
B12, Context 1043, C	1541c		BA	4.05

B30, Context 1076	1659	BA	214.85
B28, Context 1080	1648	BA	29.5
B1, Context 1021	1506	Bagan	47
Jar burial, Context 1018	-	Bagan	1.262
HL30-1/7027	7539	IA	2.6
HL-TP1/4001		Bagan	
HL-TP1/6519		Bagan	
TP6/6003		IA	
TP6/6003		IA	
TP6/6003		IA	

Corrosion	
-	
-	
-	
-	
-	
-	
-	
-	
-	
-	
-	
-	
-	
-	
-	
-	
-	
-	
-	
-	
low	
low	1
low	2
low	3
low	4
low	5
low	6
low	7
low	8
low	9
medium	10
low	11
low	12
low	13
medium	14
medium	15
low	16
low	17
medium	18
low	19
low	20
low	21
medium	22
high	23
	24
	25
	26
high	27
high	28
high	29
high	30

low	31
low	32
low	33
	34
	35
high	36
high	37
low	38
low	39
low	40

SAMPLE	Sb	Sn	Bi	Pb	Zn	Cu	Ni	Co	Fe	Mn	Al	S
B10 pXRF	1.2	7.2	*bdl*	4.1	2.9	83.2	1.1	*bdl*	0.2	*bdl*	*bdl*	*bdl*
B10 SEM-EDS	1.7	6.6	*bdl*	3.6	3.0	82.7	1.0	*bdl*	*bdl*	*bdl*	*bdl*	*bdl*
B10 certified value	1.1	7.0	0.0	4.1	2.8	83.7	1.0	0.0	0.2	0.0	0.2	0.0
B12 pXRF	0.1	10.1	*bdl*	0.2	0.7	85.2	2.8	*bdl*	0.2	0.2	*bdl*	*bdl*
B12 SEM-EDS	*bdl*	9.5	*bdl*	*bdl*	0.9	84.9	3.1	*bdl*	*bdl*	*bdl*	*bdl*	*bdl*
B12 certified value	0.1	9.6	0.0	0.2	0.6	85.7	2.6	0.0	0.2	0.2	0.1	0.0
51.13-4 pXRF	*bdl*	0.3	*bdl*	0.1	0.4	91.0	*bdl*	*bdl*	1.9	0.9	4.9	*bdl*
51.13-4 SEM-EDS	*bdl*	*bdl*	*bdl*	*bdl*	0.7	87.7	*bdl*	*bdl*	1.9	1.1	7.8	*bdl*
51.13-4 certified value	0.0	0.3	0.0	0.0	0.3	88.8	0.1	0.0	1.8	0.9	7.3	0.0
71.32-4 pXRF	0.3	6.4	*bdl*	4.3	7.1	80.5	0.8	*bdl*	0.4	*bdl*	*bdl*	*bdl*
71.32-4 SEM-EDS	*bdl*	6.4	*bdl*	3.1	7.3	81.8	0.8	*bdl*	0.4	*bdl*	*bdl*	*bdl*
71.32-4 certified value	0.3	6.5	0.1	4.4	6.5	80.5	0.7	0.0	0.4	0.1	0.1	0.0
SRM-500 pXRF	*bdl*	*bdl*	*bdl*	*bdl*	0.1	99.7	0.1	*bdl*	*bdl*	*bdl*	*bdl*	*bdl*
SRM-500 SEM-EDS	*bdl*	*bdl*	*bdl*	*bdl*	0.4	99.4	*bdl*	*bdl*	*bdl*	*bdl*	*bdl*	*bdl*
SRM-500 certified value	0.0	0.0	0.0	0.0	0.0	99.7	0.1	0.0	0.0	0.0	0.0	0.0
C1123 pXRF	*bdl*	*bdl*	*bdl*	*bdl*	*bdl*	97.4	*bdl*	2.5	*bdl*	*bdl*	*bdl*	*bdl*
C1123 SEM-EDS	*bdl*	*bdl*	*bdl*	*bdl*	*bdl*	96.5	*bdl*	3.4	*bdl*	*bdl*	*bdl*	*bdl*
C1123 certified value	0.0	0.0	0.0	0.0	0.0	97.4	0.0	2.3	0.0	0.0	0.0	0.0
SRM1275 pXRF	*bdl*	*bdl*	*bdl*	*bdl*	*bdl*	86.9	10.7	*bdl*	1.6	0.4	*bdl*	*bdl*
SRM1275 SEM-EDS	*bdl*	*bdl*	*bdl*	*bdl*	*bdl*	87.9	10.1	*bdl*	1.5	0.5	*bdl*	*bdl*
SRM1275 certified value	0.0	0.0	0.0	0.0	0.1	88.2	9.8	0.0	1.5	0.4	0.0	0.0
L-20-1 pXRF	*bdl*	0.5	*bdl*	0.3	14.4	84.2	0.2	*bdl*	*bdl*	0.1	*bdl*	*bdl*
L-20-1 SEM-EDS	*bdl*	0.5	*bdl*	*bdl*	14.6	84.0	*bdl*	*bdl*	*bdl*	*bdl*	*bdl*	*bdl*
L-20-1 certified value	0.0	0.5	0.0	0.3	13.3	85.2	0.2	0.0	0.0	0.1	0.1	0.0
B21 pXRF	0.2	5.3	*bdl*	3.7	6.5	82.2	1.3	*bdl*	0.3	*bdl*	*bdl*	*bdl*
B21 SEM-EDS	*bdl*	5.2	*bdl*	3.9	7.0	82.2	1.3	*bdl*	*bdl*	*bdl*	*bdl*	*bdl*
B21 certified value	0.2	5.1	0.0	3.8	6.2	83.0	1.2	0.0	0.3	0.0	0.1	0.0
B31 pXRF	0.5	8.0	*bdl*	10.6	0.8	79.4	0.6	*bdl*	*bdl*	*bdl*	*bdl*	*bdl*
B31 SEM-EDS	1.8	8.0	*bdl*	9.9	1.1	78.6	0.5	*bdl*	*bdl*	*bdl*	*bdl*	*bdl*
B31 certified value	0.5	7.7	0.0	11.8	0.8	78.6	0.5	0.0	0.0	0.0	0.0	0.0
UZ-52-3 pXRF	0.1	1.0	*bdl*	0.1	18.0	80.3	0.1	*bdl*	0.3	*bdl*	*bdl*	*bdl*
UZ-52-3 SEM-EDS	*bdl*	1.0	*bdl*	*bdl*	18.2	80.2	*bdl*	*bdl*	*bdl*	*bdl*	*bdl*	*bdl*
UZ-52-3 certified value	0.1	1.1	0.0	0.1	17.0	81.1	0.1	0.0	0.3	0.0	0.0	0.0

#	Sample	Site	Object	O	Ba	Sb	Sn	Cd	Pd	Ag	Ru	Mo	Nb	Zr	Bi	Pb	Se	As	Au	W	Zn
1	SEALIP/MY/HL28/1	Halin HL28	wire bundle	4.7	bdl	bdl	bdl	bdl	bdl	bdl	bdl	bdl	bdl	bdl	bdl	bdl	bdl	bdl	bdl	bdl	bdl
2	SEALIP/MY/HL28/2	Halin HL28	wire bundle	bdl	bdl	bdl	bdl	bdl	bdl	bdl	bdl	0.0	0.0	bdl	bdl	bdl	bdl	0.0	bdl	bdl	bdl
3	SEALIP/MY/HL28/3	Halin HL28	wire bundle	1.2	bdl	bdl	bdl	bdl	bdl	bdl	bdl	bdl	bdl	bdl	bdl	bdl	bdl	bdl	bdl	bdl	bdl
4	SEALIP/MY/HL28/4	Halin HL28	wire bundle multi	bdl	bdl	bdl	bdl	bdl	bdl	bdl	bdl	0.0	bdl	bdl	bdl	bdl	bdl	0.0	bdl	bdl	bdl
5	SEALIP/MY/HL28/5	Halin HL28	wire bundle multi	bdl	bdl	bdl	bdl	bdl	bdl	bdl	bdl	0.0	bdl	bdl	bdl	bdl	bdl	0.0	bdl	bdl	bdl
6	SEALIP/MY/HL28/6	Halin HL28	wire bundle multi	bdl	bdl	bdl	bdl	bdl	bdl	bdl	bdl	bdl	bdl	bdl	bdl	bdl	bdl	0.0	bdl	bdl	bdl
7	SEALIP/MY/HL28/7	Halin HL28	wire bundle	bdl	bdl	bdl	bdl	bdl	bdl	bdl	bdl	0.0	0.0	bdl	bdl	bdl	bdl	0.0	bdl	bdl	bdl
8	SEALIP/MY/HL28/8	Halin HL28	wire bundle	1.2	bdl	bdl	bdl	bdl	bdl	bdl	bdl	bdl	bdl	bdl	bdl	bdl	bdl	bdl	bdl	bdl	bdl
9	SEALIP/MY/HL28/9	Halin HL28	wire bundle	1.8	bdl	bdl	bdl	bdl	bdl	bdl	bdl	bdl	bdl	bdl	bdl	bdl	bdl	bdl	bdl	bdl	bdl
10	SEALIP/MY/HL28/10	Halin HL28	possible casting spillage	17.5	bdl	bdl	15.7	bdl	bdl	bdl	bdl	bdl	bdl	bdl	bdl	bdl	bdl	bdl	bdl	bdl	bdl
11	SEALIP/MY/HL28/11	Halin HL28	wire bundle	bdl	bdl	bdl	bdl	bdl	bdl	bdl	bdl	0.0	0.0	bdl	bdl	bdl	bdl	0.0	bdl	bdl	bdl
12	SEALIP/MY/HL28/12	Halin HL28	large bell/rattle	bdl	bdl	bdl	4.5	bdl	bdl	bdl	bdl	0.0	0.0	bdl	bdl	bdl	bdl	0.0	bdl	bdl	bdl
13	SEALIP/MY/HL28/13	Halin HL28	small bell/rattle	bdl	bdl	bdl	bdl	bdl	bdl	bdl	bdl	0.1	0.1	bdl	bdl	bdl	bdl	bdl	bdl	bdl	bdl
14	SEALIP/MY/HL28/14	Halin HL28	small bell/rattle	bdl	bdl	bdl	4.2	bdl	bdl	bdl	bdl	bdl	bdl	bdl	bdl	bdl	bdl	bdl	bdl	bdl	bdl
15	SEALIP/MY/HL28/15	Halin HL28	small bell/rattle	bdl	bdl	bdl	4.2	bdl	bdl	bdl	bdl	bdl	bdl	bdl	bdl	bdl	bdl	bdl	bdl	bdl	bdl
16	SEALIP/MY/HL28/16	Halin HL28	small bell/rattle	bdl	bdl	bdl	1.2	bdl	bdl	bdl	bdl	0.0	0.0	bdl	bdl	bdl	bdl	0.0	bdl	bdl	bdl
17	SEALIP/MY/HL28/17	Halin HL28	small bell/rattle	bdl	bdl	bdl	11.0	bdl	bdl	bdl	bdl	0.0	0.0	0.0	bdl	bdl	bdl	0.0	bdl	bdl	bdl
18	SEALIP/MY/HL28/18	Halin HL28	small bell/rattle	bdl	bdl	bdl	6.2	bdl	bdl	bdl	bdl	bdl	bdl	bdl	bdl	bdl	bdl	bdl	bdl	bdl	bdl
19	SEALIP/MY/HL29/1	Halin HL29	pseudo spear head	bdl	bdl	bdl	1.5	bdl	bdl	bdl	bdl	bdl	bdl	bdl	bdl	bdl	bdl	bdl	bdl	bdl	bdl
20	SEALIP/MY/HL29/2	Halin HL29	pseudo spear head	bdl	bdl	bdl	bdl	bdl	bdl	bdl	bdl	bdl	bdl	bdl	bdl	0.1	bdl	0.0	bdl	bdl	bdl
21	SEALIP/MY/HL29/3	Halin HL29	pseudo spear head	bdl	bdl	bdl	bdl	bdl	bdl	bdl	bdl	bdl	bdl	bdl	bdl	0.1	bdl	0.0	bdl	bdl	bdl
22	SEALIP/MY/HL29/4	Halin HL29	axe	20.2	bdl	bdl	5.4	bdl	bdl	bdl	bdl	bdl	bdl	bdl	bdl	bdl	bdl	bdl	bdl	bdl	bdl
23	SEALIP/MY/HL29/5	Halin HL29	axe	50.2	bdl	bdl	bdl	bdl	bdl	bdl	bdl	bdl	bdl	bdl	bdl	bdl	bdl	bdl	bdl	bdl	bdl
24	SEALIP/MY/HL29/6	Halin HL29	asymmetric curved axe	bdl	bdl	bdl	11.4	bdl	bdl	bdl	bdl	bdl	bdl	bdl	bdl	bdl	bdl	bdl	bdl	bdl	bdl
25	SEALIP/MY/HL29/7	Halin HL29	spearhead	bdl	bdl	bdl	15.9	bdl	bdl	bdl	bdl	bdl	bdl	bdl	bdl	0.6	bdl	bdl	bdl	bdl	bdl
26	SEALIP/MY/HL29/8	Halin HL29	spearhead	bdl	bdl	bdl	5.2	bdl	bdl	bdl	bdl	bdl	bdl	0.1	bdl	0.4	bdl	bdl	bdl	bdl	bdl
27	SEALIP/MY/HL29-1/1	Halin HL29-1	bangle	bdl	bdl	bdl	10.8	0.1	bdl	bdl	bdl	bdl	bdl	bdl	bdl	0.4	bdl	0.1	bdl	bdl	0.3
28	SEALIP/MY/HL29-1/2	Halin HL29-1	bangle	bdl	bdl	bdl	9.8	bdl	bdl	bdl	bdl	bdl	bdl	bdl	0.0	0.2	bdl	0.1	bdl	bdl	0.1
29	SEALIP/MY/HL29-1/3	Halin HL29-1	bangle	bdl	bdl	bdl	8.6	bdl	bdl	bdl	bdl	bdl	bdl	bdl	0.0	0.1	bdl	0.1	bdl	bdl	0.1
30	SEALIP/MY/HL29-1/4	Halin HL29-1	bangle (double line)	bdl	bdl	bdl	6.9	bdl	bdl	bdl	bdl	0.0	bdl	bdl	bdl	0.3	bdl	0.1	bdl	bdl	0.4
31	SEALIP/MY/HL29-1/5	Halin HL29-1	axe	16.4	bdl	bdl	6.5	bdl	bdl	bdl	bdl	bdl	bdl	bdl	bdl	bdl	bdl	bdl	bdl	bdl	bdl
32	SEALIP/MY/HL29-1/6	Halin HL29-1	flat ring	bdl	bdl	bdl	2.0	bdl	bdl	bdl	bdl	0.0	bdl	bdl	bdl	0.1	bdl	bdl	bdl	bdl	0.1
33	SEALIP/MY/HL29-1/7	Halin HL29-1	spiral square section ring	bdl	bdl	bdl	5.8	bdl	bdl	bdl	bdl	bdl	bdl	bdl	0.0	0.1	bdl	0.1	bdl	bdl	0.1
34	SEALIP/MY/HL29-1/8	Halin HL29-1	ring	bdl	bdl	0.1	bdl	bdl	bdl	bdl	bdl	bdl	bdl	bdl	bdl	1.5	bdl	bdl	bdl	bdl	bdl
35	SEALIP/MY/HL30-1/1	Halin HL30-1	ring	bdl	bdl	bdl	9.5	bdl	bdl	bdl	bdl	bdl	bdl	bdl	bdl	0.2	bdl	bdl	bdl	bdl	bdl
36	SEALIP/MY/HLTP1/1	Halin HLTP1	platy fragment	bdl	bdl	1.5	29.3	bdl	bdl	bdl	bdl	bdl	bdl	bdl	bdl	0.1	bdl	bdl	bdl	bdl	bdl
37	SEALIP/MY/HLTP1/2	Halin HLTP1	ring fragment	bdl	bdl	0.4	bdl	bdl	bdl	bdl	bdl	bdl	bdl	0.0	0.1	1.4	bdl	bdl	bdl	bdl	0.1
38	SEALIP/MY/MLW/1	Maliwan	fragment	bdl	bdl	0.1	7.6	bdl	bdl	bdl	bdl	bdl	bdl	0.0	0.1	13.4	bdl	0.5	bdl	bdl	bdl
39	SEALIP/MY/MLW/2	Maliwan	fragment	bdl	bdl	0.7	19.4	bdl	bdl	bdl	bdl	bdl	bdl	bdl	0.1	3.5	bdl	0.6	0.0	bdl	bdl
40	SEALIP/MY/MLW/3	Maliwan	fragment	bdl	bdl	bdl	0.1	bdl	bdl	bdl	bdl	bdl	bdl	0.0	0.7	0.0	bdl	0.0	bdl	bdl	bdl

41	SEALIP/MY/BAW/1	Baw Mountain, Kyaukse	Cu mineral	72.9	4.6	0.2	bdl	bdl	bdl	bdl	bdl	bdl	bdl	bdl	bdl	0.1	bdl	0.1	bdl	bdl	bdl
42	SEALIP/MY/BAW/2	Baw Mountain, Kyaukse	Cu mineral	60.8	2.4	0.5	bdl	bdl	bdl	bdl	bdl	bdl	bdl	bdl	bdl	0.9	bdl	0.6	bdl	bdl	bdl
43	SEALIP/MY/BAW/3	Baw Mountain, Kyaukse	Cu mineral	55.5	0.1	0.3	bdl	bdl	bdl	bdl	bdl	bdl	bdl	bdl	bdl	bdl	bdl	0.2	bdl	bdl	0.5
44	SEALIP/MY/BWD/1	Bawdwin	Cu mineral	bdl	bdl	bdl	0.1	bdl	bdl	bdl	bdl	bdl	bdl	bdl	bdl	42.9	bdl	3.6	bdl	bdl	0.2
45	SEALIP/MY/BWD/2	Bawdwin	Cu mineral																		
46	SEALIP/MY/KAW/1	Kawlin	Cu mineral	7.4	bdl	bdl	bdl	bdl	bdl	bdl	bdl	bdl	bdl	bdl	bdl	bdl	bdl	0.1	bdl	bdl	bdl
47	SEALIP/MY/KAW/2	Kawlin	Cu mineral	bdl	bdl	0.2	bdl	bdl	bdl	bdl	bdl	bdl	bdl	bdl	bdl	bdl	bdl	2.1	bdl	bdl	bdl
48	SEALIP/MY/KAW/3	Kawlin	Cu mineral	15.3	bdl	bdl	bdl	bdl	bdl	0.1	bdl	bdl	bdl	bdl	bdl	bdl	bdl	0.1	bdl	bdl	bdl
49	SEALIP/MY/MIN/1	Mingan	Cu mineral	68.2	bdl	bdl	bdl	bdl	bdl	bdl	bdl	bdl	bdl	bdl	bdl	bdl	bdl	bdl	bdl	bdl	bdl
50	SEALIP/MY/MIN/2	Mingan	Cu mineral	53.1	bdl	bdl	bdl	bdl	bdl	bdl	bdl	bdl	bdl	0.5	bdl	bdl	bdl	bdl	bdl	bdl	bdl
51	SEALIP/MY/MIN/3	Mingan	Cu mineral	64.9	bdl	bdl	bdl	bdl	bdl	bdl	bdl	bdl	bdl	0.2	bdl	bdl	bdl	bdl	bdl	bdl	bdl
52	SEALIP/MY/NTL/1	Nant Twin village	Cu mineral	66.1	bdl	1.9	bdl	bdl	bdl	bdl	bdl	bdl	bdl	bdl	bdl	bdl	bdl	bdl	bdl	bdl	bdl
53	SEALIP/MY/NTL/2	Nant Twin village	Cu mineral	58.9	bdl	0.1	bdl	bdl	bdl	bdl	bdl	bdl	bdl	bdl	bdl	0.1	bdl	0.1	bdl	bdl	0.8
54	SEALIP/MY/NTL/3	Nant Twin village	Cu mineral	73.0	1.3	0.4	bdl	bdl	bdl	bdl	bdl	bdl	bdl	bdl	bdl	0.1	bdl	bdl	bdl	bdl	0.1
55	SEALIP/MY/PDHT/1	Pala Dauk Hter Taung	Cu mineral																		
56	SEALIP/MY/PDHT/2	Pala Dauk Hter Taung	Cu mineral																		
57	SEALIP/MY/PDHT/3	Pala Dauk Hter Taung	Cu mineral																		
58	SEALIP/MY/ST/1	Sabad Taung	Cu mineral																		
59	SEALIP/MY/ST/2	Sabad Taung	Cu mineral																		
60	SEALIP/MY/ST/3	Sabad Taung	Cu mineral																		
61	SEALIP/MY/TKN/1	Thabeik Kyinn	Cu mineral	46.7	0.1	bdl	bdl	bdl	bdl	bdl	bdl	bdl	bdl	bdl	bdl	bdl	bdl	bdl	bdl	bdl	bdl
62	SEALIP/MY/TKN/2	Thabeik Kyinn	Cu mineral	55.0	0.4	bdl	bdl	bdl	bdl	bdl	bdl	bdl	bdl	bdl	bdl	bdl	bdl	bdl	bdl	bdl	bdl
63	SEALIP/MY/TKN/3	Thabeik Kyinn	Cu mineral	35.6	bdl	bdl	bdl	bdl	bdl	bdl	bdl	bdl	bdl	bdl	bdl	bdl	bdl	bdl	bdl	bdl	bdl
64	SEALIP/MY/YTCM/1	Yang Tse Copper	Cu ingot																		

Cu	Ni	Co	Fe	Mn	Cr	V	Ti	Al	S	Cl	P	Si	Mg	Analytical total	Analytical technique	Corrosion products	Probable alloy	Working techniques
93.4	bdl	bdl	0.2	bdl	bdl	bdl	bdl	bdl	1.4	0.3	bdl	0.1	bdl	100.0	SEM-EDS	Medium	copper	As cast
99.1	bdl	bdl	0.8	bdl	bdl	bdl	bdl	bdl	bdl	bdl	bdl	bdl	bdl	100.0	pXRF	Low	copper	As cast
97.5	bdl	bdl	0.4	bdl	bdl	bdl	bdl	bdl	0.9	bdl	bdl	0.0	bdl	100.0	SEM-EDS	Low	copper	As cast
99.5	bdl	bdl	0.4	bdl	bdl	bdl	bdl	bdl	bdl	bdl	bdl	bdl	bdl	100.0	pXRF	Low	copper	As cast
98.8	bdl	bdl	0.4	bdl	bdl	bdl	bdl	bdl	0.8	bdl	bdl	bdl	bdl	99.9	pXRF	Low	copper	As cast
97.5	bdl	bdl	0.5	bdl	bdl	bdl	bdl	bdl	1.2	bdl	bdl	0.8	bdl	100.0	pXRF	Low	copper	As cast
99.5	bdl	bdl	0.4	bdl	bdl	bdl	bdl	bdl	bdl	bdl	bdl	bdl	bdl	100.0	pXRF	Low	copper	As cast
97.2	bdl	bdl	0.5	bdl	bdl	bdl	bdl	bdl	1.1	bdl	bdl	0.1	bdl	100.0	SEM-EDS	Low	copper	As cast
96.1	bdl	bdl	0.3	bdl	bdl	bdl	bdl	bdl	1.1	0.4	bdl	0.3	bdl	100.0	SEM-EDS	Low	copper	As cast
66.3	bdl	bdl	bdl	bdl	bdl	bdl	bdl	bdl	bdl	0.4	0.1	0.2	bdl	100.2	SEM-EDS	High	bronze	As cast
99.2	bdl	bdl	0.8	bdl	bdl	bdl	bdl	bdl	bdl	bdl	bdl	bdl	bdl	100.0	pXRF	Low	copper	As cast
92.7	bdl	bdl	0.1	bdl	bdl	bdl	bdl	bdl	bdl	bdl	bdl	2.6	bdl	100.0	pXRF	Medium	bronze	As cast
99.4	bdl	bdl	bdl	bdl	bdl	bdl	bdl	bdl	bdl	bdl	bdl	bdl	bdl	99.6	pXRF	Low	copper	Hammered/annealed
80.3	bdl	bdl	bdl	bdl	bdl	bdl	bdl	bdl	bdl	bdl	bdl	bdl	bdl	84.5	SEM-EDS	High	bronze	As cast
83.4	bdl	bdl	bdl	bdl	bdl	bdl	bdl	bdl	bdl	bdl	bdl	bdl	bdl	87.6	SEM-EDS	High	bronze	As cast
98.0	bdl	bdl	bdl	bdl	bdl	bdl	bdl	bdl	bdl	bdl	bdl	0.7	bdl	100.0	pXRF	Medium	bronze	As cast
88.2	bdl	bdl	bdl	bdl	bdl	bdl	bdl	bdl	bdl	bdl	bdl	0.6	bdl	100.0	pXRF	Medium	bronze	As cast
80.1	bdl	bdl	bdl	bdl	bdl	bdl	bdl	bdl	bdl	bdl	bdl	0.6	bdl	86.9	SEM-EDS	High	bronze	As cast
97.8	bdl	bdl	bdl	bdl	bdl	bdl	bdl	bdl	bdl	bdl	bdl	bdl	bdl	99.3	SEM-EDS	High	bronze	As cast
96.7	bdl	bdl	1.7	bdl	bdl	bdl	bdl	bdl	0.2	bdl	bdl	1.3	bdl	100.0	pXRF	Low	copper	As cast
99.5	bdl	bdl	0.5	bdl	bdl	bdl	bdl	bdl	bdl	bdl	bdl	bdl	bdl	100.1	pXRF	Low	copper	As cast
63.6	bdl	bdl	bdl	bdl	bdl	bdl	bdl	bdl	bdl	10.6	bdl	0.1	bdl	100.0	SEM-EDS	High	bronze	As cast
7.3	bdl	bdl	5.3	bdl	bdl	bdl	bdl	8.1	bdl	0.5	bdl	22.6	2.2	96.2	SEM-EDS	High	copper	Corroded
88.1	0.0	bdl	0.0	bdl	bdl	bdl	bdl	bdl	bdl	bdl	bdl	bdl	bdl	99.6	pXRF	High	bronze	As cast
82.9	bdl	bdl	bdl	bdl	0.1	0.0	0.1	bdl	bdl	bdl	bdl	bdl	bdl	99.6	pXRF	High	bronze	As cast
91.5	bdl	bdl	1.6	bdl	0.1	0.1	0.3	bdl	bdl	bdl	bdl	bdl	bdl	99.3	pXRF	High	bronze	Corroded
87.1	bdl	bdl	1.0	bdl	bdl	bdl	bdl	bdl	bdl	bdl	bdl	0.3	bdl	100.0	pXRF	Medium	bronze	As cast
87.1	bdl	bdl	2.3	bdl	bdl	bdl	bdl	bdl	0.1	bdl	bdl	0.2	bdl	100.0	pXRF	Medium	bronze	Annealed
90.9	bdl	bdl	0.1	bdl	bdl	bdl	bdl	bdl	bdl	bdl	bdl	0.1	bdl	100.0	pXRF	Medium	bronze	Hammered
86.4	bdl	0.0	4.3	bdl	bdl	bdl	bdl	bdl	bdl	bdl	bdl	1.7	bdl	100.0	pXRF	Medium	bronze	Hammered/annealed
73.3	bdl	bdl	bdl	bdl	bdl	bdl	bdl	0.1	1.2	0.9	1.1	1.0	bdl	100.4	SEM-EDS	High	bronze	Corroded
97.9	bdl	bdl	bdl	bdl	bdl	bdl	bdl	bdl	bdl	bdl	bdl	bdl	bdl	100.0	pXRF	Low	bronze	Hammered/annealed
93.9	bdl	bdl	0.1	bdl	bdl	bdl	bdl	bdl	bdl	bdl	bdl	bdl	bdl	100.0	pXRF	Medium	bronze	As cast
96.4	bdl	bdl	0.1	bdl	0.1	0.0	0.0	bdl	bdl	bdl	bdl	bdl	bdl	98.4	pXRF	Low	leaded copper	Hammered/annealed
89.3	bdl	bdl	0.6	bdl	bdl	bdl	bdl	bdl	bdl	bdl	bdl	bdl	bdl	99.7	pXRF	High	bronze	As cast
67.6	bdl	bdl	0.8	bdl	bdl	bdl	0.2	bdl	bdl	bdl	bdl	bdl	bdl	99.5	pXRF	High	bronze	Corroded
97.1	bdl	bdl	0.1	bdl	0.1	0.0	bdl	bdl	bdl	bdl	bdl	bdl	bdl	99.3	pXRF	Low	leaded copper	Hammered/annealed
78.1	0.1	bdl	bdl	bdl	bdl	bdl	0.1	bdl	bdl	bdl	bdl	bdl	bdl	100.0	pXRF	Low	leaded bronze	As cast
75.0	0.1	0.1	0.4	bdl	bdl	bdl	0.1	bdl	bdl	bdl	bdl	bdl	bdl	100.1	pXRF	Medium	leaded bronze	As cast
98.4	bdl	bdl	0.1	bdl	bdl	bdl	bdl	bdl	0.8	bdl	bdl	bdl	bdl	100.0	pXRF	Medium	copper	As cast

3.9	bdl	bdl	0.3	0.1	bdl	bdl	bdl	bdl	6.4	bdl	bdl	12.3	bdl	99.7	pXRF	Mineral
5.4	bdl	bdl	0.7	bdl	bdl	bdl	bdl	0.3	3.0	bdl	bdl	24.9	bdl	99.7	pXRF	Mineral
1.4	bdl	bdl	1.5	bdl	bdl	bdl	bdl	0.3	5.8	bdl	bdl	33.5	bdl	99.1	pXRF	Mineral
37.0	0.5	0.3	0.1	0.1	bdl	bdl	bdl	bdl	13.2	bdl	bdl	1.3	bdl	99.3	pXRF	leaded copper
																Mineral
27.0	bdl	bdl	26.0	bdl	bdl	bdl	bdl	bdl	32.2	bdl	bdl	6.7	bdl	99.3	pXRF	Mineral
26.7	bdl	bdl	22.8	0.2	bdl	bdl	bdl	bdl	29.4	bdl	bdl	14.9	bdl	96.4	pXRF	Mineral
18.3	bdl	bdl	21.1	1.5	bdl	bdl	bdl	bdl	23.1	bdl	bdl	19.8	bdl	99.3	pXRF	Mineral
0.6	bdl	bdl	0.7	bdl	bdl	bdl	bdl	1.5	bdl	bdl	bdl	28.7	bdl	99.7	pXRF	Mineral
9.6	bdl	bdl	3.7	0.6	bdl	bdl	1.4	7.1	bdl	bdl	bdl	20.3	1.7	97.9	pXRF	Mineral
9.4	bdl	bdl	0.6	0.1	bdl	bdl	0.1	6.4	0.1	bdl	bdl	17.9	bdl	99.6	pXRF	Mineral
17.8	bdl	bdl	bdl	bdl	bdl	bdl	bdl	0.3	0.2	bdl	bdl	13.2	bdl	99.5	pXRF	Mineral
15.2	bdl	bdl	0.2	bdl	bdl	bdl	bdl	0.2	0.2	bdl	bdl	24.0	bdl	99.8	pXRF	Mineral
8.7	bdl	bdl	0.1	bdl	bdl	bdl	bdl	0.2	0.2	bdl	bdl	15.8	bdl	99.8	pXRF	Mineral
																Mineral
																Mineral
																Mineral
																Mineral
																Mineral
																Mineral
34.6	bdl	bdl	6.7	bdl	bdl	bdl	bdl	1.9	0.5	bdl	bdl	7.9	bdl	98.4	pXRF	Mineral
29.1	bdl	bdl	6.4	bdl	bdl	bdl	bdl	1.1	0.1	bdl	bdl	6.5	bdl	98.5	pXRF	Mineral
45.8	bdl	bdl	2.9	bdl	bdl	bdl	bdl	1.7	0.1	0.7	bdl	8.1	2.3	97.1	pXRF	Mineral
																pure copper

	SEALIP ID	Lab ID	Material type	206Pb/204Pb	err (2σ)	207Pb/204Pb	err (2σ)
1	SEALIP/MY/BAW/1	1907566	Mineral	18.428	0.002	15.764	0.002
2	SEALIP/MY/BAW/2	1907567	Mineral	18.425	0.002	15.768	0.001
3	SEALIP/MY/BAW/3	1907568	Mineral	18.433	0.002	15.757	0.001
4	SEALIP/MY/BWD/1	1907569	Mineral	18.385	0.002	15.793	0.002
5	SEALIP/MY/BWD/2	1907570	Mineral	18.391	0.002	15.797	0.002
6	SEALIP/MY/KAW/1	1907571	Mineral	18.306	0.002	15.646	0.002
7	SEALIP/MY/KAW/2	1907572	Mineral	18.305	0.002	15.646	0.002
8	SEALIP/MY/KAW/3	1907573	Mineral	18.322	0.001	15.652	0.001
9	SEALIP/MY/MIN/1	1907560	Mineral	18.833	0.003	15.704	0.003
10	SEALIP/MY/MIN/2	1907561	Mineral	19.099	0.002	15.719	0.002
11	SEALIP/MY/MIN/3	1907562	Mineral	19.260	0.002	15.725	0.002
12	SEALIP/MY/NTL/1	1907563	Mineral	19.189	0.002	15.763	0.002
13	SEALIP/MY/NTL/2	1907564	Mineral	19.186	0.002	15.764	0.002
14	SEALIP/MY/NTL/3	1907565	Mineral	19.226	0.012	15.763	0.011
15	SEALIP/MY/PDHT/1	1804225	Mineral	18.414	0.001	15.605	0.001
16	SEALIP/MY/PDHT/2	1804226	Mineral	18.356	0.003	15.615	0.002
17	SEALIP/MY/PDHT/3	1804227	Mineral	18.795	0.001	15.592	0.001
18	SEALIP/MY/ST/1	1804222	Mineral	28.219	0.002	16.258	0.002
19	SEALIP/MY/ST/2	1804223	Mineral	21.635	0.001	15.885	0.001
20	SEALIP/MY/ST/3	1804224	Mineral	21.204	0.001	15.889	0.001
21	SEALIP/MY/TKN/1	1907574	Mineral	18.552	0.003	15.746	0.003
22	SEALIP/MY/TKN/2	1907575	Mineral	18.356	0.003	15.725	0.002
23	SEALIP/MY/TKN/3	1907576	Mineral	18.350	0.002	15.757	0.002
24	SEALIP/MY/YTCM/1	1907577	Mineral equivalent	17.885	0.004	15.596	0.005
25	SEALIP/MY/HL28/1	1804228	Consumption artefact	18.501	0.009	15.569	0.009
26	SEALIP/MY/HL28/2	1804229	Consumption artefact	18.430	0.002	15.616	0.002
27	SEALIP/MY/HL28/3	1804230	Consumption artefact	18.589	0.002	15.614	0.002
28	SEALIP/MY/HL28/4	1804231	Consumption artefact	18.596	0.002	15.618	0.001
29	SEALIP/MY/HL28/5	1804232	Consumption artefact	18.589	0.001	15.616	0.001
30	SEALIP/MY/HL28/6	1804233	Consumption artefact	18.580	0.001	15.618	0.001
31	SEALIP/MY/HL28/7	1804234	Consumption artefact	18.608	0.001	15.616	0.002
32	SEALIP/MY/HL28/8	1804235	Consumption artefact	18.597	0.002	15.618	0.002
33	SEALIP/MY/HL28/9	1804236	Consumption artefact	18.611	0.002	15.617	0.001
34	SEALIP/MY/HL28/10	1804237	Production artefact	18.292	0.001	15.703	0.001
35	SEALIP/MY/HL28/11	1804238	Consumption artefact	18.593	0.002	15.618	0.002
36	SEALIP/MY/HL28/12	1804239	Consumption artefact	18.687	0.002	15.627	0.002
37	SEALIP/MY/HL28/13	1901264	Consumption artefact	17.984	0.001	15.598	0.001
38	SEALIP/MY/HL28/14	1901265	Consumption artefact	18.120	0.001	15.605	0.001
39	SEALIP/MY/HL28/15	1901266	Consumption artefact	18.542	0.008	15.700	0.006
40	SEALIP/MY/HL28/16	1901267	Consumption artefact	18.531	0.002	15.669	0.002
41	SEALIP/MY/HL28/17	1901268	Consumption artefact	19.080	0.002	15.697	0.002
42	SEALIP/MY/HL28/18	1901269	Consumption artefact	18.565	0.005	15.700	0.003
43	SEALIP/MY/HL29/1	1901270	Consumption artefact	18.583	0.002	15.607	0.002
44	SEALIP/MY/HL29/2	1804240	Consumption artefact	18.573	0.002	15.616	0.001
45	SEALIP/MY/HL29/3	1804241	Consumption artefact	18.573	0.002	15.616	0.001
46	SEALIP/MY/HL29/4	1804242	Consumption artefact	19.192	0.001	15.771	0.001
47	SEALIP/MY/HL29/5	1804243	Consumption artefact	18.718	0.001	15.704	0.001
48	SEALIP/MY/HL29/6	1907640	Consumption artefact	18.399	0.004	15.620	0.004
49	SEALIP/MY/HL29/7	1907641	Consumption artefact	18.842	0.002	15.689	0.002
50	SEALIP/MY/HL29/8	1907642	Consumption artefact	18.060	0.002	15.541	0.002
51	SEALIP/MY/HL29-1/1	1804244	Consumption artefact	18.331	0.001	15.718	0.001

52	SEALIP/MY/HL29-1/2	1804245	Consumption artefact	18.332	0.001	15.725	0.001
53	SEALIP/MY/HL29-1/3	1804246	Consumption artefact	18.343	0.001	15.727	0.002
54	SEALIP/MY/HL29-1/4	1804247	Consumption artefact	18.326	0.001	15.720	0.001
55	SEALIP/MY/HL29-1/5	1804248	Consumption artefact	18.469	0.003	15.660	0.003
56	SEALIP/MY/HL29-1/6	1804249	Consumption artefact	19.024	0.001	15.748	0.001
57	SEALIP/MY/HL29-1/7	1804250	Consumption artefact	18.376	0.002	15.712	0.002
58	SEALIP/MY/HL29-1/8	1907638	Consumption artefact	18.393	0.002	15.794	0.002
59	SEALIP/MY/HL30-1/1	1907639	Consumption artefact	18.324	0.002	15.719	0.002
60	SEALIP/MY/HLTP1/1	1907643	Consumption artefact	18.596	0.002	15.748	0.002
61	SEALIP/MY/HLTP1/2	1907644	Consumption artefact	18.357	0.002	15.738	0.002
62	SEALIP/MY/MLW/1	1804394	Consumption artefact	18.425	0.001	15.705	0.001
63	SEALIP/MY/MLW/2	1804395	Consumption artefact	17.784	0.001	15.576	0.001
64	SEALIP/MY/MLW/3	1804396	Consumption artefact	18.357	0.002	15.770	0.003

208Pb/204Pb	err (2σ)	207Pb/206Pb	err (2σ)	206Pb/207Pb	err (2σ)	208Pb/206Pb	err (2σ)
38.805	0.006	0.856	0.00003	1.1683	0.00003	2.106	0.0001
38.814	0.004	0.856	0.00003	1.1679	0.00003	2.107	0.0006
38.796	0.004	0.855	0.00002	1.1690	0.00002	2.105	0.0010
38.767	0.004	0.859	0.00002	1.1635	0.00002	2.109	0.0001
38.787	0.005	0.859	0.00002	1.1636	0.00002	2.109	0.0001
38.904	0.006	0.855	0.00004	1.1700	0.00004	2.125	0.0002
38.900	0.006	0.855	0.00003	1.1700	0.00003	2.125	0.0001
38.921	0.004	0.854	0.00003	1.1706	0.00003	2.124	0.0001
39.445	0.008	0.834	0.00003	1.1986	0.00003	2.094	0.0001
41.699	0.005	0.823	0.00003	1.2144	0.00003	2.183	0.0001
42.711	0.005	0.817	0.00003	1.2241	0.00003	2.218	0.0001
39.175	0.005	0.822	0.00003	1.2167	0.00003	2.042	0.0001
39.133	0.006	0.822	0.00004	1.2153	0.00004	2.040	0.0001
39.172	0.030	0.820	0.00013	1.2190	0.00013	2.037	0.0005
38.522	0.003	0.848	0.00002	1.1799	0.00002	2.092	0.0001
38.326	0.006	0.851	0.00003	1.1757	0.00003	2.088	0.0001
38.160	0.004	0.829	0.00002	1.2061	0.00002	2.030	0.0001
40.422	0.005	0.576	0.00002	1.7360	0.00002	1.433	0.0001
42.281	0.004	0.734	0.00002	1.3618	0.00002	1.955	0.0001
41.796	0.004	0.749	0.00001	1.3344	0.00001	1.971	0.0001
38.999	0.007	0.849	0.00003	1.1775	0.00003	2.102	0.0001
38.759	0.007	0.857	0.00004	1.1667	0.00004	2.112	0.0001
38.673	0.005	0.859	0.00003	1.1646	0.00003	2.108	0.0001
37.853	0.012	0.873	0.00008	1.1461	0.00008	2.117	0.0002
38.643	0.021	0.841	0.00007	1.1884	0.00007	2.089	0.0001
38.634	0.009	0.847	0.00010	1.1803	0.00012	2.096	0.0002
38.811	0.009	0.840	0.00010	1.1906	0.00012	2.088	0.0002
38.826	0.004	0.840	0.00002	1.1906	0.00002	2.088	0.0001
38.809	0.004	0.840	0.00001	1.1904	0.00001	2.088	0.0001
38.799	0.003	0.840	0.00001	1.1898	0.00001	2.088	0.0001
38.829	0.005	0.839	0.00002	1.1918	0.00002	2.087	0.0001
38.825	0.009	0.840	0.00010	1.1908	0.00012	2.088	0.0002
38.839	0.005	0.839	0.00001	1.1920	0.00001	2.087	0.0001
38.542	0.003	0.859	0.00001	1.1647	0.00001	2.107	0.0001
38.814	0.005	0.840	0.00002	1.1904	0.00002	2.088	0.0001
38.532	0.006	0.836	0.00002	1.1958	0.00002	2.062	0.0001
37.925	0.004	0.868	0.00002	1.1523	0.00002	2.109	0.0001
38.103	0.004	0.862	0.00002	1.1605	0.00002	2.103	0.0001
38.691	0.017	0.847	0.00002	1.1805	0.00002	2.087	0.0001
38.664	0.005	0.846	0.00002	1.1820	0.00002	2.086	0.0001
39.201	0.005	0.823	0.00002	1.2148	0.00002	2.055	0.0001
38.636	0.009	0.846	0.00005	1.1819	0.00005	2.081	0.0001
38.787	0.004	0.840	0.00003	1.1900	0.00003	2.087	0.0001
38.776	0.005	0.841	0.00002	1.1896	0.00002	2.088	0.0001
38.776	0.005	0.841	0.00002	1.1896	0.00002	2.088	0.0001
39.196	0.002	0.822	0.00001	1.2171	0.00001	2.042	0.0001
39.010	0.003	0.839	0.00001	1.1921	0.00001	2.084	0.0001
38.460	0.009	0.849	0.00004	1.1772	0.00004	2.090	0.0002
38.786	0.006	0.833	0.00004	1.2003	0.00004	2.059	0.0001
38.037	0.005	0.861	0.00003	1.1615	0.00003	2.106	0.0001
38.645	0.004	0.857	0.00001	1.1663	0.00001	2.108	0.0001

38.659	0.004	0.858	0.00001	1.1659	0.00001	2.109	0.0001
38.671	0.005	0.857	0.00001	1.1663	0.00001	2.108	0.0001
38.644	0.005	0.858	0.00001	1.1657	0.00001	2.109	0.0001
38.645	0.008	0.848	0.00003	1.1794	0.00003	2.092	0.0001
39.085	0.004	0.828	0.00002	1.2081	0.00002	2.054	0.0001
38.670	0.006	0.855	0.00002	1.1696	0.00002	2.104	0.0001
38.771	0.005	0.859	0.00002	1.1639	0.00002	2.108	0.0001
38.665	0.005	0.858	0.00003	1.1650	0.00003	2.110	0.0001
38.840	0.005	0.847	0.00002	1.1802	0.00002	2.089	0.0001
38.602	0.006	0.858	0.00005	1.1658	0.00005	2.103	0.0002
38.981	0.004	0.852	0.00001	1.1731	0.00001	2.116	0.0001
38.472	0.004	0.876	0.00000	1.1417	0.00000	2.164	0.0001
38.653	0.008	0.859	0.00001	1.1640	0.00001	2.106	0.0002